Aus dem

Institut für Schlaganfall- und Demenzforschung (ISD)

Klinikum der Ludwig-Maximilians-Universität München

Characterization of novel NEDDylation inhibitors in in vitro models of atherogenesis

Dissertation

zum Erwerb des Doktorgrades der Medizin

an der Medizinischen Fakultät

der Ludwig-Maximilians-Universität München

vorgelegt von

Eva-Maria Preuner

aus

Vöcklabruck, Österreich

Jahr

2025

Mit Genehmigung der Medizinischen Fakultät der
Ludwig-Maximilians-Universität München

Erstes Gutachten:	Prof. Dr. Jürgen Bernhagen
Zweites Gutachten:	Prof. Dr. Christian Behrends
Drittes Gutachten:	Priv. Doz. Dr. Philipp Freiherr von Hundelshausen
weitere Gutachten:	

Dekan:	Prof. Dr. med. Thomas Gudermann

Tag der mündlichen Prüfung:	30.01.2025

Table of content

Zusammenfassung

Das Ubiquitin-Proteasom-System (UPS) steuert den intrazellulären Proteinabbau durch posttranslationale Modifikation der Zielproteine mit Ubiquitin. Die zentralen Schaltstellen des UPS sind Cullin-RING-Ligasen (CRLs), deren Ubiquitin-Ligase-Aktivität durch NEDD8 (*neural precursor cells expressed developmentally downregulated-8*) reguliert wird. Die NEDDylierung beeinflusst die Zellhomöostase und physiologische Zellfunktionen, indem sie den Abbau regulatorischer Proteine vermittelt. Das CSN (*constitutive photomorphogenesis 9* (COP9) *signalosome*), welches die Entfernung von NEDD8 katalysiert, gilt daher als vielversprechendes therapeutisches Ziel in der Krebsforschung. Des Weiteren deuten verschiedene Studien darauf hin, dass das CSN auch bei Entzündungen und Atherosklerose eine wichtige Rolle spielt. In den letzten Jahren wurden mehrere Verbindungen identifiziert, die die NEDDylierung inhibieren und somit zumindest teilweise die Aktivität des CSN widerspiegeln. MLN4924, ein Inhibitor welcher die gesamte NEDDylierung blockiert, wirkt *in vivo* und *in vitro* atheroprotektiv. DCN1 (*defective in cullin NEDDylation protein 1*) Inhibitoren, die einen späteren Zeitpunkt in der NEDDylierungskaskade beeinträchtigen und nicht die NEDDylierung aller Culline beeinflussen, ermöglichen es, den Einfluss der Cullin-NEDDylierung gezielter zu erforschen.

In dieser Arbeit wurden die Wirkungen der neuartigen DCN1 Inhibitoren NAcM-OPT und -COV, welche bis dato nur an Krebszellmodellen getestet wurden, in murinen und humanen Monozyten- und Makrophagenmodellen *in vitro* im Kontext atherosklerotischer Entzündungsprozesse evaluiert. Die Ergebnisse deuteten auf einen weniger ausgeprägten Einfluss auf die CUL1- und CUL3-NEDDylierung im Vergleich zu MLN4924 hin. Dennoch führte das kovalent bindende NAcM-COV zu einer stärkeren Reduktion der Cullin-NEDDylierung als das nicht kovalent bindende NAcM-OPT. Die starke atheroprotektive Wirkung von MLN4924 auf die Sekretion inflammatorischer Mediatoren aus Makrophagen *in vitro* wurde mit den neuen DCN1 Inhibitoren nicht beobachtet. Interessanterweise beeinträchtigte die Behandlung mit NAcM-COV und MLN4924 die Mobilität und Vitalität der Monozyten *in vitro*.

Zusammenfassend lieferte diese Dissertation erste Einblicke in die Wirksamkeit der neuartigen DCN1 Inhibitoren an murinen und menschlichen Monozyten- und Makrophagenmodellen im Kontext der Atherogenese *in vitro*. Hierbei wurden die neuartigen DCN1 Inhibitoren als vielversprechende Ergänzung der Erforschung des CSN identifiziert, da sie Einblicke in die gezielte Regulation der CUL1- und CUL3-NEDDylierung ermöglichen. Perspektivisch könnten sich spezifischere NEDDylierungsinhibitoren auch als nebenwirkungsärmere therapeutische Alternativen zu MLN4924 etablieren.

Abstract

Intracellular protein degradation is controlled by the ubiquitin-proteasome system (UPS) through post-translational modification of target proteins with ubiquitin. The central components of the UPS are cullin-RING ligases (CRLs). The CRLs' ubiquitin ligase activity is regulated by post-translational modification with NEDD8 (*neural precursor cells expressed developmentally downregulated-8*), a protein structurally similar to ubiquitin. NEDDylation impacts cell homeostasis, cell death, and physiological cell functions by mediating the degradation of critical regulatory proteins. Especially the CSN (*constitutive photomorphogenesis 9* (COP9) *signalosome*), which catalyzes the removal of NEDD8, is considered a promising therapeutical target in cancer research. Still, various studies indicate that the CSN also has a central role in inflammation and atherosclerosis. Recent efforts have identified multiple compounds that negatively impact NEDDylation. These compounds, at least partially, mimic, and consequently allow to study the CSN. MLN4924, which affects the E1 enzyme and therefore fully blocks NEDDylation, is atheroprotective *in vivo* and *in vitro*. To target cullin-NEDDylation more specifically, novel defective in cullin NEDDylation protein 1 (DCN1) inhibitors, which impair a later timepoint in the NEDDylation cascade, have been developed.

This thesis evaluated the effects of the novel DCN1 inhibitors NAcM-OPT and -COV, which had only been applied in cancer cell models so far, in murine and human monocyte and macrophage models in the context of atherosclerosis *in vitro.* The results suggested a less pronounced impact on CUL1- and CUL3-NEDDylation levels compared to MLN4924 *in vitro*. Still, the covalently binding NAcM-COV resulted in a more potent reduction of cullin-NEDDylation than the non-covalently binding NAcM-OPT. The atheroprotective effect of MLN4924 on macrophage protein secretion *in vitro* could not be observed when using the novel DCN1 inhibitors. Interestingly, treatment with NAcM-COV and MLN4924 significantly impaired monocyte mobility and viability *in vitro*.

This study provided first insights into the effectiveness of the novel DCN1 inhibitors on murine and human monocyte and macrophage models in the context of atherogenesis *in vitro*. This thesis pinpointed novel DCN1 inhibitors as a promising addition to the research of the CSN as they allow insight into specifically targeting CUL1- and CUL3-NEDDylation. These more specific inhibitors of NEDDylation could be future therapeutic alternatives to MLN4924 as they might result in fewer side effects.

Key words: COP9 signalosome, DCN1 inhibitors, NEDDylation, inflammation, atherosclerosis

List of Abbreviations

ABCA1	ATP-binding cassette transporter 1
ABCG1	ATP-binding cassette sub-family G member-1
ACAT1	Acylcholesterol transferase 1
ApoE	Apolipoprotein E
ARG1	Arginase-1
BMDMs	Bone marrow-derived macrophages
BSA	Bovine serum albumin
CANTOS	Canakinumab anti-inflammatory thrombosis outcomes study
CCK8	Cell counting kit 8
CCL	Chemokine (C-C motif) ligand
cDNA	Complementary DNA
CIRT	Cardiovascular Inflammation Reduction Trrial
COP9	Constitutive photomorphogenesis 9
CRL	Cullin-RING ligase
CRP	C-reactive protein
CSN	COP9 signalosome
CUL1	Cullin 1
CUL3	Cullin 3
CUL4A	Cullin 4A
CXCL12	CXC-Motif-chemokine 12
DAMPs	Damage-associated molecular patterns
DCs	Dendritic cells
DCN1	Defective in cullin NEDDylation protein 1
DMSO	Dimethylsulfoxide
DNA	Deoxyribonucleic acid
DTT	Dithiothreitol
EDTA	Ethylenediaminetetraacetic acid
ELISA	Enzyme-linked immunosorbent assay
FCS	Fetal calf serum
FIZZ1	Found in inflammatory zone
GM-CSF	Granulocyte-macrophage colony-stimulating factor
HCC95	Non-small-cell lung and tongue carcinoma cell lines
HIF	Hypoxia-inducible factor

ICAM-1	Intercellular adhesion molecule-1
IFN-ɣ	Interferon-gamma
IL	Interleukin
INOS	Inducible nitric oxide synthase
JAB1	c-Jun-activation domain-binding protein-1
JAK	Janus kinases
JAMM	JAB1-MPN-domain metalloenzyme
LDL	Low-density lipoprotein
LPS	Lipopolysaccharide
MAP	Mitogen-activated protein
M-CSF	Macrophage colony-stimulating factor
MI	Myocardial infarction
MM6	Mono Mac 6
mpi	Mean pixel intensities
MRC1	Mannose receptor 1
NAE	Nedd8 E1-activating enzyme
NEDD8	Neural-precursor-cell-expressed developmentally down-regulated 8
NF-κB	Nuclear factor-kappaB
oxLDL	Oxidized LDL
PAMPs	Pathogen-associated molecular patterns
PBMCs	Peripheral blood mononuclear cells
PBS	Phosphate-buffered saline
PCR	Polymerase chain reaction
PCSK9	Proprotein convertase subtilisin/kexin type 9
Pen-Strep	Penicillin-streptomycin
PI	Propidium iodide solution
RNA	Ribonucleic acid
RT-qPCR	Quantitative real-time PCR
SMC	Smooth muscle cell
SR	Scavenger-receptor
STAT	Signal transducer and activator of transcription proteins
TBS	Tris-buffered saline
TEMED	Tetramethylethylendiamin
TGM2	Transglutaminase 2

TNF-α	Tumor necrosis factor-alpha
Ub	Ubiquitin
UPS	Ubiquitin-proteasome system
VCAM-1	Vascular cell adhesion molecule-1
VSMCs	Vascular smooth muscle cells
YM1	Chitinase-like 3

List of Figures

List of Tables

1 Introduction

1.1 Atherosclerosis

Cardiovascular diseases account for over one-third of all deaths in the Western world today [5]. One of the main contributors to the cardiovascular burden is atherosclerosis, a chronic inflammatory condition of the medium and large arteries. It is characterized by vessel inflammation and plaque formation, which can cause pathologies like cerebrovascular disease, peripheral artery disease, and coronary artery disease [6]. Eventually, plaque rupture or erosion, and thrombus formation can occur, leading to ischemic events like stroke or ischemic heart disease [7].

1.1.1 Lesion development and plaque formation

Atherosclerotic development is triggered by disturbed laminar flows and shear stress, leading to endothelial activation. Adhesion molecules are upregulated within this process, resulting in atherogenic leukocyte arrest and transmigration [8-10].

In pro-atherogenic predilection sites, the atherogenic process starts with a buildup of plasma lipoproteins, such as Low-Density Lipoprotein (LDL), within the *tunica intima* [11]. Here, reactive oxygen species, as well as myeloperoxidases and lipoxygenases, modify the LDL to oxidized LDL (oxLDL), which is recognized with high affinity by macrophage scavenger receptors (SRs) [12]. The accumulation of LDL correlates with well-known risk factors like smoking, hypertension, and metabolic dysregulation [13, 14]. These vascular lipid deposits facilitate the activation and proliferation of macrophages, endothelial cells, and smooth muscle cells (SMCs). This results in enhanced production of chemokines and adhesion molecules to attract T-cells, neutrophils, monocytes, and dendritic cells (DCs) into the *tunica intima* [13, 15]. A growing number of studies indicate that mononuclear cells are crucial in the formation and advancement of atherosclerotic plaques [16-18]. After different T-cell subsets, macrophages and monocytes account for the largest cell populations in the human atherosclerotic plaque [19]. In mouse aortae, the number of macrophages increases up to 20-fold during atherogenesis due to local proliferation and predominant derivation from circulating monocytes [20, 21].

Predominant differentiation to monocyte-derived macrophages is stimulated by atheroma factors like macrophage colony-stimulating factor (M-CSF) or granulocyte/macrophage colony-stimulating factor (GM-CSF), which are produced by activated endothelial cells and SMCs [13, 22, 23]. These monocyte-derived macrophages proliferate and secrete growth factors and cytokines that amplify the inflammatory response. Additionally, heightened expression of scavenger receptors on the cell surface results in an upregulation of receptor-mediated endocytosis of oxLDL, subsequently leading to foam cell formation [7, 24, 25].

This atherogenic process typically begins clinically asymptomatic and starts at an early age. Over the course of decades, it progresses from a reversible fatty streak to severe fibrous lesions with necrotic cores containing lipid crystals. These plaques can narrow the vessel volume and are prone to plaque rupture, resulting in cardiovascular events like myocardial infarctions (MIs) or strokes [26].

1.1.2 Monocytes in atherosclerosis

Monocytes and macrophages are the second and third-largest cell populations within human atherosclerotic plaques after T cells [19]. These cells are crucial for the initiation and progression of atherosclerosis as well as the chronic inflammatory state characterizing the condition. Monocyte differentiation happens in the bone marrow from hematopoietic stem cells due to the involvement of various progenitors, resulting in a polarization of the cells towards one of three main monocyte subsets: classical ($CD14^{++}CD16^{-}$), non-classical ($CD14^{+}CD16^{++}$), and intermediate monocytes ($CD14^{++}CD16^{+}$). These subsets vary by their surface proteins and their specific function in disease and homeostasis [27]. Classical monocytes have been suggested to express higher levels of chemokine receptors and, therefore, have a higher potential to migrate towards inflammatory cues [27, 28]. Furthermore, they are linked to the emission of pro-inflammatory cytokines such as interleukin (IL)-6, IL-8, and CCL2 and the differentiation into monocyte-derived macrophages [28, 29]. Intermediate monocytes were shown to secrete IL-1β, IL-6, and tumor necrosis factor-alpha (TNF-α) and to express the highest protein levels related to antigen presentation [19, 28, 30, 31]. Non-classical monocytes do not mirror the classical monocyte secretion of pro-inflammatory cytokines but are associated with wound healing [31, 32].

Monocytes in circulation are drawn to the lesion by a variety of adhesion molecules, like intercellular adhesion molecule-1 (ICAM-1), vascular cell adhesion molecule-1 (VCAM-1), P-selectin and S-Selectin **(Figure 1)** [33]. These molecules are exhibited by activated endothelial cells in lesion-prone areas and border areas of atherosclerotic plaques [34].
In animal models, the adhesion of monocytes was demonstrated to be the initial step in early atherogenesis [35]. After the attachment of monocytes to the endothelium of the aorta, the cells migrate into the vessel wall. There, because of elevated levels of M-CSF and/or GM-CSF in their microenvironment, classical monocytes predominantly transform into pro-inflammatory macrophages and DCs within the subendothelial space of the aorta [20, 21, 25, 36]. Furthermore, monocytes can take up lipids and differentiate into foam cells [27, 37].

Monocyte levels in human blood samples have been suggested as a prediction marker for cardiovascular risks [38]. A study containing more than 600 patients with no known cardiovascular disease revealed that increased numbers of classical monocytes predicted

cardiovascular events within an average monitoring period of 15 years [39]. Furthermore, after MIs, the number of circulating monocytes was shown to be increased for more than three days [40].

1.1.3 Macrophages in atherosclerosis

Macrophages are crucial players in all stages of atherogenesis. After T cells, they are the second-largest cell population in the human plaque, contributing to inflammatory signaling and foam cell formation by taking up oxLDL [19].

Specialized tissue-resident macrophages, as well as monocyte-derived macrophages, take part in the inflammatory response. Answering to signaling molecules, damage-associated molecular patterns (DAMPs), and pathogen-associated molecular patterns (PAMPs), the macrophages polarize towards different functional phenotypes [21, 41].

The classical model of macrophage polarization distinguishes between a pro-inflammatory M1 macrophage, which is elicited by interferon-gamma (IFN-ɣ) and/or bacterial lipopolysaccharide (LPS), and an anti-inflammatory M2 phenotype that can be induced by, for instance, IL-4 [13, 42]. Still, macrophage polarization is not limited to these two extremes but lies within a broad spectrum of phenotypes. Using single-cell RNA sequencing technology, Zernecke et al. recently identified three sub-groups of both human and mouse macrophages: aortic resident, inflammatory, and foamy ($Trem2^{hi}$) macrophages [43]. Different phenotypes are associated with individual functional characteristics and cytokine secretion patterns [43-46]. In this thesis, macrophage markers were still analyzed according to the traditional pro-inflammatory M1 and anti-inflammatory M2 classification, as this paradigm has been used in many papers that this work refers to [47, 48].

Chronic inflammation, which underlines atherosclerotic plaques, can lead to a shift towards an increase of pro-inflammatory macrophages [49]. Within the atherosclerotic plaque, macrophages are exposed to various stimuli like LPS, IFN-ɣ, T-helper cells, hypoxia, and necrotic cells, resulting in a pro-inflammatory state **(Figure 1)**[50]. Analyses of human and murine transcriptomes have shown that the markers used for phenotype determination are species-specific [51]. Among others, human M1-macrophages secrete high levels of inducible nitric oxide synthase (iNOS), TNF-α, IL-1β, and chemokine (C-C motif) ligand (CCL) 2, whereas IL-6, IL-1β, IL-12, TNF-α, and CCL2 can be considered murine M1-markers. This plethora of pro-inflammatory cytokines can produce hyper-inflammatory, tissue-destroying effects [41]. However, plaque macrophages can still have anti-inflammatory characteristics involved in fibrotic tissue repair by expressing higher protein quantities of scavenger and mannose receptors, as well as increased levels of Arginase-1 (ARG1), IL-10, and CCL22 secreted by human M2-macrophages. Murine M2-macrophages secrete Arg1, found in inflammatory zone

1 (Fizz1), chitinase-like 3 (Ym1), mannose receptor 1 (Mrc1), and transglutaminase 2 (Tgm2) [52-54]. Pro- and anti-inflammatory macrophage activation signaling depends on the nuclear factor-κB (NF-κB)-, and Janus kinases (JAK)/signal transducer and activator of transcription proteins (STAT)-pathways [55].

1.1.4 Foam cell formation

Foam cells originate from macrophages, vascular SMCs (VSMCs), endothelial cells, and stem/progenitor cells [56]. In the subendothelial space, macrophages internalize modified lipoproteins through sets of different scavenger receptors (SR), resulting in foam cell formation [25]. Foam cells are a significant subpopulation associated with the progression of atherosclerosis. They contribute to the forming of a necrotic core and destabilizing of the plaque, skewing the plaque towards a more unstable phenotype. Different SRs are specific for certain lipoproteins. For example, the SR-A classes SR-AI and SR-AII have a strong affinity to oxLDL [57]. Still, it is not yet shown whether the high expression of these receptors exacerbates foam cell formation. Different studies suggest that inhibition of SR-A in mice can lead to pro- and anti-atherogenic effects [58, 59]. Still, these conflicting results indicate complex regulatory mechanisms within the lipid metabolism [25]. After the macrophages internalize the modified lipoproteins, they are hydrolyzed into fatty acids and free cholesterol (FC) by intracellular lysosomes. The FC accumulates in the cell as cytoplasmic lipid droplets as it is re-esterified by the acylcholesterol transferase 1 (ACAT-1) [60]. However, these esterized lipid droplets have not yet been proven to cause foam cell formation. Pharmacological inhibition of ACAT-1 even increased foam cell formation in murine *in vivo* models [61].

Foam cell formation initiates numerous apoptotic pathways, resulting in the formation of a necrotic core. OxLDL can prompt the initiation of the caspase cascade, proteasomal dysfunction, toxic cell injury, as well as increased activity of degradative enzymes [25, 62-64]. Inadequate removal of these post-apoptotic foam cells within the necrotic core is considered a key driver of inflammation in the atherosclerotic lesion [25, 65].

Cholesterol efflux, the active transportation of phospholipids and cholesterol out of the cells, is mediated by various transporters like ATP-binding cassette transporter 1 (ABCA1), ATP-binding cassette sub-family G member-1 (ABCG1) and SR-B1 [24, 66]. Via a reverse cholesterol transport system, the cholesterol is attached to high-density lipoproteins (HDL) and Apolipoprotein A1 (ApoA1), and transported out of the cell towards the liver [25, 67]. This cholesterol efflux prevents intracellular cholesterol accumulation and, subsequently, foam cell formation.

In summary, monocytes, macrophages, and foam cells are closely connected cell populations and significant players in atherogenesis. These cell populations and their interactions affect

the inflammatory process and plaque formation alike and are therefore considered a promising target for studying and treating atherosclerosis.

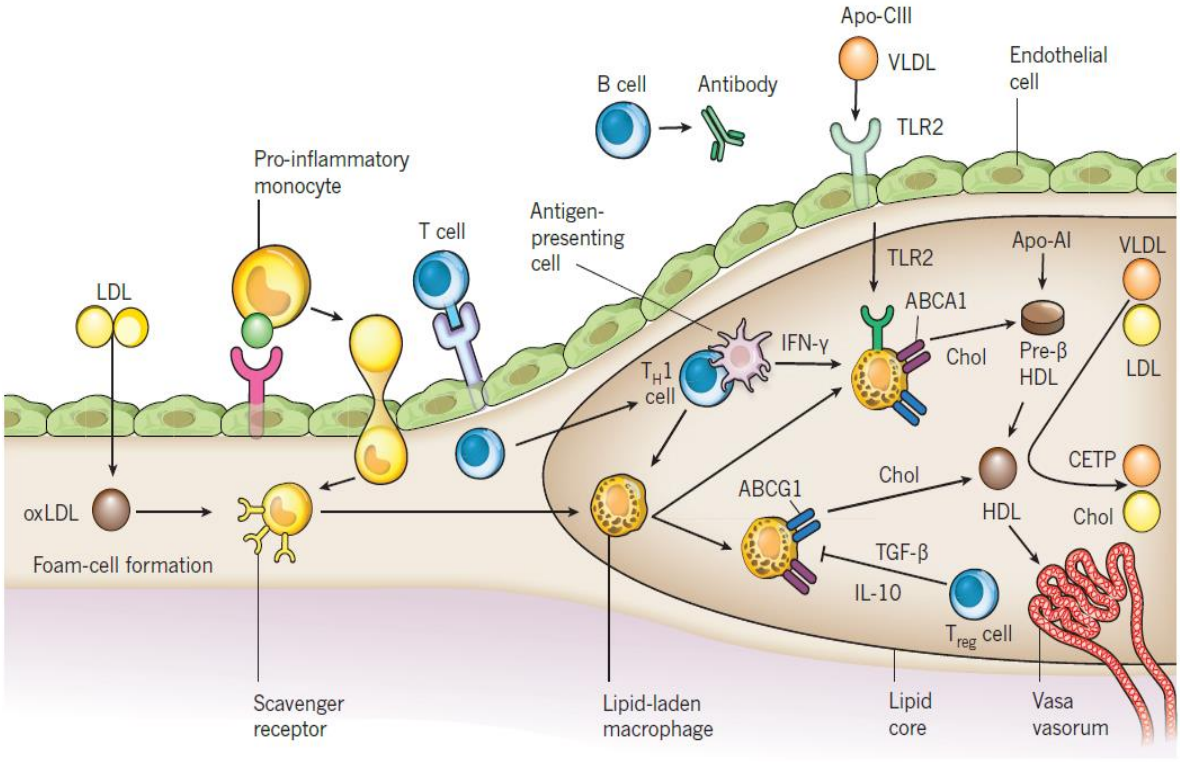

Figure 1 Inflammation and lipid metabolism are closely connected in the modulation of atherosclerosis. Initially, inflammatory cells, including blood monocytes, are recruited to the intima. During inflammatory activation, monocytes and macrophages can take up oxLDL via scavenger receptors, resulting in foam cell formation and an even further advanced inflammatory micro-environment and necrotic core formation. For cholesterol efflux, ABCA1 and ABCG1 can load HDL particles with cholesterol and transport them out of the cells. (Figure taken from Libby P. et al., 2011 [1], permission obtained from Springer Nature, license number 5712731048741).

1.1.5 Cell death in myeloid cells

The molecular mechanisms of cell death have been the focus of countless studies during the last decades. In inflammation and atherosclerosis, cell death can be both a physiological part of cell homeostasis or a pathological mechanism enhancing inflammation and leading to the formation of necrotic areas within the plaque. Different cell death mechanisms can be distinguished: apoptosis, necrosis, pyroptosis, and necroptosis. Also, efferocytosis, the process of phagocytosis of damaged and dead cells, has been suggested to be connected to atherosclerotic lesion development [68].

1.1.5.1 Apoptosis

Apoptosis is characterized by various structural and biochemical changes to the cell's composition, enabling cells with phagocytic capacities to detect and remove the apoptotic cell. Typical morphological criteria are massive membrane blebbing, hypercondensation, and disintegration of the nucleus [69]. The cells are engulfed before they leak their contents, reducing

the risk of damaging the surrounding cells or triggering inflammation by releasing DAMPs [70]. Thus, apoptosis is a characteristic type of cell death within tissue undergoing homeostatic cell death. Typically, apoptosis is activated via caspases-3, -6, -7, -8, and -9, which control the disposal of apoptotic cells [69, 70]. Monocytes, for example, are programmed to undergo apoptosis when there is no stimulation towards monocyte-macrophage differentiation. Stimuli like M-CSF therefore not only lead to cellular changes but also inhibit the default apoptosis of monocytes [71].

1.1.5.2 Necrotic cell death, pyroptosis, and necroptosis

Necrosis is defined by a sudden uncontrolled loss of membrane integrity and extensive organelle and cell swelling, causing the release of DAMPs and other cellular contents. This results in the activation of the immune system, as well as, subsequently, an upregulation of inflammatory signaling [70, 72].

Even though necrositic cell death is not typically liked to caspase activation, there is an exception termed pyroptosis. Pyroptosis is a type of programmed necrosis activated upon intracellular infections in the presence of DAMPs or PAMPs, which is typically induced in cells of the nonspecific immune system, like monocytes and macrophages [73, 74]. In this case, cell death occurs subsequent to the activation of an inflammatory subgroup of caspases (caspases-1, -4, and -5), leading to an immune response and the secretion of pro-inflammatory chemokines and cytokines [55, 75].

Another type of programmed inflammatory necrosis is necroptosis. It is characteristically seen as a reaction to the activation of specific TNF ‘death receptor’ subset receptors when the activity of caspases is actively impaired by synthetic or viral-derived caspase inhibitors [70, 76]. Consequently, cell death and the inflammatory pathways triggered by necrosis can be considered key factors in cell physiology and pathology. Particularly, the inflammatory aspect has been the target in drug trials for treating and preventing atherosclerosis.

1.1.5.3 Efferocytosis

The removal of cellular corpses, efferocytosis, is performed by ‘professional’ phagocytes (mostly macrophages, as well as monocytes, and DCs), and ‘non-professional phagocytes’ like epithelial cells [77]. This removal of dead and dying cells is crucial for homeostasis. For instance, it has been suggested that macrophage efferocytosis, by impacting intravascular homeostasis, contributes to the prevention of atherogenesis [68]. Vice versa, disruption of functional efferocytosis has been associated with various pathologies including atherosclerosis. During the initial steps of atherosclerotic plaque development, macrophages carry out an intense process of foam cell efferocytosis, which restricts atherosclerotic lesion development [13, 77]. With further progression of the disease, the capacity of the macrophage

efferocytosis decreases, leading to a buildup of apoptotic cells and the development of a necrotic core [68].

1.1.6 Current clinical treatment approaches for atherosclerosis

Current approaches for treating atherosclerosis and preventing cardiovascular events mainly focus on LDL blood levels. Patients are asked to change their lifestyle and diet as a first attempt, which might reduce LDL levels by up to 40% [78]. If this does not sufficiently reduce the patient's LDL levels or the hyperlipidemia is genetically caused, it is possible to treat with statins additionally. These lower the LDL levels up to 50% by competitively inhibiting the HMG-CoA-reductase; thus, novel cholesterol production is impacted directly [78]. Combining statins with Ezetimibe, a drug that selectively inhibits intestinal cholesterol absorption [79], can reduce LDL levels by up to 65%. Proprotein Convertase Subtilisin/Kexin type 9 (PCSK9)-inhibitors which lessen lysosomal degradation of LDL-receptors are also commonly used. Combined with statins and Ezetimibe, these can decrease the patient's LDL levels by up to 85% [80, 81].

1.1.7 Clinical trials for an anti-inflammatory attempt in treating atherosclerosis

Some of the leading clinical studies testing new approaches for treating atherosclerosis have validated the "inflammatory hypothesis" of atherosclerosis. The Canakinumab Anti-inflammatory Thrombosis Outcomes Study (CANTOS), the Cardiovascular Inflammation Reduction Trial (CIRT), and the Colchicine Cardiovascular Outcomes Trial (COLCOT) have been the biggest and most recognized ones [82].

CANTOS, with over 10,000 patients included, proved that specific inhibition of IL-1β significantly reduces cardiovascular risks, measured by event rates. Canakinumab injected in doses of 150 mg or 300 mg every three months led to reduced IL-6- and C-reactive protein (CRP)-levels by 35% in comparison to the placebo group. A 17% decrease in recurrent MIs, strokes, or cardiovascular death was observed without any lipid level or blood pressure lowering involved. This trial can be considered proof of principle regarding the critical role of inflammation within atherosclerosis [83]. Still, this study has been criticized for overinterpreting its clinical significance [84-86]. The actual relative risk reduction has been calculated to be 15%, corresponding to a number needed to treat of 156 [84-86]. Considering the high costs and adverse effects, like a higher risk of infections, it is unclear whether Canakinumab will ever be implemented as an actual clinical strategy [85, 87].

Contrary to this, the 4786 patient CIRT presented fewer promising results. In this trial, patients were treated with low-dose methotrexate, a drug commonly used in inflammatory diseases like rheumatoid arthritis and psoriasis. Its effect is less well-understood but is most likely mediated through adenosine signaling, leading to a broader impact on inflammation [88]. The weekly dose

of 15-20 mg methotrexate did not reduce cardiovascular events or lower IL-1β, IL-6, or CRP levels [89].

In COLCOT, a study with 4745 participants with a recent history of MI, the colchicine group received 0.5 mg of colchicine daily. Colchicine is a well-known anti-inflammatory drug, commonly used in conditions like gout and pericarditis. Within a follow-up period of 23 months, patients subjected to colchicine treatment experienced significantly fewer cardiovascular events (5.5% versus 7.1% in the placebo group) [90]. CRP levels were only measured in a small subgroup of 207 patients. Within 6 months a significant reduction of CRP levels occurred in both groups, with no significant difference between patients treated with colchicine or placebo [90]. Interestingly, other studies have suggested, that low-dose colchicine treatment can significantly decrease CRP levels in patients with cardiovascular risk factors [91, 92].

These studies draw attention towards focused cytokine inhibition instead of broad-spectrum anti-inflammatory strategies as treatments for atherosclerosis. Especially the NLRP3 inflammasome and its subsequent IL-1 to IL-6 pathway appear to be promising targets [82]. Nevertheless, these anti-inflammatory strategies are associated with side effects, like lethal infections and sepsis. The CANTOS trial, for instance, did not reveal a significant difference in all-cause mortality amid the canakinumab and placebo cohorts, as there were, for example, significantly more deaths attributed to infections or sepsis in the canakinumab group [82]. These side effects highlight the necessity for more targeted therapeutic strategies when intervening in inflammatory pathways.

1.2 COP9 signalosome[1]

1.2.1 Structure and functions

The constitutive photomorphogenesis 9 (COP9) signalosome (CSN) controls cell homeostasis by regulating the ubiquitin-proteasome system (UPS) and serving as a docking platform for various cell-regulatory factors. This multi-protein complex was first discovered in 1996 from *Brassicaoleracea* (cauliflower) and found to act as a repressor of photomorphogenesis [94]. In 1998, the mammalian COP9 was first purified from human erythrocytes [95]. In mammals, the evolutionarily conserved complex is formed by eight subunits (CSN1-CSN8). For some of these subunits, additional complex-independent functions have been indicated [96-98]. For example, the CSN5 subunit was first identified complex-independently as c-Jun-activation domain-binding protein-1 (JAB1) for stabilizing the complexes of target gene activation for certain transcription factors like c-Jun. [99]

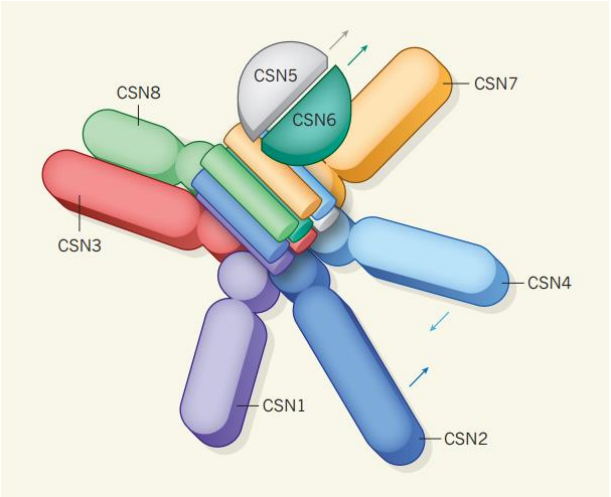

Figure 2 Structure of the CSN. The enzyme complex is formed by eight protein subunits. Six subunits form a *"hand"* where the N-terminals end at the fingertips and the C-terminals are bundled as a *"box"* that sits on the *"hand".* The CSN5 and CSN6 form a *"tomato atop".* The arrows represent the conformational changes of the subunits after binding to a NEDDylated substrate. (Figure taken from Deshaies et al., 2014 [3], permission obtained from Springer Nature, license number 5712730785233)

The CSN's enzymatic effect catalyzes the removal of neural-precursor-cell-expressed developmentally down-regulated 8 (NEDD8) from substrate proteins like cullin-RING Ligases (CRLs) ("deNEDDylation"), resulting in regulation of the CRLs' activity [100]. Cullins are the major substrate class of the CSN. The CSN's enzymatic activity is regulated by the Zn^{2+}-containing JAB1-MPN-domain metalloenzyme (JAMM) motif of the CSN5 subunit. Still, the holocomplex of all eight subunits is required for the actual function as an isopeptidase [101-103]. Additionally, CRL-independent NEDDylation targets have been discussed in recent years [104].

The human CSN's crystal structure was first determined in 2014, providing detailed information about the control of the CSN's enzymatic activity and its interaction with CRLs [105]. The holocomplex structure can be compared to *"a widely splayed hand holding a box with a tomato atop"* [3]. In this visualization, the "fingers" represent the ends of CSN1, 2, 4, 7, 3, and 8, whereas six PCI domain proteins form the "palm" in a horseshoe-shaped ring. The carboxy-

[1] This section uses significant amount of information from the review "Role of the COP9 Signalosome (CSN) in Cardiovascular Diseases" by Milic et al. [93. Milic, Tian and Bernhagen. Role of the COP9 Signalosome (CSN) in Cardiovascular Diseases. *Biomolecules*. 2019;9:217.]

terminal ends of the CSN-subunits build a “box”, whereas the “*tomato atop*” represents the subunits CSN5 and CSN6, which contain the MPN. There are two structural centers: a “*horseshoe-shaped ring*” and a “*tomato*” [3] **(Figure 2)**.
The crystal structure furthermore illustrates that when there is no NEDDylated substrate present, CSN5 is inactivated by a glutamate residue 104, blocking the Zn^{2+} atom in the catalytically active site. Once a NEDDylated substrate binds to the complex, CSN4 and CSN6 mediate conformational changes, activating the enzymatic deNEDDylation-activity in CSN5 [3, 105] **(Figure 2)**.

It is known that the cycle of NEDDylation and deNEDDylation is necessary for the physiological function of the UPS. Consequently, the CSN broadly impacts Deoxyribonucleic acid (DNA) repair mechanisms, cell cycle control, inflammatory gene expression, and other functions within the cell [106-109].

1.2.2 The ubiquitin-proteasome system

The UPS is a multi-enzyme pathway that regulates more than 80% of all protein degradation in the cell [110]. It is closely connected to and regulated by NEDDylation and the CSN-mediated deNEDDylation [106]. The UPS covalently conjugates a poly-ubiquitin chain to the substrate protein. This tagged protein is then recognized and broken down by the proteasome, the core multicomponent proteolytic complex of the UPS [111, 112]. This poly-ubiquitination does not only apply to damaged or misfolded proteins but also regulates various cellular processes, such as immune response [113], cell cycle control [114], apoptosis [115], cell signaling [116, 117], and protein turnover under both physiological and pathological conditions [112, 118].

The process of ubiquitination consists of three different enzymes. First, an E1 activating enzyme activates and transfers Ub (ubiquitin) to an E2 conjugating enzyme ATP-dependently. This E2 enzyme is bridged to a target protein via an E3 Ub ligase, facilitating the transfer of Ub to an N-terminus or lysine of the substrate protein [119]. To facilitate substrate-selectivity, an immense diversity in E3 ligases is necessary. Over 600 different E3 ligases are known, categorized into three subfamilies: HECT, RING and U box, and RBR. CRLs, the biggest subtype of the RING ligases, account for over 200 E3 ligases, making them responsible for about 20% of all cellular ubiquitination [120, 121].
Mammals express seven different cullin proteins (cullin 1 (CUL1), cullin 2, cullin 3 (CUL3), cullin 4A (CUL4A), cullin 4B, cullin 5, and cullin 7) that form multi-subunit CRLs, CRL1-7 [122]. All CRLs share a universal structure: a catalytic RING domain subunit, either Rbx1 or Rbx2, recruiting the Ub-tagged E2 enzymes and a rigid scaffold. To enable distinctive protein-ubiquitination patterns as a response to various signals, the CRLs differ in their adaptor

proteins and substrate receptors [93, 123, 124]. In CRL1, for instance, the Skp1 adaptor protein attaches to the F-box substrate receptor protein family [111].

1.2.3 NEDDylation of Cullin-RING ligases

The CRLs' ubiquitin-ligase activity is dependent on its degree of post-translational NEDD8 conjugation ("NEDDylation"). NEDD8, structurally similar to but not interchangeable with Ub, is conjugated to its target protein by an isopeptide bond in a three-enzyme process that is similar to the respective process of the ubiquitination cascade [125]. NEDD8 is first activated ATP-dependently by the NEDD8 E1-activating enzyme (NAE), resulting in a thioester-linked E1-NEDD8 complex. NEDD8 is then relocated to a NEDD8-specific E2-conjugating enzyme (UBC12 or UBE2F) and eventually attached to a lysine residue of the target protein by an E3 enzyme **(Figure 3)** [104, 126-128]. A defective in cullin NEDDylation protein 1 (DCN1)-UBC12 protein-protein interaction stabilizes this complex. DCN1 is a component of the E3 enzyme complex and contains a binding pocket for UBC12. Most of the NEDD8 E3 enzymes are of the RING-subclass [127]. Depending on the E2 enzyme and the RING domain subunits, different cullins and, consequently, CRLs are modified and activated [128, 129].

The CRL's impact on substrate degradation links NEDDylation and the CSN to various pathologies. As the CSN holocomplex and its subunits are key players in the regulation of cell proliferation, cell cycle control, and homeostasis, much research concerning the CSN has been focused on its role in cancer development and treatment [130]. An overexpression of CSN5, for instance, has been correlated with gastric cancer [131], non-small cell lung cancer [132], gliomas [133], and many others [130].

Furthermore, the CSN is suggested to regulate inflammatory and stress pathways like hypoxia-inducible factor (HIF)-1α signaling and the NF-κB pathway, as well as cell survival responses [47, 134-137]. This, subsequently, connects NEDDylation to atherogenesis, via various pathologies like atherosclerotic plaque formation and VSMC proliferation [93] (see chapter 1.2.5).

Additionally, a study from 2020 by Vogl et al. revealed that NEDDylation also impacts various non-cullin proteins. One standout candidate appears to be the actin regulator cofilin. Global inhibition of NEDDylation in developing neurons led to altered actin dynamics followed by cytoskeletal defects and cellular growth impairments. Conversely, site-specific NEDDylation of cofilin impacted neurite outgrowth [138]. This data indicates that NEDDylation alters actin reorganization and, therefore, might impact more areas of the organic system than initially implied.

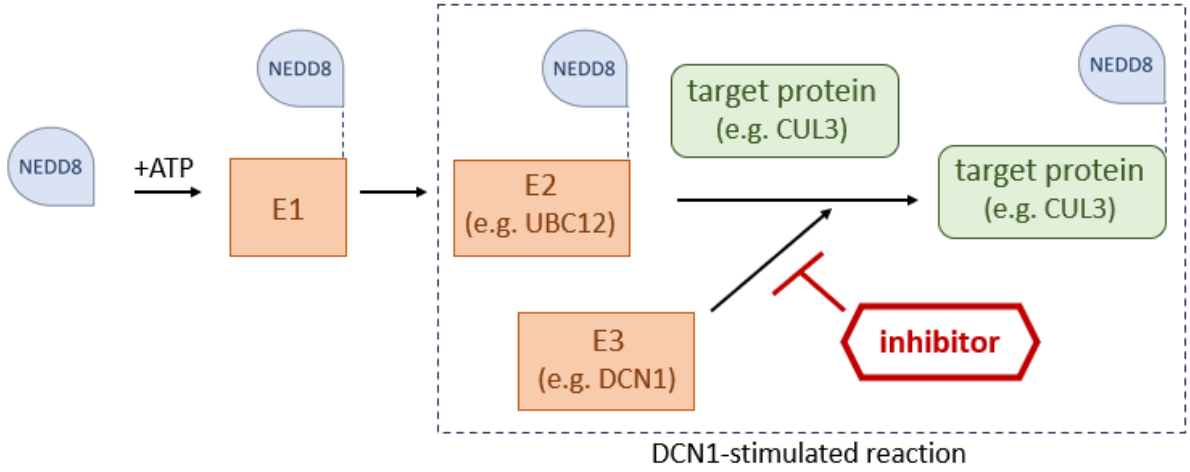

Figure 3 The NEDDylation cascade. After activation by the an E1-enzyme, NEDD8 is transferred to an E2-conjugating enzyme. Eventually, it is attached to a target protein by an E3-enzyme. A DCN-UBC12 protein-protein interaction stabilizes the complex. The novel DCN1 inhibitors (depicted as red hexagon) affect the E3 enzyme. (Figure inspired by Kim et al., 2019 [2])

1.2.4 Small molecule inhibitors

As the CSN broadly impacts protein turnover and is subsequently connected to various signaling pathways, different inhibitors have been designed for therapeutic purposes and to further study the effects of NEDDylation. Small molecule inhibitors have been promising candidates, as through their small molecular weight (<900 daltons), they can diffuse through the cell membrane and impact specific intracellular proteins and processes [139].

1.2.4.1 MLN4924

MLN4924 (Pevonedistat) is a highly selective and potent small-molecule inhibitor of the NAE, the first enzyme in the NEDDylation cascade **(Figure 3, Figure 5 D)**. It covalently binds to NEDD8, producing a pevodenistat-NEDD8 adduct that is impossible to conjugate further. This NEDDylation leads to a broad downregulation of the CRL's NEDDylation and, therefore, an activation and accumulation of CRL-dependent substrates [140, 141].

Pevonedistat was tested in phase 2/3 clinical trials for individuals with solid tumors [142], acute myeloid leukemia, myelodysplastic syndromes, and nonhematological malignancies [143, 144]. However, due to its broad effects, various side effects have been reported, including pyrexia, peripheral edemas, myalgia, febrile neutropenia, and even multi-organ failure [144].

In *in vivo* studies with atherogenic *Apolipoprotein E*$^{-/-}$ *(Apoe*$^{-/-}$*)*-mice, regular injections of MLN4924 led to inhibition of initial atherosclerotic lesion development in the aortic root and the aorta along with downregulation of acute atherogenic inflammation [47]. Considering that MLN4924 mirrors CSN overexpression, this suggests that the CSN impacts atherosclerosis and highlights its potential pharmacological value in treating cardiovascular diseases.

1.2.4.2 DCN1 inhibitors

DCN1 inhibitors target a later timepoint in the NEDDylation cascade and can thus be considered more specific inhibitors than MLN4924 [145]. This approach of inhibition of NEDDylation has been developed as the clinical results of MLN4924 were promising in principle. However, many side effects occurred, which might be explainable by the broad impact of MLN494 on NEDDylation. The more specific inhibitors might circumvent such problems and will allow further investigation into the effects of CUL1- and CUL3-NEDDylation.

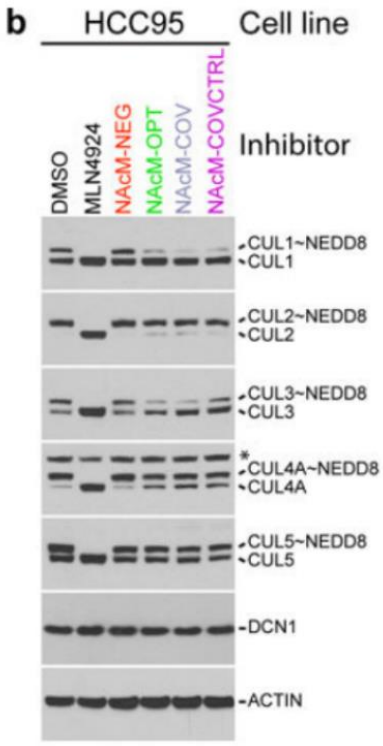

Figure 4 CUL1- and CUL3-NEDDylation was impacted by NAcM-OPT and COV in HCC95 cells. Immunoblot of NEDD8 levels upon MLN4924, NAcM-COV and -OPT treatment for 24 h. (Figure taken from Scott et al., 2017 [4], permission: open access)

Among others, there are “NAcM-inhibitors”, which are small molecule inhibitors affecting the DCN1-UBC12 protein-protein interaction by blocking the acetylation of the UBC12’s N-terminal methionine **(Figure 5 A, B)**. UBC12 typically docks to a binding pocket in DCN1, stabilizing the enzymatic complex [145] **(Figure 3)**. Two different NAcM-inhibitors have been developed: First, NAcM-OPT, which selectively reduces CUL1- and CUL3-NEDDylation by attaching to DCN1 and DCN2 **(Figure 4)**. It is considered a promising candidate *in vivo* due to its stability and high oral bioavailability in mice [145]. Furthermore, NAcM-COV, an inhibitor irreversibly targeting DCN1, reduced steady-state levels of NEDDylated CUL1 and CUL3 [145] **(Figure 4)**. Both compounds did not induce any significant side effects during a 48 h observation period in murine *in vivo* cancer models [145].

These small molecule inhibitors still have several limitations: Their moderate murine half-life requires high dosing and frequent treatment. Furthermore, they cannot access the actual N-acetyl as they lack three-dimensional character as they only have one stereocenter [4]. For this reason, another inhibitor (compound 27), based on a pyrazolopyridone’s structure, has been developed **(Figure 5 C)**. Its’ more pronounced three-dimensional structure allows it to reach the binding pocket of DCN1 more efficiently, and it is generally found to be more potent than the NAcM-inhibitors [2, 146].

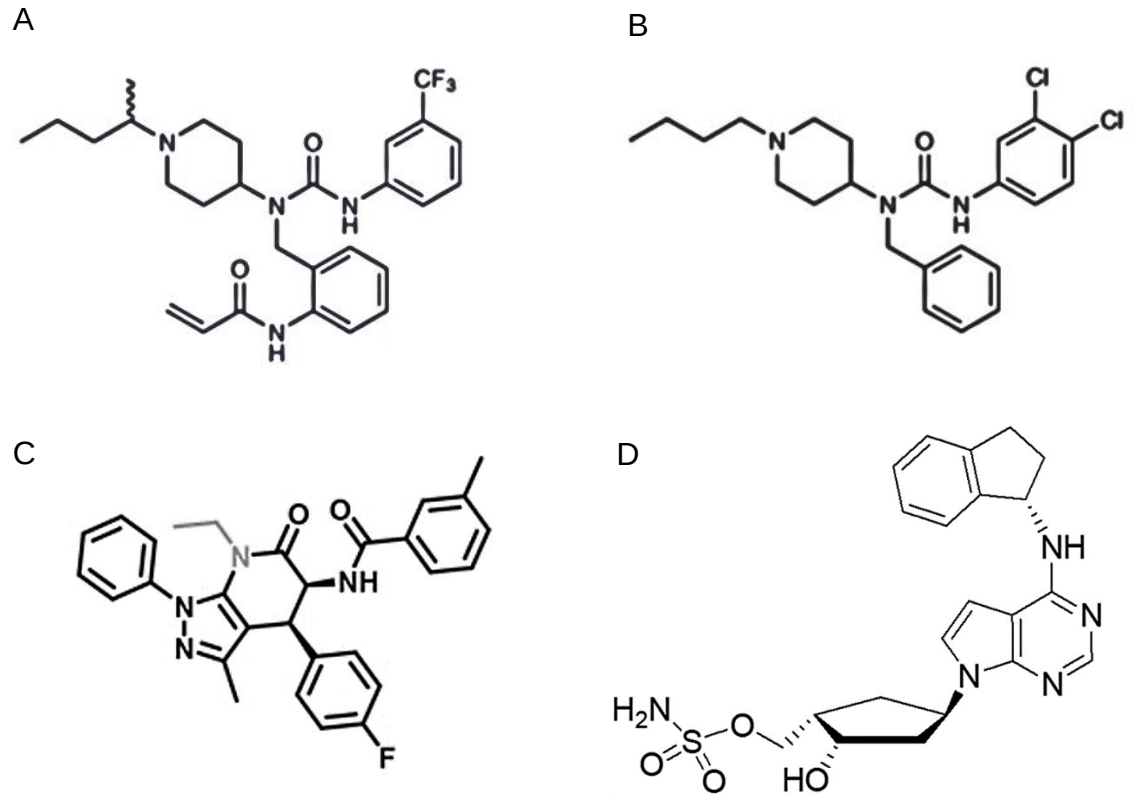

Figure 5 Chemical structures of A NAcM-COV (Figure taken from Scott et al., 2017 [4]) **B NAcM-OPT** (Figure taken from Scott et al., 2017 [4]) **C compound 27** (Figure taken from Kim et al., 2019 [2]) **D MLN4924** (Figure taken from Brownell et al., 2010 [140])

1.2.4.3 CSN5i-3

CSN5i-3 was initially developed as a specific and orally available drug for targeted cancer-treatment. It inhibits the activity of CSN5, the catalytic core of the CSN. Hence, deNEDDylation is impacted, stabilizing cullin-NEDDylation and enhancing CRL-activity [147]. Still, as the compound traps CRLs in a NEDDylated state, degradation of their substrate recognition modules can occur, resulting in an inactivation of certain subsets of CRLs. CSN5i-3 and MLN4924 can, therefore, induce similar, downregulating effects on some CRLs, even though through opposing mechanisms [148].

1.2.5 COP9 in atherosclerosis

The CSN impacts various pathways connected to atherosclerosis and inflammation, like NF-κB, JNK/AP1, or Mitogen-activated protein (MAP)-Kinases, resulting in a broad impact on different cell populations [93]. Various studies have connected the CSN to atherosclerosis, primarily via the NF-κB pathway [47, 134-137].

Increased levels of CSN5 were found in human atherosclerotic lesions during atherogenesis [136]. Additionally, CSN5-inhibition by CSN5-i3 in human umbilical vein endothelial cells (HUVECs) proved to trigger activation of the NF-κB pathway, inflammatory signaling, and Rho/ROCK-dependent damage of endothelial integrity [147].

In HUVECs, silencing of CSN5 led to decreased IκBα levels, increased NF-κB activity, and elevated adhesion molecules and atherogenic chemokine secretion *in vitro* [136]. Conversely, atheroprotective effects were found when using MLN4924, which mirrors CSN5 activity and consequently results in decreased levels of NEDDylated cullins [47]. MLN4924 led to enhanced levels of IκB-α and HIF-1α in HUVECs and human and mouse aortic endothelial cells *in vitro*. MLN4924 also reduced early atherosclerotic lesion sizes in murine aortae and aortic roots *in vivo* [47].

In human monocytes, *in vitro* usage of MLN4924 led to a downregulation of NF-κB activity and increased TNFR1-induced cell death. These results suggest that MLN4924 alters anti-apoptotic and anti-necrotic capacities in monocytes [149].

Furthermore, CUL3 has been identified as the E3 ligase mediating ABCA1 degradation and subsequently inhibiting cholesterol efflux, resulting in the formation of foam cells [150]. Additionally, it was demonstrated that oxLDL enhances CSN5 expression in human macrophages *in vitro*. However, when macrophages were stimulated with oxLDL, JAB1 did not have a direct impact on intracellular cholesterol levels or the NF-κB signaling. Still, alterations in p38 MAP-kinases upon oxLDL treatment were observed *in vitro* [151].

2 Aim of the study

The CSN holocomplex has been shown to broadly influence atherogenesis [93]. Currently, a common way of studying the CSN is by employing MLN4924, an inhibitor of the NAE. As the NAE is the first enzyme in the NEDDylation cascade, MLN4924 application leads to a broad ablation of CRL NEDDylation [140, 141]. Although recent studies suggest MLN4924's beneficial effects in combating the development of atherosclerosis, this small molecule inhibitor is connected to adverse side effects as concluded from cancer studies [152]. In 2018, the more specific novel DCN1 inhibitors NAcM-OPT and NAcM-COV were developed [145]. The more targeted approach of these inhibitors allows a distinction between the activity of CUL1 and CUL3 versus the five residual cullins.

In this MD thesis, I aimed to investigate how the novel DCN1 inhibitors, compared to the well-studied MLN4924, impact monocytes and macrophages *in vitro*. More specifically, I aimed to address the following questions:

- To what extent do the novel DCN1 small molecule inhibitors impact CUL1- and CUL3-NEDDylation in murine and human monocytes and macrophages *in vitro*?
- The UPS is a crucial regulator of cell homeostasis, and it has been demonstrated that MLN4924 can sensitize monocytes for cell death [149]. Therefore, I wanted to address whether NAcM-OPT and NAcM-COV also affected human and murine monocyte viability *in vitro*.
- Global ablation of NEDDylation has been shown to alter cellular actin remodeling in developing neurons *in vitro* [138]. In this thesis, I wanted to evaluate whether treatment with the novel DCN-1 small molecule inhibitors results in impaired monocyte mobility *in vitro*.
- Can the anti-inflammatory effects of MLN4924 on human and murine macrophages in the context of NF-κB signaling and M2-skewing, shown by Asare et al. [47], be recapitulated by employing the novel DCN1 inhibitors *in vitro*?
- Treatment with MLN4924 in atherogenic mice *in vivo* has previously been associated with a decrease in early atherosclerotic lesion size in the aorta and the aortic root [47]. To further the investigation *in vitro*, I wished to evaluate the effect of NAcM-OPT and NAcM-COV on mouse and human macrophage-derived foam cell formation.

3 Materials

3.1 General laboratory equipment

Table 1: List of general laboratory equipment

Equipment	Manufacturer
Biometra TRIO PCR Thermocycler	Analytik Jena AG (Jena, Germany)
Bosch Economic Super Freezer	Bosch (Gerlingen, Germany)
Centrifuge Heraeus Fresco17	Thermo Fisher Scientific (Dreieich, Germany)
Centrifuge Heraeus Megafuge 16R	Thermo Fisher Scientific (Dreieich, Germany)
DMi8 Fluorescent Microscope	Leica Microsystems GmbH (Wetzlar, Germany)
DMIL LED Microscope	Leica Microsystems GmbH (Wetzlar, Germany)
Elmasonic S40	Elma Electronics AG (Dreieich, Germany)
EnSpire Plate Reader	Perkin Elmer (Walham, USA)
FACSVerse™ Flow Cytometer	BD Bioscience (Franklin Lakes, USA)
Fisherbrand™ Mini Vortex Mixer	Thermo Fisher Scientific (Dreieich, Germany)
Heracell™ VIOS 160i CO2 Incubator	Thermo Fisher Scientific (Dreieich, Germany)
Incubation Water Bath	GFL (Burgwedel, Germany)
Liebherr Premium Fridge	Liebherr (Bulle, Switzerland)
Microbiological Safety Cabinet class II	Kojair (Tampere, Finland)
Mini Blot Modul	Life Technologies (Carlsbad, USA)
Mini Gel Tank	Life Technologies (Carlsbad, USA)
Nanodrop™ ONE	Thermo Fisher Scientific (Dreieich, Germany)
Odyssey Fc Imaging System	LI-COR (Lincoln, USA)
Power Supply EV3020	Consort bvba (Turnhout, Belgium)
QuadroMACS Separator	Miltenyi Biotec (Bergisch-Gladbach, Germany)
Real-Time PCR machine Rotorgene Q	Qiagen (Hilden, Germany)
Rocker RK-2D	Witeg (Wertheim am Main, Germany)
Roller Mixer SRT6D	Stuart Equipment (New Bern, USA)
TC20TM-Automated Cell Counter	Biorad (Feldkirchen, Germany)
Thermo Shaker 7001200	4 more Labor (Harthausen, Germany)

3.2 Consumables

Table 2: List of consumables

Consumable	Manufacturer
12/ 24/ 96 well cell culture plates	Corning Incorporated (Berlin, Germany)
6.5mm Transwell with 5.0 µm pore polycarbonate membrane insert, sterile	Corning Incorporated (Berlin, Germany)
Cell counting slides	Biorad (Feldkirchen, Germany)
Cell scraper	Falcon® (USA)
Cell strainer (40 µm nylon)	Corning Incorporated (Berlin, Germany)
Empty gel cassettes, mini, 1.0 mm	Thermo Fisher Scientific (Dreieich, Germany)
FACS tubes	Corning Incorporated (Berlin, Germany)
Falcon tubes (15 ml/50 ml)	Corning Incorporated (Berlin, Germany)
Flasks 25 cm^2	Corning Incorporated (Berlin, Germany)
Flasks 75 cm^2	Thermo Fisher Scientific (Dreieich, Germany)
LS columns	Miltenyi Biotec (Bergisch-Gladbach, Germany)
PCR softtubes 0.2 ml	Biozym Scientific GmbH (Hessisch Oldendorf, Germany)
Reaction tubes (0.5 ml, 1.5 ml; 2 ml)	Carl Roth GmbH (Karlsruhe, Germany)

RotiPVDF membranes (0.45 µm)	Carl Roth GmbH (Karlsruhe, Germany)
Rotor-Gene strip tubes	Starlab (Brussels, Belgium)
Syringe 10 ml/30 µM (Omnifix Luer Solo)	Braun (Kronberg im Taunus, Germany)

3.3 Software

Table 3: List of software used

Software	**Company**
BioRender	BioRender.com (Toronto, Canada)
FIJI	[153, 154]
FlowJo version 10.2	Treestar (Ashland, USA)
GraphPad Prism 8.4.3	GraphPad Prism (La Jolla, USA)
Image Studio Ver. 5.2.	Image Studio (Salt Lake City, USA)
Leica Application Suite X (version 3.0.15878.1)	Leica Microsystems GmbH (Wetzlar, Germany)

3.4 Chemicals and reagents

Table 4: List of chemicals and reagents

Product	**Manufacturer**
30% acrylamide/bis solution 29:1	Biorad (Feldkirchen, Germany)
Annexin binding buffer (5x)	Thermo Fisher Scientific (Dreieich, Germany)
Annexin V, Alexa Fluor 488 conjugate	Thermo Fisher Scientific (Dreieich, Germany)
BODIPY™ 493/503	Invitrogen (Karlsruhe, Germany)
Bovine serum albumin (BSA)	Carl Roth GmbH (Karlsruhe, Germany)
Chloroform	Sigma-Aldrich (Taufkirchen, Germany)
Count Bright absolute counting beads	Thermo Fisher Scientific (Dreieich, Germany)
CozyHi™ prestained protein ladder	HighQu (Kraichtal, Germany)
Dimethylsulfoxide (DMSO)	Carl Roth GmbH (Karlsruhe, Germany)
Dithiothreitol (DTT)	Sigma-Aldrich (Taufkirchen, Germany)
DRAQ5™ 5 mM	BioLegend (San Diego, USA)
Ethanol	Merck (Darmstadt, Germany)
Ethylenediaminetetraacetic acid (EDTA)	AppliChem Panreac (Darmstadt, Germany)
Fetal calf serum (FCS)	Invitrogen (Karlsruhe, Germany)
GoTaq qPCR mastermix	Promega (Madison, Wisconsin, USA)
Isopropanol	Merck (Darmstadt, Germany)
Lipopolysaccharides from salmonella enterica serotype enteritidis	Sigma-Aldrich (Taufkirchen, Germany)
Mayers hematoxylin solution	Sigma-Aldrich (Taufkirchen, Germany)
Methanol	Carl Roth GmbH (Karlsruhe, Germany)
MLN4924	Chemgood (Glen Allen, USA)
NAcM-OPT NAcM-COV NAcM-NEG	University Kentucky, College of Pharmacy (Kentucky, USA)
NuPage LDS sample buffer (4x)	Novex (Darmstadt, Germany)
NuPAGE transfer buffer (20x)	Novex (Darmstadt, Germany)
Oil Red O	Sigma-Aldrich (Taufkirchen, Germany)
oxLDL	Invitrogen (Karlsruhe, Germany)
oxLDL from human plasma	Thermo Fisher Scientific (Dreieich, Germany)

Penicillin-streptomycin (Pen-Strep)	Gibco Life Technologies (Darmstadt, Germany)
Phosphate-buffered saline (PBS)	Invitrogen (Karlsruhe, Germany)
PhosStop	Roche (Basel, Switzerland)
Propandiol	Carl Roth GmbH (Karlsruhe, Germany)
Propodium iodide solution (PI)	Sigma-Aldrich (Taufkirchen, Germany)
Recombinant human M-CSF	PeproTech (Hamburg, Germany)
Recombinant human SDF-1α (CXCL12)	Peprotech (Hamburg, Germany)
RPMI medium	Invitrogen (Karlsruhe, Germany)
SuperSignal™ West Femto substrate	Thermo Fisher Scientific (Dreieich, Germany)
Tetramethylethylendiamin (TEMED)	Biorad (Feldkirchen, Germany)
TNF-α (human)	PeproTech (Hamburg, Germany)
TNF-α (murine)	PeproTech (Hamburg, Germany)
Tris	Carl Roth GmbH (Karlsruhe, Germany)
TRIzol™ Reagent	Thermo Fisher Scientific (Dreieich, Germany)
Trypan Blue	Biorad (Feldkirchen, Germany)
Tween20	Biorad (Feldkirchen, Germany)

3.5 Media, buffers, and solutions

Table 5: List of media, buffers, and solutions

Description	**Composition**
General buffers	
MACS buffer	1X PBS 0.5% BSA 2 mM EDTA
Phosphate-buffered saline (PBS)	137 mM NaCl 2.7 mM KCl 1.5 mM KH_2HPO_4 8.1 mM Na_2HPO_4 in ddH_2O
RPMI media for culture	RPMI-media 10% FCS 1% Pen-Strep
TBS-T	1XTBS 0.1% Tween™-20
Tris-buffered saline (TBS)	20 mM Tris-HCl 150 mM NaCl in ddH_2O
Western Blot	
Blocking buffer	5% BSA in TBS-T
LDS-DTT	1 ml 4x NuPage LDS 500 µl 1 M DTT 2.5 ml ddH_20
Resolving gel (11%)	13.2 ml 30% acrylamid/bis-solution 15 ml Tris-HCL 1 M pH 8.8 7.5 ml ddH_2O 360 µl 10% SDS 120 µl 10% APS 36 µl TEMED
Resolving gel (7.5%)	10 ml 30% acrylamid/bis-solution 10 ml Tris-HCL 1 M pH 8.8 19 ml ddH_2O

	400 µl 10% SDS 200 µl 10% APS 30 µl TEMED
Running buffer (5x)	15.14 g Tris 72.05 g glycine 50 ml 10% SDS 950 ml ddH_2O
Stacking gel (4%)	2 ml 30% acrylamid/bis-solution 1.5 ml Tris-HCl 1 M pH 6.8 7.8 ml ddH_2O 120 µl 10% SDS 60 µl 10% APS 18 µl TEMED
ELISA	
Blocking buffer	2% BSA in PBS
Stop solution	2 M H2SO4 in ddH2O
Wash buffer	1XPBS 0.05% Tween™-20

3.6 qPCR-primers

Table 6: List of qPCR-primers

Description	**Sequence**
human	
ARG1	5'- CAA GGT GGC AGA AGT CAA GA -3' 5'- GCTTCC AAT TGC CAA ACT GT -3'
CCL2	5'- AGT CTC TGC CGC CCT TCT -3' 5' GTG ACT GGG GCA TTG ATT G -3'
CCL22	5'- CCC CTG ACC CCT CTA ACC -3' 5'- GGG AAC AGG ACC CTC TGA CT -3'
RPLP0	5'- GGC ACC ATT GAA ATC CTG AG -3' 5'- GAC CAG CCC AAA GGA GAA G- 3'
IL-10	5'- GCA ACC CAG GTA ACC CTT AAA -3' 5'- ATG AAG GAT CAG CTG GAC AAC- 3'
INOS	5'- CAA CGT GGA ATT CAC TCA GC -3' 5' ATC GAA GCG GCC GTA CTT -3'
TNF-α	5'- AGC CCA TGT TGT AGC AAA CC- 3' 5'- TCT CAG CTC CAC GCC ATT -3'
murine	
Abca1	5'- AGC ATG CCA GCC CTT GTT AT -3' 5'- AGT TTC GGT ATG GCG GGT TT -3'
Abcg1	5'- GGT GCC AAA GAA ACG GGT TC -3' 5'- ACC TAC CAC AAC CCA GCA GAC TTT -3'
Arg1	5'- TTT TTC CAG CAG ACC AGC TT -3'

	5’- AGA GAT TAT CGG AGC GCC TT -3’
Ccl2	5’- CAT CCA CGT GTT GGC TCA -3’ 5’- GAT CAT CTT GCT GGT GAA TGA GT -3’
Csn5	5’- CCA ATG CTC AGA TTT TGC AG -3’ 5’- TCA CCT CCG GTC TCA AGT G -3’
Csn8	5’- GCC AGT GTA CGG TCA GCT TC -3’ 5’- TTC CAC AGA TAT CTT GCA TTA TTC AT -3’
Fizz1	5’- CCC TCC ACT GTA ACG AAG ACT C -3’ 5’- CAC ACC CAG TAG CAG TCA TCC -3’
Il-1β	5’- TGG ATG CTC TCA TCA GGA CAG -3’ 5’- GAA ATG CCA CCT TTT GAC AGT G -3’
Il-6	5’- ATG GAT GCT ACC AAA CTG GAT -3’ 5’- TGA AGG ACT CTG GCT TTG TCT -3’
Il-10	5’- CAG AGC CAC ATG CTC CTA GA -3’ 5’- TGT CCA GCT GGT CCT TTG TT -3’
Il-12α	5‘-CAT GAT GAG CTG ATG CAG T -3’ 5‘-GCA GAG CTT CAT TTT CAC TCT GT -3’
Mrc1	5’- CCA CAG CAT TGA GGA GTT TG -3’ 5’- ACA GCT CAT CAT TTG GCT CA -3’
Rplp0	5’- ACT GGR CTA GGA CCC GAG APG -3’ 5’- CTC CCA CCT TGT CTC CAG TC -3’
Tgm2	5’- GAG AGC AAC AAG AGC GAG ATG -3’ 5’- TGT AGG TCT GGC CTG GTC AT -3’
Tnf-α	5’- CAT CTT CTC AAA ATT CGA GTG ACA A -3’ 5’- TGG GAG TAG ACA AGG TAC AAC CC -3‘
Ym1	5’- GGT CTG AAA GAC AAG AAC ACT GAG -3’ 5’- GAG ACC ATG GCA CTG AAC G -3’

3.7 Antibodies

The following antibodies were used for Western Blot.

Table 7: List of antibodies used for Western Blot

Antibody	Host	Manufacturer
Primary		
β-actin	mouse	MP Biologicals (Santa Ana, USA)
α-tubulin	mouse	Santa Cruz (Dallas, USA)
Caspase-3	rabbit	Cell Signaling (Danvers, USA)
Cleaved caspase-3	rabbit	Cell Signaling (Danvers, USA)
Cullin1 (71-8700)	rabbit	Invitrogen (Karlsruhe, Germany)
Cullin3 (PA5-17397)	rabbit	Invitrogen (Karlsruhe, Germany)
Secondary		
Goat anti-mouse IgG H&L (HRP)	goat	Abcam (Cambridge, UK)
Mouse anti-rabbit IgG (HRP)	mouse	Jackson Immuno Research (West Grove, USA)

3.8 Kits

Table 8: List of commercial kits

Kit	Manufacturer
Cell counting kit 8 (CCK8)	Sigma-Aldrich (Taufkirchen, Germany)
First Strand cDNA synthesis kit	Thermo Scientific (Dreieich, Germany)
Human pan monocyte isolation kit	Miltenyi Biotec (Bergisch-Gladbach, Germany)
Mouse Il-1 beta uncoated ELISA	R&D Systems (Minneapolis, USA)

3.9 Mice

Table 9: List of mice lines

Genotype	Origin
Apoe$^{-/-}$	Charles River Laboratories and own breeding at the Center for Stroke and Dementia Research

3.10 Cell Lines

Table 10: List of cell lines

Cell Line	Origin
Mono Mac 6 (MM6)	Acute monocytic leukemia-derived cell line 155

4 Methods

4.1 Cell culture

Cell culture was performed in a laminar flow hood under sterile conditions. The cells were cultured at 37°C in a humidified 5% CO2 atmosphere. For cell counting, a TC20TM Automated Cell Counter (Biorad) was used according to the manufacturer's instructions. To determine the number of viable cells, equal amounts of the cell suspension in media and filtered Trypan Blue were applied to the counting slides.

4.1.1 Monocyte isolation

Primary human monocytes were isolated from Peripheral Blood Mononuclear Cells (PBMCs) using a human pan monocyte isolation kit (Miltenyi Biotec).

The cells were centrifuged and resuspended in MACS buffer (40 µl per 10^7 cells). A blocking reagent (10 µl per 10^7 cells) and biotin-antibody cocktail (10 µl per 10^7 cells) were added, followed by incubation of the cell suspension at 4°C for 20 min. After that, MACS buffer (30 µl per 10^7 cells) and anti-biotin microbeads (20 µl per 10^7 cells) were added, and the mixture was put at 4°C for 30 min. After that, another 500 µl of MACS buffer per 10^7 cells was added.

Magnetic cell separation was carried out using LS columns (Miltenyi Biotec). The columns were positioned in the magnetic field of a MACS separator and primed by rinsing them with 3 ml of MACS buffer. After that, the cell suspension was added to the columns and washed with 3x3 ml of MACS buffer. The flow-through was collected and centrifuged (300 x g, 5 min). The cell pellet was resuspended in RPMI-media containing 10% FCS and 1% pen/strep, and the cells were used for the following experiments.

4.1.2 Macrophage derivation from PBMCs

PBMCs were obtained from healthy, anonymous donors. The cells were cultured in RPMI-media containing 10% FCS, 1% Pen/Strep, and M-CSF (100 ng/ml). Half of the media was replaced with fresh media every other day to guarantee stable levels of fresh M-CSF. After seven days, the macrophages were adherent and could be used for the following experiments.

4.1.3 Bone marrow-derived macrophage- obtainment

Bone marrow-derived macrophages (BMDMs) were generated from *Apoe*$^{-/-}$ mice. The tibia and femur were flushed with cold PBS. The extracted bone marrow was homogenized in cold PBS by repeated pipetting and filtered through a 40 µm cell strainer. This cell suspension was centrifuged (300 x g, 5 min), and the resulting pellet was resuspended in RPMI-media containing 10% FCS, 1% Pen-Strep and 12% L929-supernatant. L929 is a fibroblast cell line which stems from a clone of subcutaneous adipose and areolar tissue of a male C3H/An mouse [156]. These cells were found to secrete M-CSF, and using L929

supernatant instead of recombinant M-CSF is known to result in considerably higher numbers of differentiated macrophages [156]. The L929 was kindly provided to us by Dichgans Lab (ISD, Munich, Germany).

The cells were planted in uncoated culture dishes (12 or 96 wells). After three days, another 5% of L929 supernatant were added. After five days, the cells were differentiated to macrophages and could be used for the following experiments.

4.1.4 Treatments

Cells were treated with 10 µM of NAcM-COV, NAcM-OPT, or NAcM-NEG, a negative isotype control, for 16 h. The inhibitors were kindly provided by Dr. Jared T Hammill et al. For controls, the cells were treated with 0.1% DMSO in RPMI media containing 10% FCS and 1% Pen/Strep as vehicle control. Treatment with 1 µM of MLN4924 was used as a positive control. If simulation of inflammatory conditions was indicated, the cells were incubated with 20 ng/ml of TNF-α or 100 ng/ml of LPS for 6 h after inhibitor treatment.

4.1.5 Foam cell assay

To simulate foam cell formation, an oxLDL uptake assay was performed. Macrophages were washed with cold PBS and then “starved” in RPMI media containing 1% FCS and 1% Pen/Strep for 3 h. Afterwards, they were incubated with RPMI media containing 10% FCS, 1% Pen/Strep, and oxLDL (50 µg/ml) for 48 h.

For the analysis and quantification of the lipid uptake, the cells were stained with Oil Red O or BODIPY (see chapter 4.8).

4.2 CCK8 viability assay

5.000 PBMC-derived macrophages each were plated in a 96-well plate and treated for 16 h with a vehicle control (0.1% DMSO) or DCN1 inhibitors (10 µM) diluted in RPMI media containing 10% FCS and 1% Pen/Strep.

After that, 10 µl of unthawed CCK8 was added to each well, and the plate was incubated for 3 h at 37°C. The absorbance was measured using a microplate reader, and a calibration curve was done using cells that had not been incubated with any toxicant.

4.3 Annexin/PI staining

Monocytes (MM6 or primary human monocytes) were centrifuged (300 x g, 5 min) and resuspended in Annexin binding buffer (100 µl per 10^6 cells) and Annexin V-FITC (2 µl per 10^6 cells). After 10 min incubation in the dark, binding buffer (400 µl per 10^6 cells) and PI (10 µl per 10^6 cells) were added. The samples were analyzed via FACS shortly after adding the PI to prevent its toxicity.

4.4 Chemotaxis assay

The migration assay was performed using Transwell cell culture plate inserts for 24-well plates with a pore size of 5 µm (Corning Incorporated).
500.000 viable, pre-treated cells (MM6 or primary human monocytes) diluted in 100 µl of RPMI-media containing 10% FCS and 1% Pen/Strep were suspended in the upper chamber. 100 ng/ml of CXC-Motif-Chemokin 12 (CXCL12) diluted in 600 µl of media was used as a chemo-attractant in the lower chamber. After a migration period of 6-8 h, cell numbers were analyzed via FACS using Count Bright Absolute Counting Beads (Thermo Fisher Scientific).

4.5 Western blot

The cells were washed with cold PBS, and total cell lysates were prepared by lysis in LDS-DTT buffer containing phosphatase inhibitors (PhosSTOP, Roche) where indicated. Before usage, the samples were boiled (95°C for 5 min), syringed, and sonicated to prevent clumps.

The immunoblots were performed according to standard protocols [157] using homemade Bis-Tris gels (7.5% and 11%) and running- buffers. The transfer buffer was purchased from Novex. Running was performed at 120V. The transfer was performed at 20V for 2 h with PVDF-membranes, which were first activated in methanol. After the transfer, the membranes were blocked in a filtered blocking buffer for 1 h at room temperature or overnight at 4°C.

Antibodies were diluted according to the manufacturer's recommendations in 1% BSA in TBS-T. The membranes were incubated with primary antibodies overnight at 4°C, then washed 3x15 min with TBS-T and incubated with secondary antibodies for 1 h at room temperature. Before imaging, the membranes were washed 3x15 min with TBS-T. The blots were developed using SuperSignal™ west Femto-substrate. Protein bands were obtained with a LI-COR Odyssey FC and visualized and quantified using Image Studio Version 5.2.

4.6 Quantitative real-time PCR assay

Quantitative real-time PCR assays (RT-qPCR) were used to analyze gene expression. After isolation of the ribonucleic acid (RNA) of BMDMs and PBMC-derived macrophages, reverse transcriptase (Thermo Fisher Scientific) was used to transcribe the RNA into complementary copy DNA (cDNA). This cDNA could then be quantified via the RT-qPCR reaction.

4.6.1 RNA isolation

After removing the media, 300 µl of TRIzol reagent (Thermo Fisher Scientific) was added directly to each well (~ 500.000 macrophages). TRIzol reagent (Thermo Fisher Scientific) was used per the manufacturer's protocol. A cell scraper was used to lyse and collect the cells. The samples were then stored at +4°C overnight and used further the next day. After incubation at room temperature for 5-10 min to allow complete dissociation of the

nucleoprotein complexes, 200 µl of chloroform per 1 ml of TRIzol reagent were added to the samples. After vortexing the samples, they were incubated for 3 min and centrifuged at 4°C at 12.000 x g for 15 min. The suspension had now separated into a lower red phenol-chloroform-phase, an interphase, and a transparent upper phase containing the RNA. The upper phase was transferred to a new tube to which 500 µl of isopropanol, and 1 ml TRIzol reagent were added. After incubating for 10 min, the samples were centrifuged at 4°C at 12.000 x g for 10 min. The supernatant was discarded, and the RNA pellet was resuspended in 1 ml of 75% ethanol/1 ml TRIzol reagent. After briefly vortexing, the samples were centrifuged at 4°C at 7.500 x g for 5 min. The supernatant was removed, and the pellets were air-dried in a sterile hood for 2 h. The RNA was dissolved in 25 µl RNase-free water containing 0.1 mM EDTA and incubated in a water bath at 55°C for 15 min. The RNA was stored short-term at -20°C.

4.6.2 cDNA synthesis

For cDNA synthesis, First Strand cDNA synthesis kit (Thermo Fisher Scientific) was used as suggested in the manufacturer´s protocol. The following reaction mix was used for each reaction containing 0.2 µg of isolated RNA:

5x RT-buffer	4 µl
dNTPs	2 µl
RiboLock RNAse Inhibitor	1 µl
OligoDTs	1 µl
RTase	2 µl

For the reverse transcription reaction, a thermocycler (Analytik Jena AG) was used. Three incubation steps were performed: 1 h at 37°C, 5 min at 70°C, and cooling down and short-term storage at 4°C.

4.6.3 RT- qPCR

A GoTaq qPCR mastermix (Promega) containing SYBR-Green was used for the RT-qPCR. This fluorescent dye of SYBR-GREEN preferentially binds to double-stranded DNA and, therefore, allows quantifying the increase of DNA product during each PCR- cycle. The following scheme was used for each reaction:

RT-qPCR mix:	
GoTaq qPCR mastermix	5 µl
cDNA	2.5 µl
Primer forward	1.25 µl
Primer backward	1.25 µl
RT-qPCR instrument settings:	
Initial denaturation	1 cycle: 95°C- 2 min
Denaturation	40 cycles: 95°C- 5 s
Annealing/extension	40 cycles 60°C- 30 s

4.6.4 Calculation of relative mRNA levels

GAPDH or RPLP0 were used as housekeeping genes to calculate relative mRNA levels. Ct values are defined as the cycle number at which the measured fluorescence exceeds a specific threshold set in the exponential region of amplification. For relative mRNA expression levels, the following calculation was used:

The Ct value of the target gene is normalized to the Ct value of the housekeeping gene.
Ct (target) - Ct (housekeeping)= ∆Ct (sample)

∆Ct (sample) is then normalized to the ΔCT-value of a control:
∆Ct - ∆Ct (control)= ∆∆Ct

Subsequently, the relative mRNA expression in a sample is calculated as:
$2^{(-\Delta\Delta Ct)}$

4.7 ELISA

To determine murine Il-1β protein levels in cell supernatant, an enzyme-linked immunosorbent assay (ELISA) (R&D Systems) was used as described in the manufacturer's instructions. First, at room temperature, a 96-well plate was coated with capture antibody in a coating buffer for 16 h. The plates were washed with wash buffer three times afterward, blocked with blocking solution for 1 h at room temperature, and washed three times. A standard titration was prepared (1000 pg/ml to 15.6 pg/ml). 100 µl/well of standard titration or supernatant was added to each well, followed by incubation for 2 h at room temperature. After washing three times, the detection antibody solution was added to the wells and incubated at room temperature for 2 h. After washing three times, 100 µL/well of diluted streptavidin-horseradish-peroxidase was added to each well and incubated in the dark for 20 min at room temperature. After five washes, 100 µL/well of Substrate Solution was added and incubated in the dark for 20 min at room temperature. The reaction was then stopped using 50 µl of Stop Solution. The optical density was measured at 450 nm with wavelength correction at 570 nm using an EnSpire microplate reader (Perkin Elmer).

4.8 Immunocytochemistry and stainings

4.8.1 Oil Red O staining

After incubation with oxLDL for 48 h, the macrophages were washed with PBS and fixed with 4% PFA for 10 min at 4°C. After rehydrating the cells with PBS for 1 min, they were rinsed with 70% propanediole in PBS for 15 s. The staining was performed with filtered Oil-Red-O solution (0.5% in propylene glycol) at 37°C for 1 h. After that, the cells were rinsed with 70% Propanediol in PBS for 15 s and PBS 3x3 min. A counterstaining was performed, incubating with Mayer´s hematoxylin solution for 4 min at room temperature and rinsing with ddH_2O before

and after the staining. The images were obtained with a Dmi8 Fluorescent Microscope (Leica) in 20x and 40x with LAS X (Leica) and analyzed using FIJI [153, 154].

4.8.2 BODIPY- staining

The cells were rinsed with PBS and fixed in 4% PFA for 30 min at +4°C. After this, they were stained with BODIPY (2 µM) and DRAQ5™ fluorescent probe solution (1:1000) in the dark for 30 min at 4°C. After removing the staining solution, the cells were rinsed with PBS and imaged as soon as possible. The images were obtained using a Dmi8 fluorescent microscope (Leica) in 20x and 40x with LAS X and analyzed using FIJI [153, 154].

4.9 Statistics

Statistical analyses were performed using GraphPad Prism 8.4.3 (*GraphPad Software Inc.*). Data are represented as means ± SD. The results were analyzed using one-way ANOVA with Dunnett multiple comparisons test. Significance levels were marked according to the APA scheme (*p<0.05, **p<0.01, ***p<0.001, n.s.= not significant). N represents the number of biological replicates (mice, patients, or experimental biological repeats).

5 Results

This thesis aimed to analyze the effects of the novel DCN1 inhibitors in the context of atherosclerosis *in vitro*. To do so, first, the impact of NAcM-OPT and NAcM-COV on monocyte mobility and viability was established. Since monocytes are key players in the progression of atherosclerosis and studies have suggested that NEDDylation patterns can impact actin dynamics [138] and MLN4924 sensitizes monocytes for cell death [149], monocytes appeared to be a promising target to study the effects of the DCN1 inhibitors on atherogenesis. Secondly, the DCN1 inhibitors' impact on macrophages in the context of NF-κB signaling and M2 skewing compared to the already well-studied atheroprotective effects of MLN4924 on monocytes [47, 136] was investigated. As the DCN1 compounds have been designed as more specific alternatives to MLN4924, I sought to determine whether these inhibitors can mirror the effects of MLN4924 in this setting. Finally, the impact of the NAcM compounds on foam cell formation *in vitro* was checked, as it is known that ABCA1-degradation is dependent on CUL3-NEDDylation [150].

5.1 NAcM-COV but not NAcM-OPT impacts monocyte viability and mobility *in vitro*

5.1.1 NAcM-OPT and NAcM-COV impact CUL1- and CUL3-NEDDylation in monocyte cell models

NAcM-OPT and NAcM-COV have not been used in clinical trials or extensive studies yet, so the effects of the inhibitors have only been tested in certain cell types so far. Scott et al., for example, used non-small-cell lung and tongue carcinoma cell lines (HCC95) and CAL-33 to study the novel DCN1 inhibitors, as these cell lines provided high levels of endogenous DCN1 [4]. In that setup, the NAcM compounds primarily affected NEDDylation levels of CUL1 and CUL3 and had less pronounced effects on CUL4A.

To establish the effects of the novel DCN1 inhibitors on cell types relevant to atherogenesis, first, immunoblots of NEDDylation levels of CUL1 and CUL3 after 16 h inhibitor treatment at a dose of 10 µM were performed. Primary human monocytes obtained from voluntary healthy donors were used to analyze the impact of NAcM-OPT and NAcM-COV in monocytes. As these primary cells are sensitive to external influences and the results can be donor-dependent, MM6 monocytes were employed in certain setups.

In MM6, CUL1-NEDDylation was downregulated significantly after treatments with both NAcM-OPT and NAcM-COV **(Figure 6 C)**. Likewise, CUL3-NEDDylation was impacted as well. However, compared to MLN4924, the DCN1 inhibitors' impact on NEDDylation levels of CUL1 and CUL3 was less pronounced **(Figure 6 D)**.

In primary human monocytes, similar effects for NAcM-COV were found **(Figure 6 G-H)**. Cells treated with NAcM-OPT presented a slight trend towards reduced CUL-1 NEDDylation levels **(Figure 6 G)**. Still, there was no significant effect on CUL3-NEDDylation after treatment with the DCN1 inhibitors **(Figure 6 H)**.

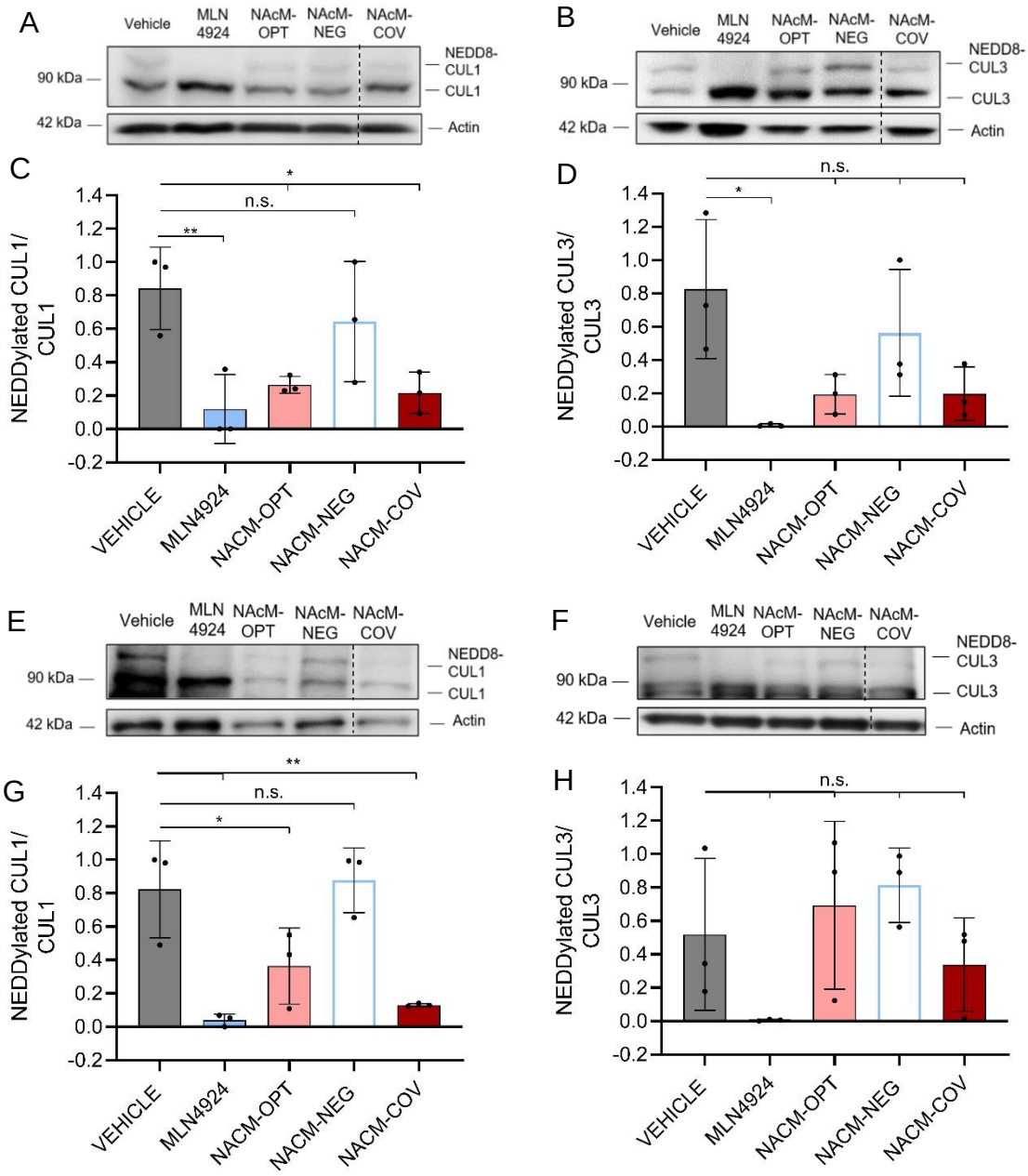

Figure 6. The DCN1 inhibitors downregulated NEDDylation levels of CUL1- and CUL3 in MM6 and primary human monocytes.Immunoblot quantification of NEDDylation levels of primary human monocytes and MM6 after 16 h of NAcM-NEG, -OPT, -COV (10 µM), and MLN4924 (1 µM) inhibitor treatments. **A-B:** Representative immunoblots of NEDDylated and non-NEDDylated CUL1-/CUL3-levels in MM6. **C-D:** Quantification of the NEDDylation levels of CUL1 and CUL3 in MM6 after small molecule inhibitor treatment or vehicle treatment (n=3 independent experiments). **E-F:** Representative immunoblots of NEDDylated and non-NEDDylated CUL1-/CUL3- levels in primary human monocytes. **G-H:** Quantification of immunoblots raised against CUL1- and CUL3-NEDDylation in primary human monocytes (n=3 biological replicates). Mean pixel intensities (mpi) were normalized to mpis of tubulin and calculated as ratios to the non-NEDDylated cullin mpis. Statistics: one-way ANOVA with Dunnett multiple comparisons test.

5.1.2 Monocyte mobility is downregulated by NAcM-COV but not by NAcM-OPT

Actin remodeling is a key player in immune functions connected to atherosclerosis, such as monocyte migration, cell differentiation, proliferation, and intra- and extracellular signaling, resulting in innate and adaptive immune responses [158]. This dynamic process of the rearrangement of cell phenotypes is only possible due to a rapid assembly and disassembly of filamentous actin [158, 159]. One of the main proteins regulating dynamic actin remodeling is cofilin. Cofilin attaching to actin filaments changes the subunits' orientation, leading to filament severing at low cofilin-to-actin ratios and filament stabilization at high cofilin-to-actin ratios [160, 161].

During the initiation and progression of atherosclerosis, monocytes undergo various changes in their phenotypes and rely on cellular outgrowth for movement and endocytosis [158, 162, 163]. Therefore, dynamic cytoskeleton reorganization is crucial for cellular integrity and functionality. Global inhibition of NEDDylation in developing neurons resulted in altered actin remodeling, cytoskeletal defects, and cellular growth impairments [138]. In a 2020 study, Vogl et al. indicated this might be due to lysine 112 of cofilin being a target for NEDDylation [138]. Additionally, Bhattacharya et al. have revealed that actomyosin rearrangement in monocyte-to-macrophage differentiation is driven by MAP-kinases [164], which have been proven to be regulated by the CSN [151].

Therefore, I hypothesized that the DCN1 inhibitors and MLN4924 affect actin remodeling in monocytes. As monocyte mobility depends on cellular outgrowth and, subsequently, dynamic actin remodeling, I chose to perform a migration assay towards the chemoattractant CXCL12 to compare the mobility of monocytes treated with small molecule inhibitors to those treated with vehicle controls.

After treatment of MM6 with NAcM-COV, a significant reduction of up to 10% less monocyte migration than in the vehicle control was observed. Likewise, treatment with MLN4924 resulted in about 20% less cell migration **(Figure 7 A)**. In primary human monocytes, NAcM-COV also impaired monocyte migration. Compared to vehicle controls, less than 70% of the monocytes migrated. Still, only the effect of MLN4924 was significant **(Figure 7 B)**. Interestingly, NAcM-OPT did not impact monocyte mobility in either MM6 or primary human monocytes **(Figure 7 A-B)**.

This data indicates that NAcM-COV but not NAcM-OPT affects monocyte mobility, which might be explained by an impact on actin remodeling. Still, alterations in NEDDylation and actin remodeling might also impair monocyte viability or fitness. Thus, I next sought to study these.

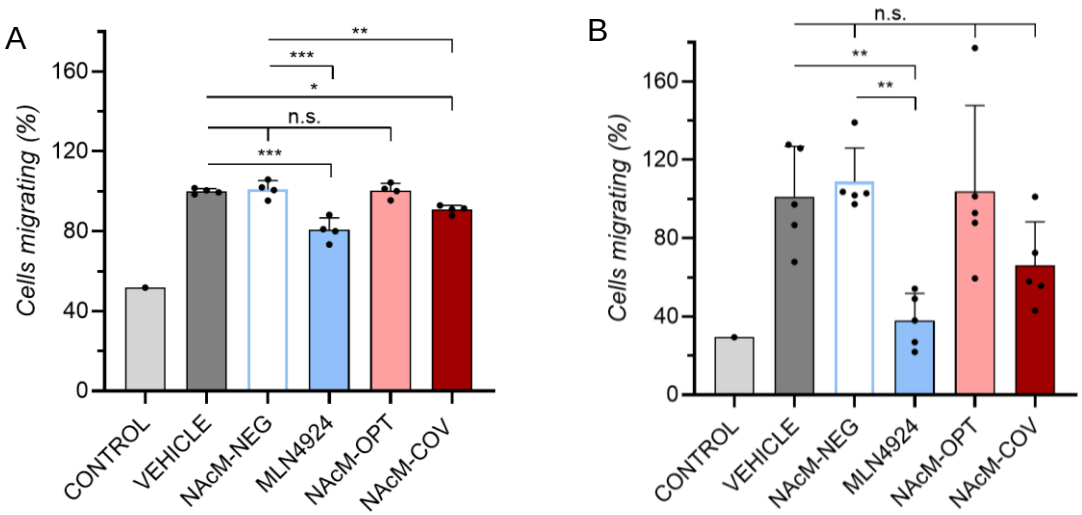

Figure 7. NAcM-COV but not NAcM-OPT significantly downregulated MM6 migration towards CXCL12. Chemotactic assay of **A:** MM6 (n=4 independent experiments, control without chemoattractant: n=1) and **B:** primary human monocytes (n=5 independent biological replicates, control without chemoattractant: n=1) after 16 h inhibitor treatment (NAcM-NEG, -OPT, -COV: 10 µM, MLN4924: 1 µM) towards CXCL12 or a random migration control (no added migration stimulus) for a migration period of 6-8 h. All values were normalized to vehicle controls. Statistics: one-way ANOVA with Dunnett multiple comparisons test.

5.1.3 NAcM-COV as well as MLN4924 impact primary human monocyte viability through both necrosis and apoptosis

By regulating the UPS, NEDDylation is strongly connected to cell homeostasis. Various studies describing how MLN4924 affects cell death in different cell types have been published with heterogeneous results. While MLN4924 was proven to sensitize cancer cells of different origins, such as endometrial carcinomas [165] and B-cell lymphomas [166] for apoptosis and/or necrosis [167], cullin-deNEDDylation appears to suppress necroptosis in cardiomyocytes [168]

As mentioned in chapter 1.2.5, El-Mesery et al. suggest that MLN4924 can sensitize monocytes for TNF-α-dependent and -independent necroptosis [149]. Furthermore, due to its impact on cytoskeletal integrity, the regulation of cofilin is connected to apoptotic cell death mechanisms [169].

As a decrease of cellular mobility towards the chemoattractant CXCL12 after inhibitor treatment was previously observed, I next sought to determine whether a loss of cellular integrity might also result in higher sensitivities towards cell death. Initially, cleaved caspase-3 protein analyses in MM6 and primary human monocytes were performed as first scouting experiments to determine whether the monocytes were sensitized towards apoptosis **(Figure A 1)**. As described in chapter 1.1.5, apoptotic cell death is prompted by the activation of various caspases, such as caspase-3. These enzymes are present as inactive zymogens and undergo autolytic cleavage upon stimulation to become active proteases. Subsequently, their cleaved fragments can be detected using specific antibodies, therefore allowing apoptosis

quantification [170]. In this experimental setup, there was a tendency towards elevated cleaved caspase-3 levels in MM6 and primary human monocytes treated with NAcM-OPT and NAcM-COV. Still, no significance was given. As this trend was also seen in NAcM-NEG, the increase of cleaved caspase-3 might be explained by external and experimental influences.

To further evaluate how small molecule inhibitor treatments alter monocyte cell death patterns, I next analyzed the percentage of viable cells as well as cells in necrosis and early and late apoptosis per cell population in an Annexin V-FITC/PI cell death assay (for exemplary gating see **Figure A 2**).

In MM6, MLN4924, in contrast to the DCN1 inhibitors, caused impaired cell viabilities *in vitro* **(Figure 8 A)**. Furthermore, the fraction of MM6 in early and late apoptosis significantly increased after MLN4924 treatments. In cells treated with NAcM-OPT and -COV, there was a trend towards a slight increase of cells in late apoptosis, but no significance was displayed **(Figure 8 C-D)**. Furthermore, treatment with the DCN1 inhibitors did not increase the percentage of MM6 in necrotic cell death. Surprisingly, MLN4924 significantly decreased the number of necrotic cells compared to vehicle controls from over 3% to 1.6% in MM6 **(Figure 8 B)**.

In primary human monocytes, *in vitro* treatment with NAcM-COV led to a significant reduction of viable cells and a significant increase of cells in necrosis and late apoptosis **(Figure 9 A, B, D)**. After 16 h of inhibitor treatments, the percentage of viable cells was reduced from 67% to 48% **(Figure 9 A)**. Likewise, the percentage of monocytes in late apoptosis increased from 3.4% in vehicle controls to 21% in the treated monocytes. These effects were similar to the impact of MLN4924 even though the effect of MLN4924 was more pronounced, reducing the number of viable cells to only 10.9% and increasing the percentage of monocytes in late apoptosis over 10-fold to 49% **(Figure 9 A, D)**. Interestingly, NAcM-OPT did not significantly decrease primary human monocyte viability **(Figure 9 A)**. Still, a trend towards an increase of cells in late apoptosis was also displayed here. Notably, in contrast to the effects of MM6, NAcM-COV, like MLN4924, significantly induced necrosis in primary human monocytes from 0.4% of the cell population in vehicle controls to 1.2% after NAcM-COV treatment and 4.2% in cells treated with MLN4924 **(Figure 9 B)**.
This data suggests that altering NEDDylation patterns *in vitro* impacts primary human monocyte viability by inducing necrosis and/or apoptosis.

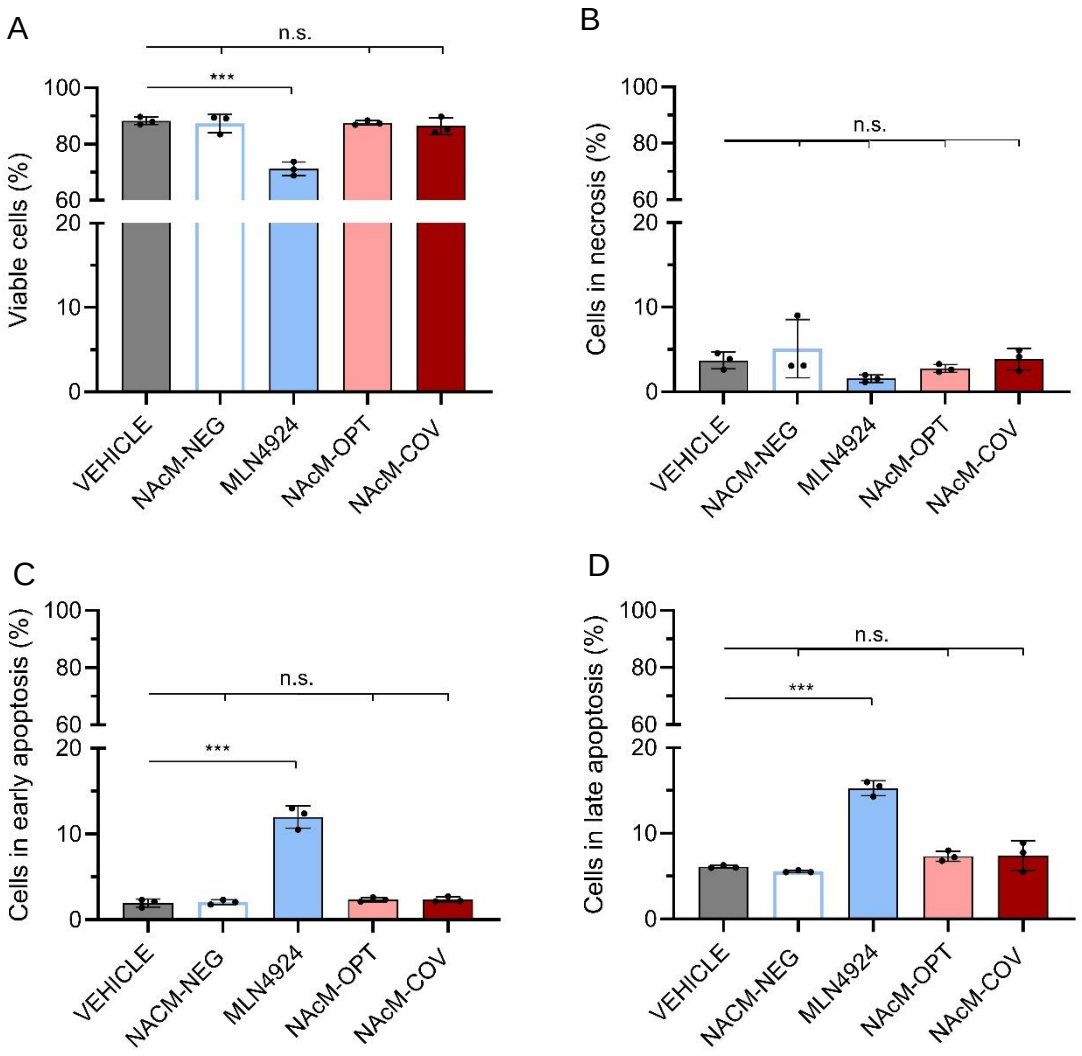

Figure 8 NAcM-OPT and NAcM-COV did not significantly impact MM6-viability *in vitro.* Annexin V-FITC/PI cell death assay of MM6 after 16 h inhibitor treatment (NAcM-NEG, -OPT, -COV: 10 µM, MLN4924: 1 µM). Percentages of viable cells, cells in necrosis, and cells in early and late apoptosis per cell population were analyzed **A:** Percentage of viable cells after inhibitor treatments **B:** Percentage of cells in necrosis after inhibitor treatments **C:** Percentage of cells in early apoptosis after inhibitor treatments **D:** Percentage of cells in late apoptosis after inhibitor treatments (n=3 independent experiments. Statistics: one-way ANOVA with Dunnett multiple comparisons test.

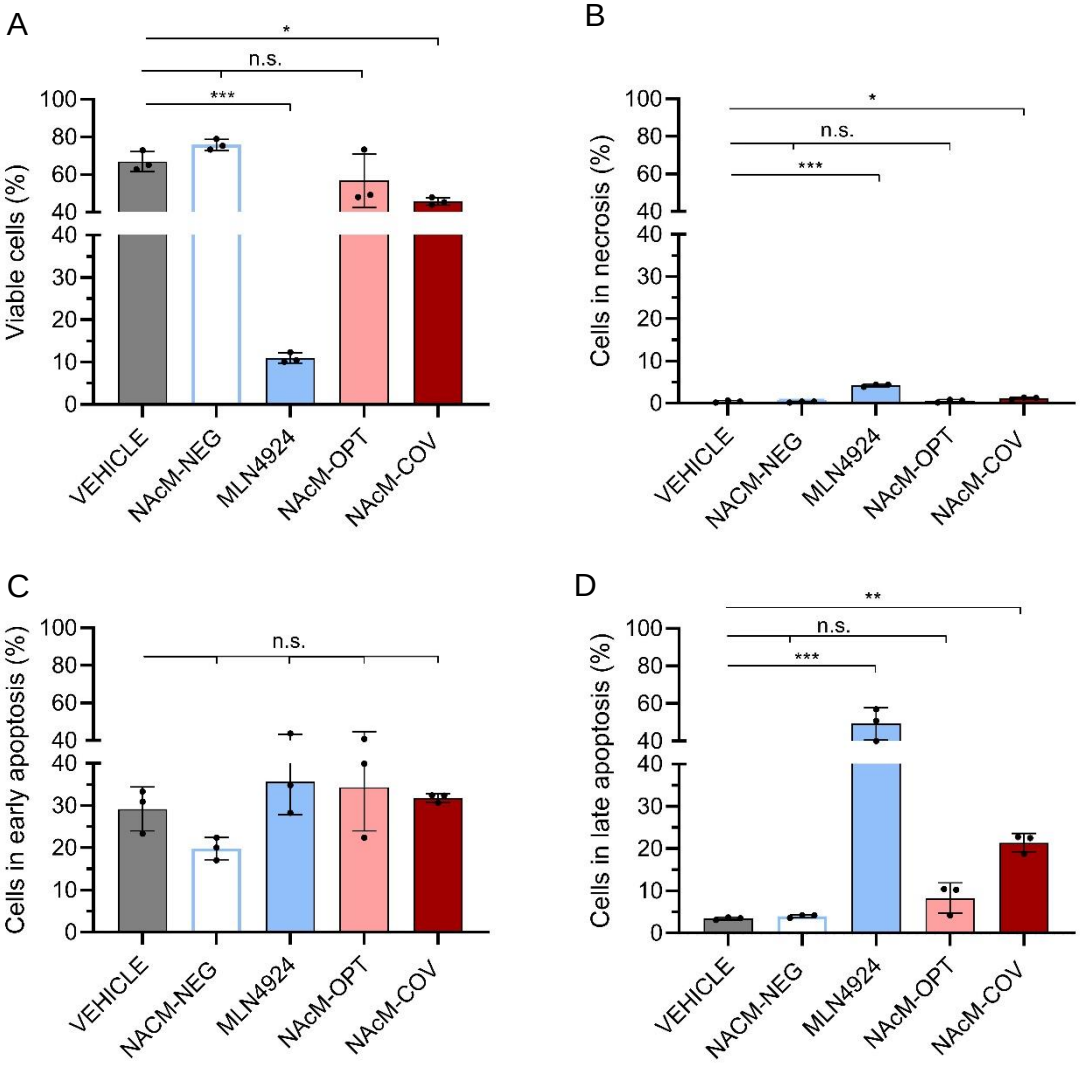

Figure 9 NAcM-COV caused both, apoptosis, and necrosis in primary human monocytes *in vitro.* Annexin V-FITC/PI- cell death assay of primary human monocytes after 16 h inhibitor treatments (NAcM-NEG/-OPT/-COV: 10 µM, MLN4924: 1 µM). Percentages of viable cells, cells in necrosis, and cells in early and late apoptosis per cell population were analyzed **A:** Percentage of viable cells after inhibitor treatments **B:** Percentage of cells in necrosis after inhibitor treatments **C:** Percentage of cells in early apoptosis after inhibitor treatments **D:** Percentage of cells in late apoptosis after inhibitor treatments (n=3 independent biological replicates). Statistics: one-way ANOVA with Dunnett multiple comparisons test.

5.1.4 NAcM-OPT and NAcM-COV impact primary human monocyte cell death patterns dose-dependently

As the previous experiments indicated that small molecule inhibitors might impact monocyte viability and cell death mechanisms, I hypothesized that these effects might depend on the degree of cullin-NEDDylation. Thus, I wanted to evaluate to which extent there is a dose- and time-dependent impact on the small molecule inhibitors' effects on cell death patterns *in vitro.* The inhibitors' impact in the default setup of a 16 h-incubation experiment and a drug dosage of 10 µM was more pronounced in primary human monocytes than in MM6. Additionally, primary cells might mirror the human system more realistically than cell lines. Therefore, primary human monocytes were also used in the following analyses.

In the dose-dependent assay, NAcM-NEG, a supposedly inactive control compound of similar structure, which does not alter NEDDylation levels in primary human monocytes, did not significantly impact cell death mechanisms **(Figure 10 A)**.
In cells treated with NAcM-OPT, cell viability was only significantly reduced from 90% to 58% at dosages as high as 30 µM. Interestingly, this high NAcM-OPT dosage caused a strong induction in necrosis from 2% to 36% within the cell population. In contrast, the fraction of cells in apoptosis was not significantly different from the vehicle controls. Still, it should be noted that compared to a dose of 1 µM, after treatment with 30 µM, there were significantly more monocytes in late apoptosis **(Figure 10 C)**.
Primary human monocytes treated with NAcM-COV significantly decreased in viability from 67% to 59% in the lowest dosage of 1 µM compared to vehicle control. The viability was similar at doses of 5 µM and 10 µM, around 60%. Notably, monocytes treated with 30 µM of NAcM-COV exhibited a strongly decreased viability of 13% of the cell population. They were, therefore, significantly less viable than the vehicle control and monocytes treated with lower doses **(Figure 10 D)**. Like NAcM-OPT, high-dosage treatment with NAcM-COV caused an increase in necrotic cell death. This effect was more substantial in NAcM-OPT, with 36% of the cell population being necrotic than in NAcM-COV, in which 7.8% of the monocyte population was necrotic in a dose of 30 µM **(Figure 10 C-D)**. Likewise, treatment with NAcM-COV also primarily resulted in apoptosis. Early apoptosis was induced in doses of 1 µM, 10 µM, and 30 µM, whereas the fraction of the cell population in late apoptosis increased in doses of 5 µM and 30 µM. Compared to the vehicle control, in a dosage of 30 µM, the number of monocytes in late apoptosis increased almost 10-fold from 5% of the monocyte population to 49% **(Figure 10 D)**. MLN4924, as a very potent drug, led to a significant reduction of viable cells in doses starting from 0.1 µM. In this concentration, the number of viable cells was reduced by more than 50%, from 67% to 31%. Notably, higher doses of up to 5 µM only reduced monocyte viability slightly more pronounced than the dosage of 0.1 µM. MLN4924 in

primary human monocytes primarily induced apoptotic cell death. Significantly more cells in late apoptosis were detected in doses of 0.1 µM and 1 µM. A trend towards upregulation of necrosis was notable **(Figure 10 B)**.

In conclusion, although these data, due to the time constraints of this thesis could so far only be acquired in n=3 technical replicates of one experiment with cells from one donor, the different small molecule inhibitors appear to trigger different cell death mechanisms dose-dependently. Treatment with very high doses of NAcM-OPT appeared to trigger necrotic cell death, whereas treatment with MLN4924 increased the percentage of cells in apoptosis. High doses of NAcM-COV significantly increased both percentages of cells in necrotic and apoptotic cell death. Thus, the increase of cells in apoptosis was more pronounced.

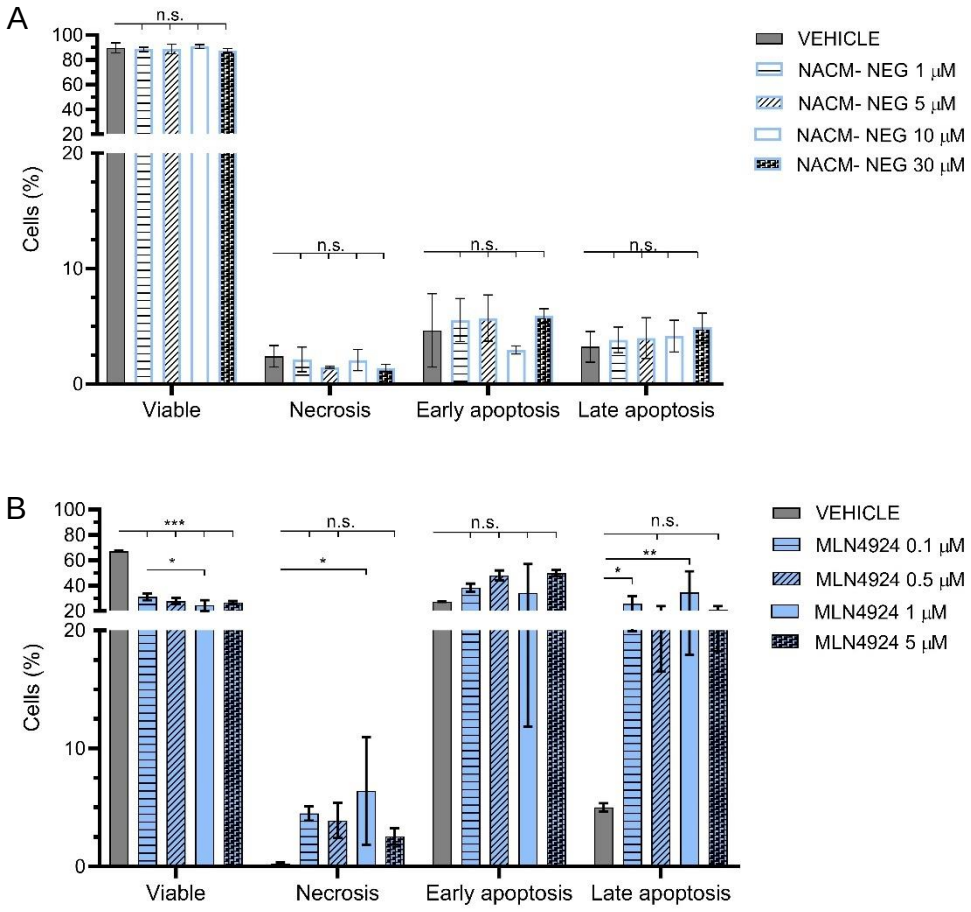

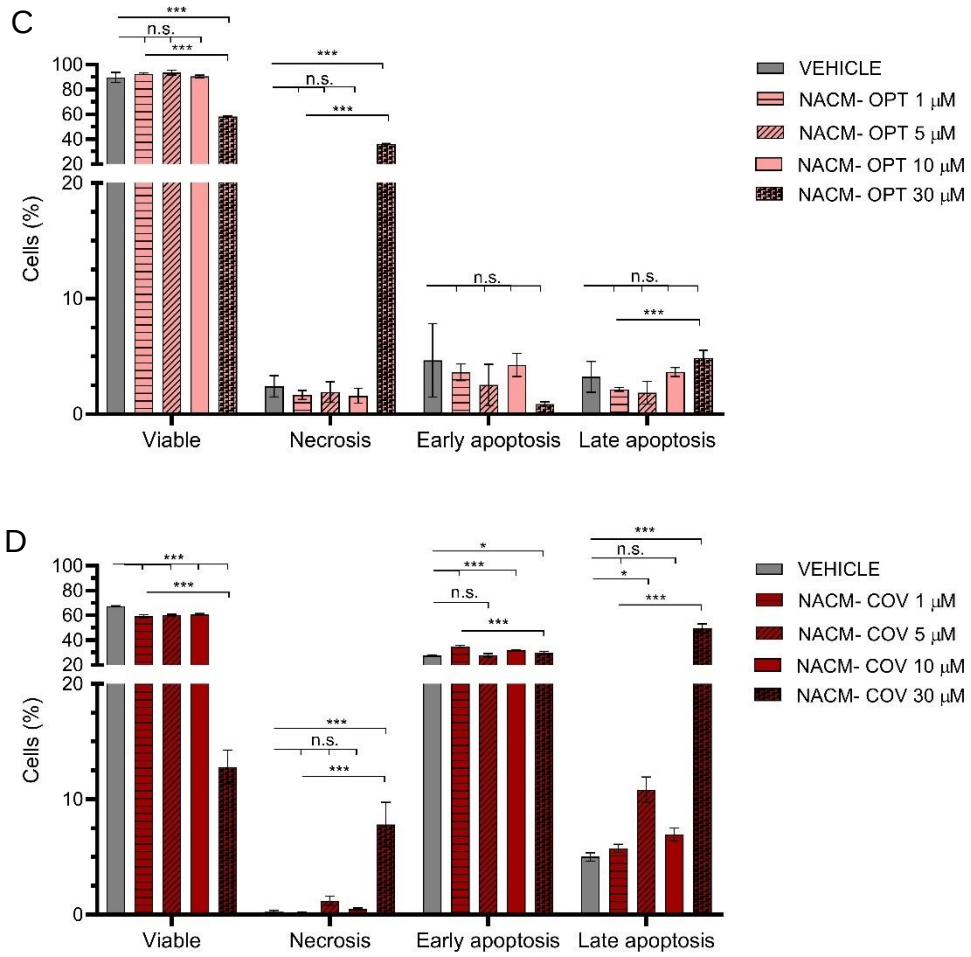

Figure 10 NacM-OPT and NAcM-COV induced different cell death mechanisms depending on the dosage. Annexin V-FITC/PI- cell death assay of primary human monocytes after 16 h inhibitor treatments in different doses. Percentages of viable cells, cells in necrosis, and cells in early and late apoptosis per cell population were analyzed. **A:** Dose-dependent assay of NAcM-NEG (1 µM, 5 µM, 10 µM, 30 µM) **B:** Dose-dependent assay of MLN4924 (0,1 µM, 0,5 µM, 1 µM, 5 µM) **C:** Dose-dependent assay of NAcM-OPT (1 µM, 5 µM, 10 µM, 30 µM) **D:** Dose-dependent assay of NAcM-COV (1 µM, 5 µM, 10 µM, 30 µM). Statistics: one-way ANOVA with Dunnett multiple comparisons test (n=3 technical replicates).

5.1.5 NAcM-OPT and NAcM-COV alter primary human monocyte viability time-dependently

In addition to analyzing the dose-dependent effects of the novel DCN1 inhibitors, time-dependent assays of the inhibitors in primary human monocytes were executed. Like the dose-dependent assay, the time-dependent assay was performed in primary human monocytes. Interestingly, significant time-dependent effects were noted in cells subjected to the vehicle control and the isotype control NAcM-NEG. As human monocytes physiologically only remain in the bloodstream for a duration of one to three days before differentiating further, cell death can occur physiologically without inhibitor treatment [171]. Thus, this should be considered in addition to the *in vitro* setting, when analyzing the following assay.

NAcM-OPT caused a steady, significant decrease of viable primary human monocytes after 4

h of treatment. After 4 h, 94% of the cell population was viable compared to 98% in the vehicle control **(Figure 11 A, D)**. After 16 h, 89% of the cell population treated with NAcM-COV was viable, whereas 97% of the cell population in the vehicle control was viable **(Figure 11 A, E)**. The results of this assay suggest that the primary type of cell death in the monocyte population treated with NAcM-OPT was apoptotic cell death, with a significant increase of early apoptosis in all time points and a significant increase of late apoptosis after 4 h, 16 h and 24 h inhibitor treatment **(Figure 11 D)**.

The effects of NAcM-COV appeared to be similar but more potent. Whereas after 4 h incubation, 95% of the monocyte population was viable, this significantly decreased to 84% after 8 h and 63% after 24 h, contrary to the percentage of viable cells in the vehicle control ranging around 97% in these time points. Like in NAcM-OPT, the primary type of cell death triggered by longer incubation times of NAcM-COV appeared to be early and late apoptosis. After 16 h, 22% of the cell population was in early apoptosis, and 11% was in late apoptosis, compared to 1.1% and 0.8% in the vehicle control group **(Figure 11 E)**. Still, also necrotic cell death was upregulated after 4 h and 24 h.

MLN4924 significantly reduced cell viabilities from 97% to 57% after 8 h of treatment. After 16 h and 24 h, about 45% of the cell population was still viable, which was less than half of the fraction of viable cells in the vehicle control group at these time points. Notably, the fraction of primary human monocytes in early apoptosis was significantly elevated after 8 h of MLN4924 treatment, whereas late apoptosis was only significantly enhanced after 16 h and 24 h of incubation. Interestingly, there was also a trend towards an elevated number of necrotic cells. Still, apoptosis also appeared to be the critical driver of cell death in this setup **(Figure 11 B)**.

This data indicates that similar to higher small molecule inhibitor doses, prolonged incubation of the NAcM compounds mainly triggers apoptotic cell death. Interestingly, in this time-dependent assay, the results of the small molecule inhibitors were in line with their degree of reduction of NEDDylation, with MLN4924 impacting cell viabilities the most pronounced, followed by NAcM-COV.

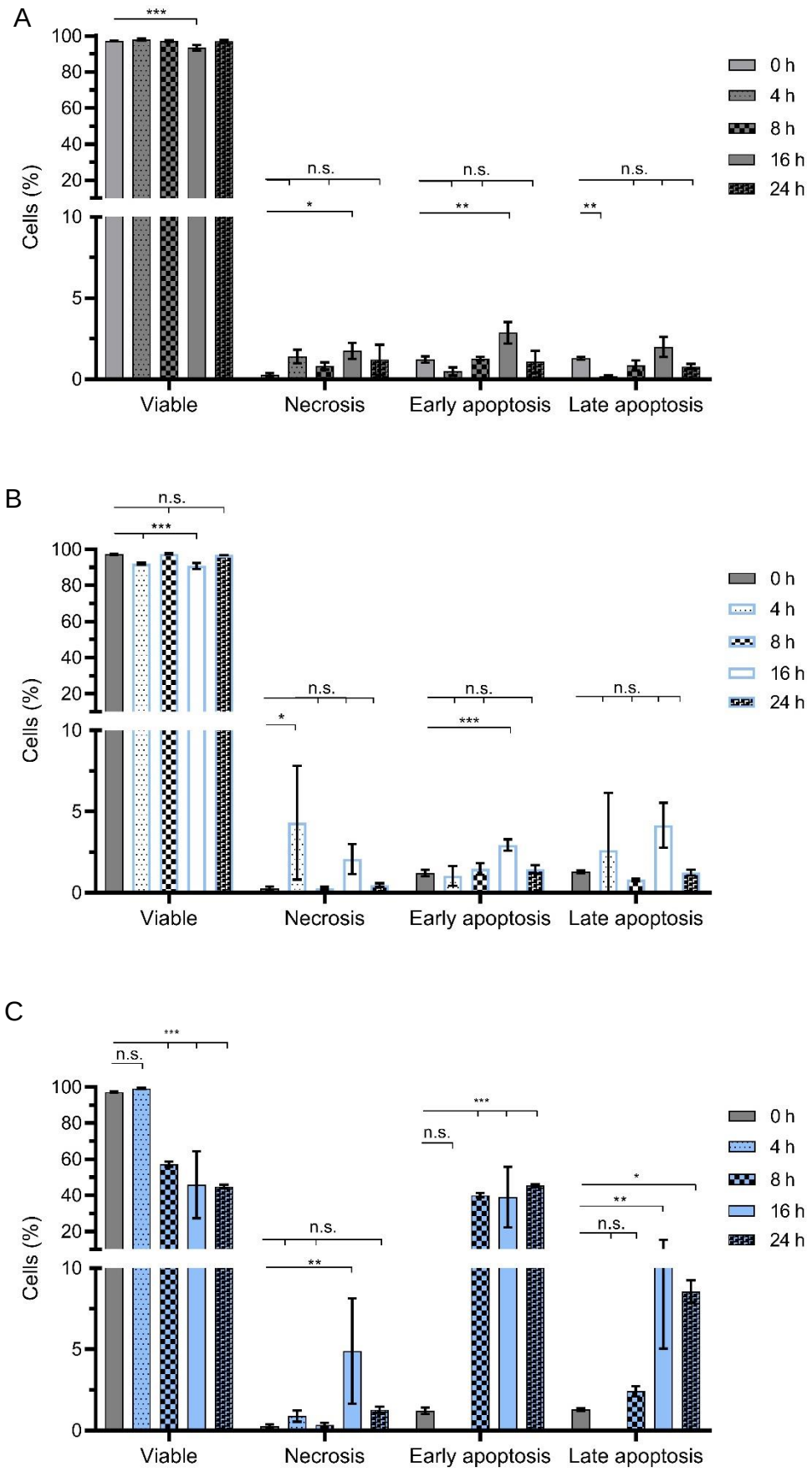
A
B
C
Cells (%)
100
80
60
40
20
10
5
0
0 h
4 h
8 h
16 h
24 h
Viable
Necrosis
Early apoptosis
Late apoptosis
n.s.
*
**
***

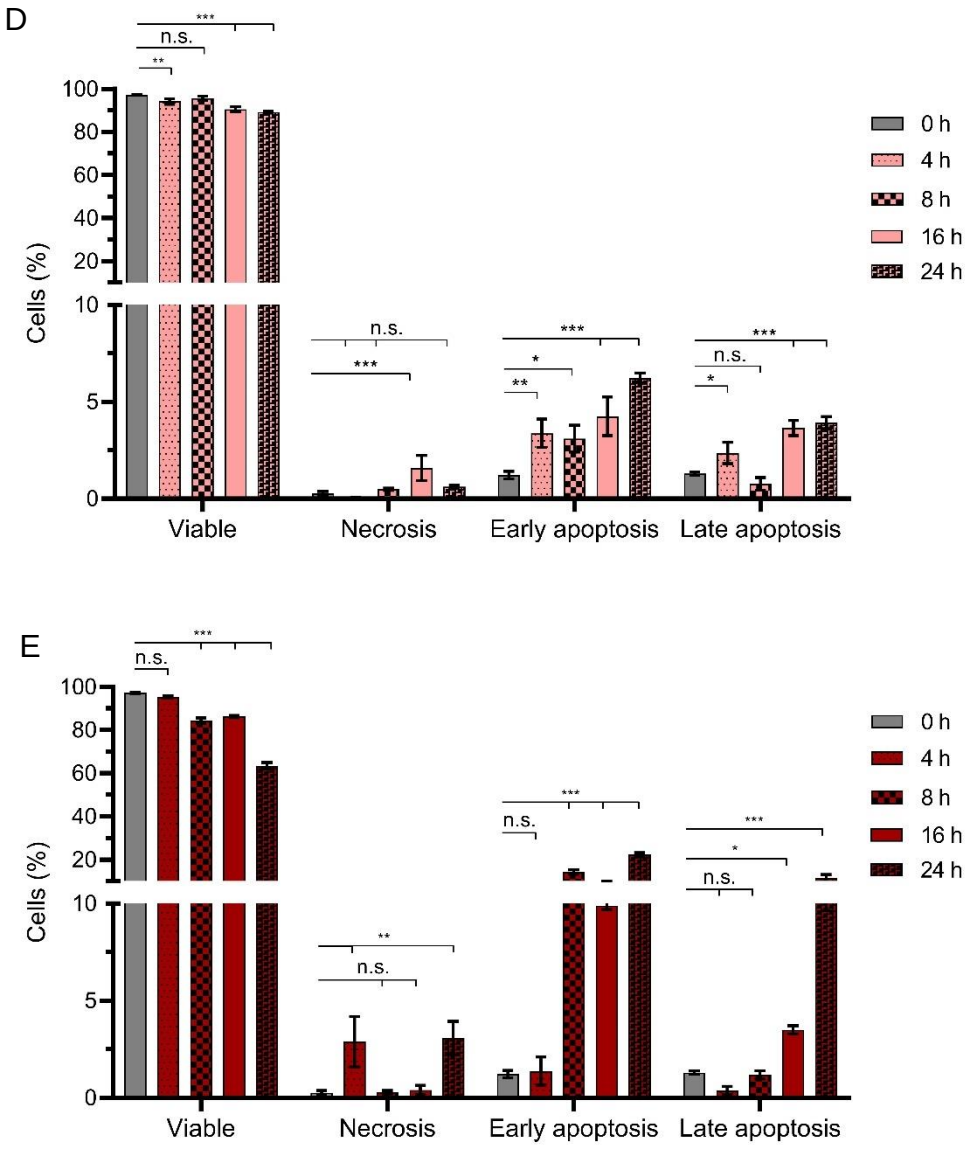

Figure 11 NAcM-OPT and NAcM-COV impacted cell viability. Annexin V-FITC/PI- cell death assay of primary human monocytes treated with vehicle control or small molecule inhibitors. Cell death was analyzed after 0 h, 4 h, 8 h, 16 h, and 24 h. Percentages of viable cells, cells in necrosis, and cells in early and late apoptosis per cell population were analyzed. **A:** Time-dependent assay of cells treated with vehicle control (0,1% DMSO) **B:** Time-dependent assay of cells treated with NAcM-NEG (10 µM) **C:** Time-dependent assay of cells treated with MLN4924 (1 µM) **D:** Time-dependent assay of cells treated with NAcM-OPT (10 µM) **E:** Time-dependent assay of cells treated with NAcM-COV (10 µM). Statistics: one-way ANOVA with Dunnett multiple comparisons test (n=3 technical replicates).

5.1.6 The DCN1 inhibitors do not impact human monocyte-derived macrophage viabilities

It has been suggested by Li et al. that MLN4924 treatment (0.1 µM) for 12 h does not impact macrophage viability, even though cullin-NEDDylation was abolished in this setup. Still, higher doses of MLN4924 (0.33 µM and 1.0 µM) significantly decreased the viability of murine RAW264.7 macrophages via apoptosis [172].

The impact of the novel DCN1 inhibitors on primary human macrophages has not been studied yet. As some impact of the DCN inhibitors on primary human monocyte viabilities could be observed in previous experiments, I wanted to elaborate on whether the inhibitors decrease primary human macrophage viability as well. The results of the cells treated with the novel DCN1 inhibitors and the vehicle control were normalized to an untreated control to ensure that the treatment procedure itself did not negatively impact the cell viability. The cell viabilities were measured by CCK8 analyses in primary human monocyte-derived macrophages subjected to 10 µM DCN1 inhibitor treatment for 16 h. No significant negative impact on cell viability could be observed in this assay **(Figure 12)**.

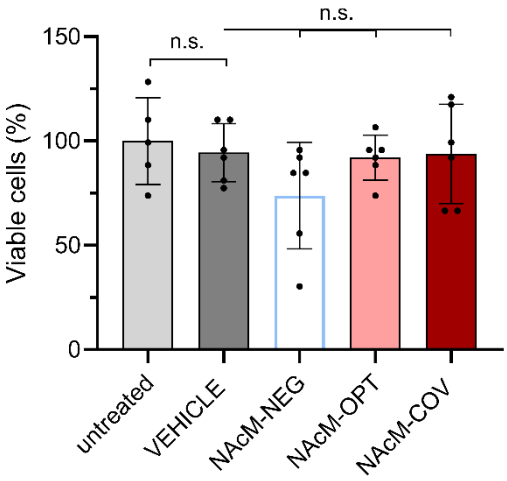

Figure 12 The DCN1 inhibitors did not impact primary human monocyte-derived macrophage-viability *in vitro.*
Cell viability was determined using CCK8 and normalized to untreated controls. Statistics: one-way ANOVA with Dunnett multiple comparisons test (n=5 technical replicates).

5.2 The DCN1 inhibitors do not significantly alter inflammatory gene expression *in vitro*

Several studies have previously reported that the CSN attenuates inflammatory signaling [47, 136, 172, 173]. Asare et al., for instance, showed that deficiency of Csn5 promotes a proinflammatory phenotype in murine macrophages. In *Csn5*$^{\Delta myeloid}$/*Apoe*$^{-/-}$-mice and *Csn5*^{wt}/*Apoe*$^{-/-}$-mice, the BMDMs from *Csn5*-deficient animals had significantly upregulated *Il-12* and *Il-6* mRNA- levels, which are considered pro-inflammatory genes. Conversely, when inhibiting NEDDylation *in vitro* with MLN4924-treatment in BMDMs from *Apoe*$^{-/-}$-mice, atheroprotective effects, like downregulated *Tnf-α*, *Il-12, and Ccl2* mRNA levels were observed [47]. This reduction of proinflammatory gene expression was even more pronounced after treatment with LPS. Additionally, expression of the M2 marker *Arg1* was significantly upregulated after MLN4924 treatment and LPS stimulation [47].

Li et al. have established that treatment with MLN4924 in murine RAW264.7 macrophages under LPS stimulation significantly reduced *Tnf*-α and *Il-6* gene expression and protein levels of Tnf-α and Il-6 [172]. Furthermore, it has been shown that MLN4924 treatment blocks murine Il-1β protein maturation and production *in vitro* and *in vivo* [173]. As mentioned in chapter 1.1.7,

the CANTOS-trial has proven that inhibition of IL-1β significantly reduces cardiovascular events [83].

I, therefore, wanted to elaborate on whether NAcM-OPT and -COV would cause similar atheroprotective effects like MLN4924 in macrophages.

5.2.1 NAcM-OPT and NAcM-COV alter CUL1- and CUL3-NEDDylation in human and murine macrophages

As discussed in chapter 5.1.1, before performing any experiments, the effects of the inhibitors on the NEDDylation levels of the cells used in the setups had to be established. For this reason, immunoblot analyses of CUL1- and CUL3-NEDDylation in primary human monocyte-derived macrophages and murine BMDMs, treated with the small molecule inhibitors or the vehicle control, were performed.

In primary human monocyte-derived macrophages, NAcM-COV and MLN4924 significantly reduced CUL1- and CUL3-NEDDylation. Still, whereas in MLN4924 an almost complete depletion of NEDDylation was observed, residual NEDDylation was left in the cells treated with NAcM-COV. In this setup, NAcM-OPT did not impact NEDDylation levels in CUL1 or CUL3 **(Figure 13 C-D)**. In murine BMDMs, CUL1- NEDDylation was significantly reduced in cells treated with MLN4924 and NAcM-COV, whereas CUL3- NEDDylation was not significantly impaired **(Figure 13 G-H)**.

Overall, cells treated with NAcM-COV presented lower levels of NEDDylated cullins than vehicle controls. This effect was similar to what was previously observed in primary human monocytes and MM6 (see chapter 5.1.1). Still, the effect was less pronounced than the almost total abolishment of NEDDylation in macrophages treated with MLN4924. Interestingly, although NAcM-OPT negatively impacted CUL1- and CUL3- NEDDylation in monocytes, it did not cause any significant effects in macrophages.

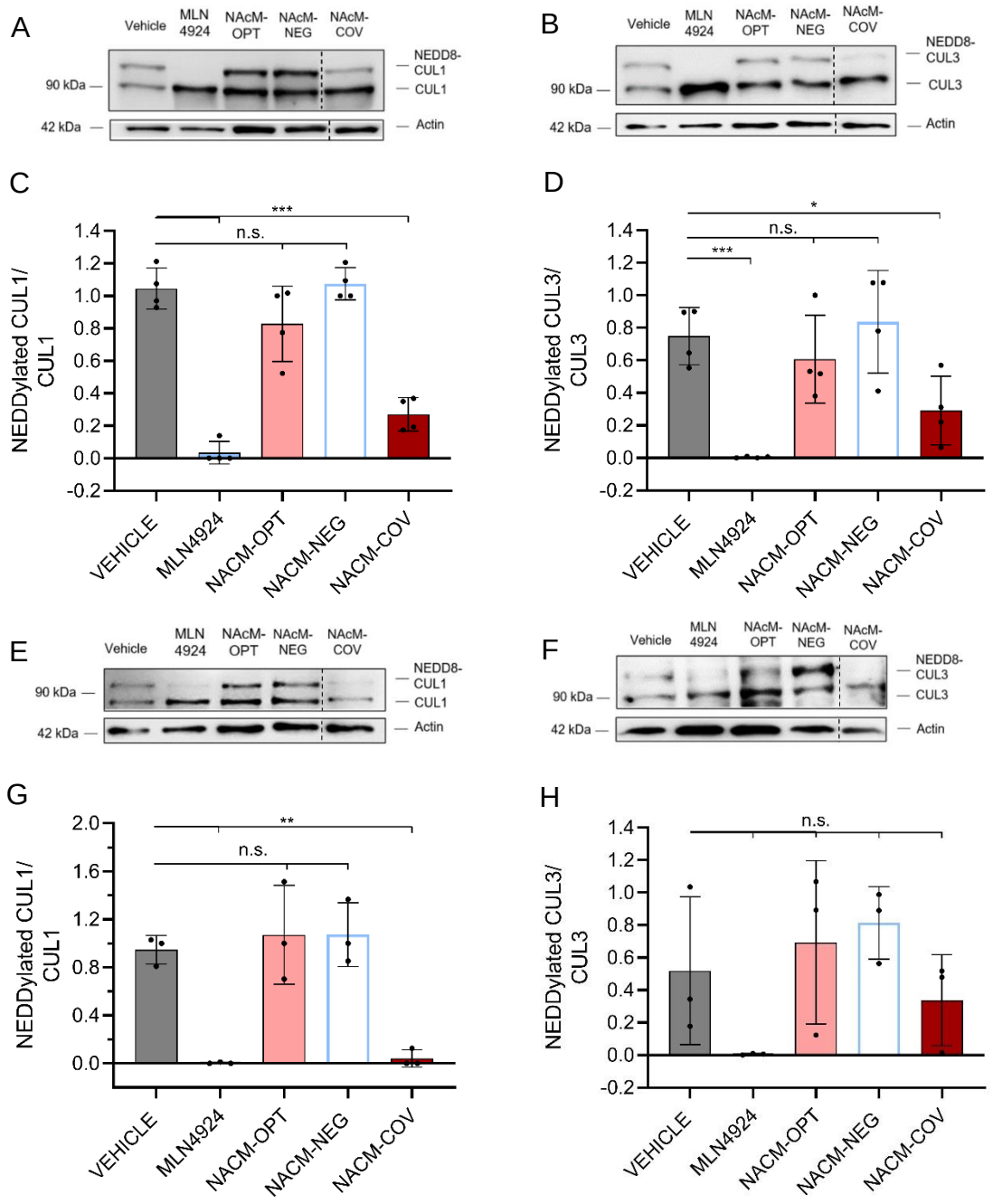

Figure 13 CUL1- and CUL3-NEDDylation levels in primary human monocyte-derived macrophages and murine BMDMs after 16 h of inhibitor treatment. Immunoblot quantification of NEDDylation levels of primary human monocyte-derived macrophages and BMDMs after 16 h inhibitor treatments (NAcM-NEG/-OPT/-COV: 10 µM, MLN4924: 1 µM). **A-B**: Representative immunoblots of NEDDylated and non-NEDDylated CUL1-/CUL3-levels in primary human monocyte-derived macrophages. **C-D:** Quantification of the NEDDylation levels of CUL1 and CUL3 in primary human monocyte-derived macrophages after small molecule inhibitor or vehicle treatment (n=3 technical replicates). **E-F:** Representative immunoblots of NEDDylated and non-NEDDylated CUL1- /CUL3-levels in BMDMs. **G-H:** Quantification of immunoblots raised against CUL1- and CUL3-NEDDylation BMDMs (n=1-3 individual biological replicates). Mpis were normalized to mpis of tubulin and calculated as ratios to the unNEDDylated cullin mpis. Statistics: one-way ANOVA with Dunnett multiple comparisons test.

5.2.2 NAcM-OPT and -COV do not significantly alter inflammatory gene expression *in vitro*

As previously discussed, MLN4924 in BMDMs has been demonstrated to downregulate *Tnf-α*, *Il-12, and Ccl2* mRNA levels while increasing *Arg1* levels [47] and decreasing murine Il-1β protein levels [173]. Thus, I wanted to investigate whether the DCN1 inhibitors cause the same atheroprotective effect.

For this reason, mRNA analyses for typical "pro-inflammatory" M1- and "anti-inflammatory" M2-genes in BMDMs and primary human monocyte-derived macrophages were performed. In primary human monocyte-derived macrophages, *TNF-α, INOS,* and *CCL2* were analyzed as markers for an M1 phenotype, whereas *ARG1, IL-10,* and *CCL22* were used for the M2 phenotype. In BMDMs *Il-10, Il-6, Tnf-α, Il-12,* and *Ccl2* were analyzed as markers for an M1 phenotype, and *Mrc1, Fizz1, Tgm2, Ym1,* and *Arg1* were used for the M2 phenotype. The genes connected to the proinflammatory M1 phenotype are associated with activating the NF-κB pathway and atherogenesis. In contrast, the genes related to the alternatively activated M2 subset can be considered atheroprotective [50, 53, 54].

No significant alterations in gene expression were observed. Still, there were certain noticeable tendencies. Firstly, in primary human monocyte-derived macrophages, treatment with NAcM-COV resulted in a downregulation of *CCL2* mRNA levels. In contrast, NAcM-OPT appeared to even upregulate inflammatory signaling **(Figure 14 A)**. Secondly, in murine BMDMs, these tendencies were even more potent. None of the inhibitors significantly downregulated inflammatory signaling in BMDMs; conversely, the M1-markers *Il-12, Il-6,* and *Ccl2* were non-significantly, yet noticeably upregulated after DCN1 inhibitor treatment **(Figure 14 B)**. Thirdly, primary human monocyte-derived macrophages treated with NAcM-OPT presented a non-significant tendency towards an M2-phenotype in their mRNA expression, both in a surrounding with and without external inflammatory stimulation. NAcM-COV appeared to positively affect *ARG1* and *CCL22* in primary human monocyte-derived macrophages, especially after stimulation with LPS **(Figure 14 C)**.

Finally, NAcM-OPT shifted BMDMs towards an M2-phenotype with and without additional Tnf-α-stimulation. NAcM-COV appeared to benefit towards an M2 shift when no additional inflammatory stimulation was applied. Mainly *Ym1* and *Tgm2* levels were upregulated after NAcM-COV treatment under Tnf-α-stimulation. In inflammatory surroundings, NAcM-COV enhanced *Mrc1* and *Fizz1* expression **(Figure 14 D)**.

Furthermore, no significant effects of the DCN1 inhibitors on murine Il-1β protein levels in the supernatant of BMDMs subjected to the DCN1 inhibitors after TNF-α stimulation were observed **(Figure 14 E)**. Still, there was a non-significant tendency towards reduced murine Il-1β protein levels in BMDMs treated with NAcM-COV.

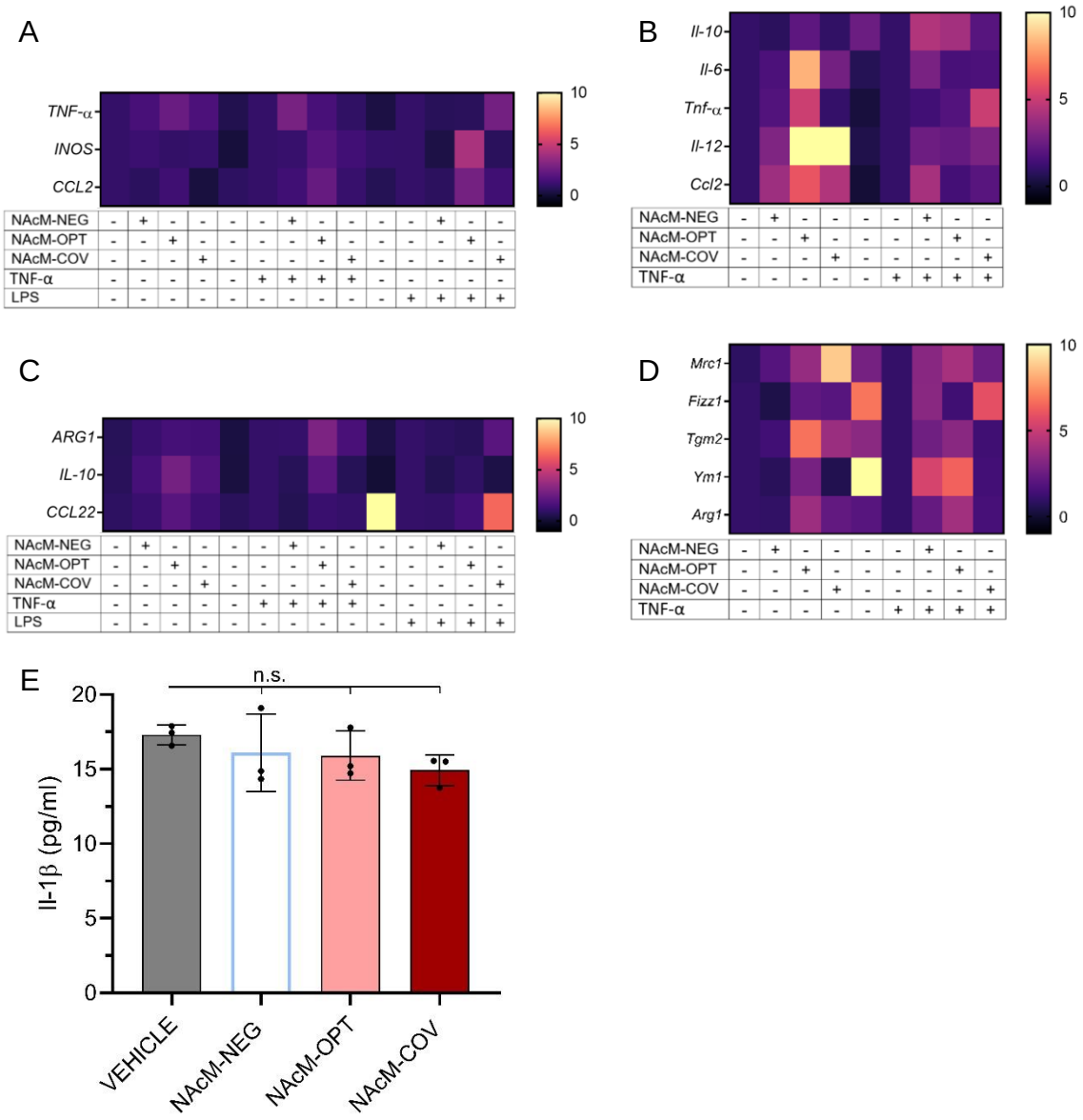

Figure 14 NAcM-OPT and -COV did not significantly alter inflammatory gene expression *in vitro*. Primary human monocyte-derived macrophages or BMDMs were treated with the inhibitors for 16 h and, if indicated, with LPS or TNF-α for 6 h. **A-D:** mRNA analyses were quantified via RT-qPCR and normalized to RPLP0 or GAPDH. Analyses were normalized to vehicle controls with or without TNF-α or LPS treatment for each setup. Data are represented as heat maps. Violet indicates repressed mRNA levels, and yellow indicates elevated levels compared to a control group. **A:** mRNA analyses of primary human monocyte-derived macrophages towards an M1 phenotype (n=5-6 biological replicates) **B:** mRNA analyses of BMDMs towards an M1 phenotype (n=4-5 biological replicates) **C:** mRNA analyses of primary human monocyte-derived macrophages towards an M2 phenotype (n=5 biological replicates) **D:** mRNA analyses of BMDMs towards an M2 phenotype (n=5-6 biological replicates) **E:** Elisa Il-1β protein quantification in the supernatant of BMDMs treated with the inhibitors for 16 h and with TNF-α for 6 h. (n=3 independent biological replicates). Statistics: one-way ANOVA with Dunnett multiple comparisons test.

5.3 Foam cell formation *in vitro* is not impacted by the novel DCN1 inhibitors

As previously discussed in chapter 1.1.4, atherogenesis is characterized by an accumulation of foam cells. Formation of foam cells can induce cell death mechanisms, subsequently leading to the progression towards a necrotic core and inflammatory signaling in the lesion [65]. This process occurs through an enhanced uptake of cholesterol and oxidized lipoproteins in macrophages and dysregulated homeostasis between cholesterol influx and efflux. Crucial players regulating cholesterol efflux are ABCA1 and ABCG1, which transport the cholesterol attached to HDL out of the cell via a reverse cholesterol transport system [174]. It was already shown in 2009 that the ubiquitination of ABCA1 is regulated by the CSN [175]. Raghavan et al. also identified CUL3 as the E3 ligase mediating ABCA1 ubiquitination and, consequently, degradation [150].

Conversely, it was indicated by Schwarz et al. that CSN5 protein expression is enhanced upon oxLDL stimulation in human macrophages [151]. Furthermore, MLN4924-treated atherogenic mice have displayed reduced early atherosclerotic lesion size in the aorta and the aortic root [47]. These findings indicate that the COP9 signalosome is essential in regulating the formation of foam cells.

As it has been shown that MLN4924 impacts foam cell formation *in vivo* and *in vitro*, I decided to analyze how the novel DCN1 inhibitors affect murine and human foam cell formation *in vitro*

5.3.1 NAcM-OPT and NAcM-COV do not impact human foam cell formation *in vitro*

To determine whether NAcM-OPT and NAcM-COV impact the formation of foam cells *in vitro,* primary human monocyte-derived macrophages were treated with the novel DCN1 inhibitors and afterward incubated with oxLDL. The cells were stained with BODIPY, a fluorescent dye binding to fatty acids, and analyzed via the ctcf of BODIPY per cell surface.
All in all, no significant differences in lipid levels in primary human monocyte-derived macrophages could be observed after treating the cells with the novel DCN1 inhibitors. Thus, there might even be a trend towards an induction of foam cell formation after treatment with NAcM-COV **(Figure 15 A)**. Still, due to the wide varieties within the samples, this effect is not significant.

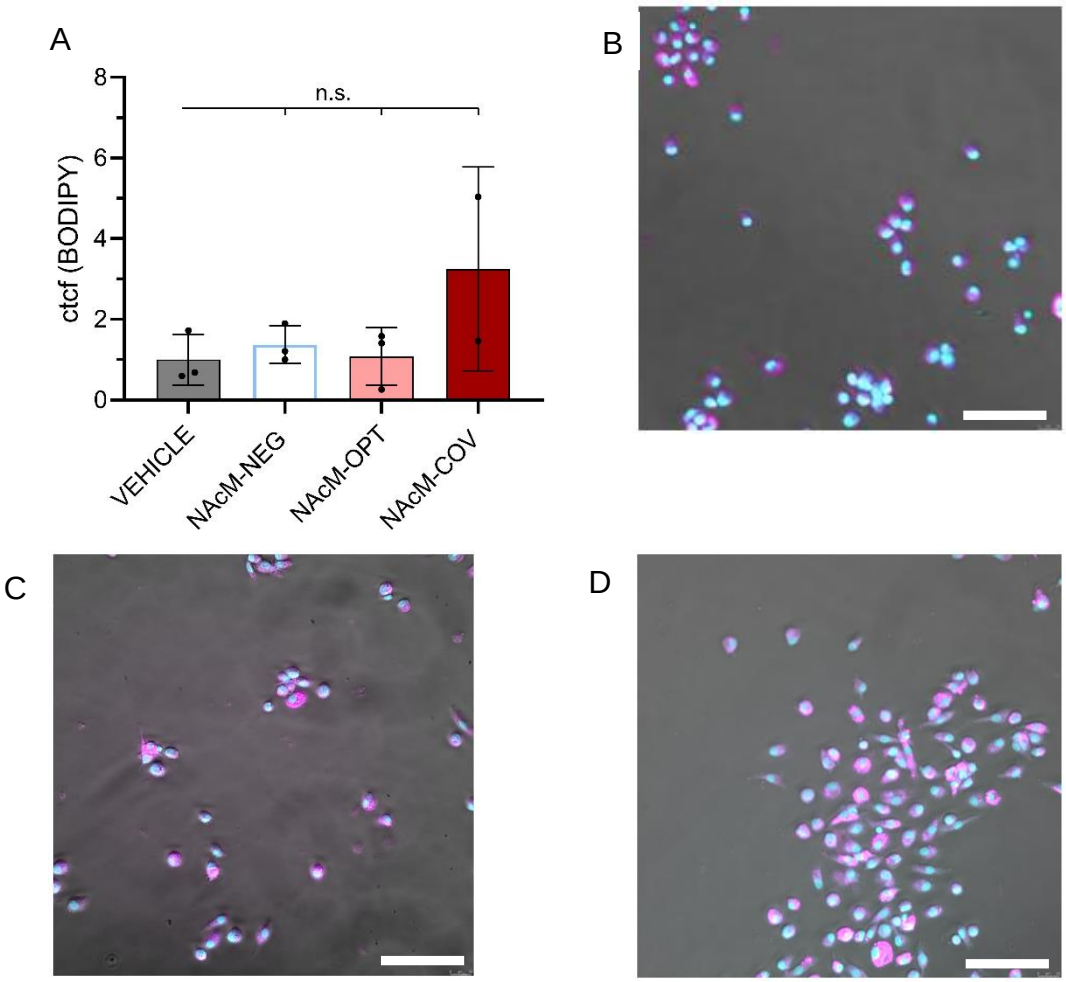

Figure 15 The DCN1 inhibitors did not impact foam cell formation in a human *in vitro* model. BODIPY/DRAQ5-Immunocytochemistry of primary human monocyte-derived macrophages treed with the inhibitors for 16 h and oxLDL for 48 h (scale bar=50 µm) A: Lipid uptake was quantified as ctcf/cell surface and normalized to vehicle controls. (n=2-3 biological replicates, data are represented as mean ± SD, n.s.=not significant) B: Representative BODIPY/DRAQ5-Immunocytochemistry of foam cell formation in the vehicle control (0.1% DMSO) C: Representative BODIPY/DRAQ5-Immunocytochemistry of foam cell formation after treatment with NAcM-OPT (10 µM for 16 h) D: Representative BODIPY/DRAQ5-Immunocytochemistry of foam cell formation after treatment with NAcM-COV (10 µM for 16 h). Statistics: one-way ANOVA with Dunnett multiple comparisons test.

5.3.2 NAcM-OPT and NAcM-COV do not impact murine foam cell formation *in vitro*

To evaluate whether NAcM-OPT and -COV affect foam cell formation in a murine *in vitro model,* BMDMs were treated with the DCN1 inhibitors and incubated with oxLDL. The cells were stained with Oil red O and hematoxylin and analyzed by pixel intensities of areas with comparable cell numbers. Similar to the results in the *in vitro* model in primary human monocyte-derived macrophages, no differences in lipid levels in BMDMs after treatment with the DCN1 inhibitors were detected **(Figure 16 A)**. Interestingly, the positive trend after NAcM-COV treatment in the previous experiment **(Figure 15 A)** was not replicated in this experimental setting.

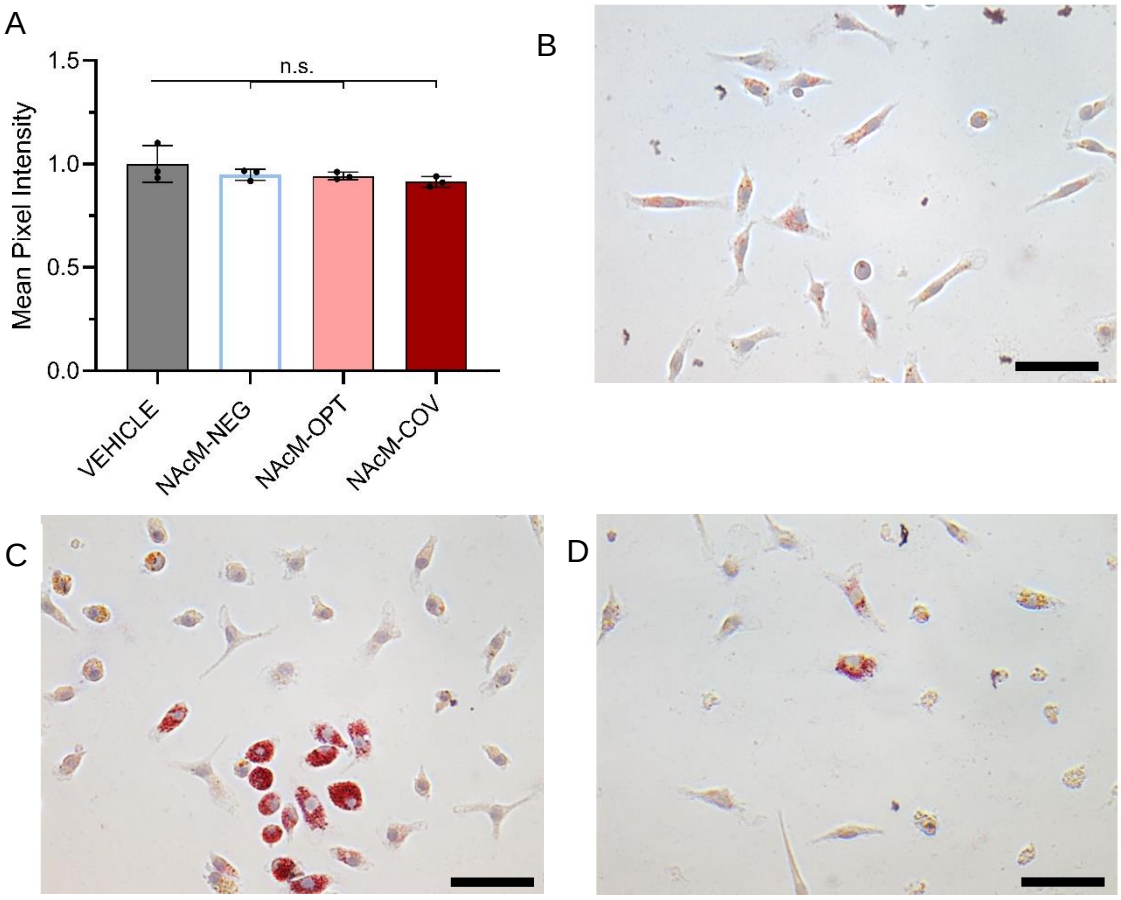

Figure 16 The DCN1 inhibitors did not impact foam cell formation in a murine *in vitro* model. Oil Red O and hematoxylin staining of BMDMs treated with the inhibitors for 16 h and incubated with oxLDL for 48 h (scale bar=50 µm) **A:** Quantification of oxLDL uptake as pixel intensity/image and normalized to vehicle controls. (n=3 biological replicates, data are represented as mean ± SD, n.s.=not significant) **B:** Representative Oil red O- and hematoxylin staining of foam cell formation in the control group (0.1% DMSO) **C:** Representative Oil red O- and hematoxylin staining of foam cell formation after treatment with NAcM-OPT (10 µM for 16 h) **D**: Representative Oil red O- and hematoxylin staining of foam cell formation after treatment with NAcM-COV (10 µM for 16 h). Statistics: one-way ANOVA with Dunnett multiple comparisons test.

6 Discussion

This thesis performed *in vitro* analyses of the effects of the novel DCN1 inhibitors NAcM-OPT and NAcM-COV in the context of atherogenesis. Numerous prior studies investigating the role of NEDDylation in chronic inflammation used MLN4924 to at least partially "mimic" the effect of CSN overexpression [47, 136, 172, 173]. As MLN4924 impacts an early stage of the NEDDylation cascade, it inhibits all cullin NEDDylation. The novel DCN1 inhibitors NAcM-OPT and NAcM-COV allow a more targeted approach, facilitating the distinction between the activity of CUL1 and CUL3 and the five other cullins [4].

6.1 NAcM-OPT and NAcM-COV are not as potent as MLN4924 as inhibitors of CUL1- and CUL3-NEDDylation in monocytes and macrophages *in vitro*

Scott et al. previously designed and showed an initial comparative effect of the DCN1 small molecule inhibitors and MLN4924 on cullin NEDDylation[4] **(Figure 4)**. In a human lung squamous carcinoma cell line model, the novel DCN1 inhibitors mainly impacted the steady-state levels of NEDDylated CUL1, CUL3, and CUL4A. This cell line was selected for its high expression of DCN1, as in many other mammalian cell lines with lower expression of DCN1 knocking out or inhibiting DCN1 affected steady-state levels of cullin NEDDylation rather subtly [4]. This might be explained by other DCN-family members compensating for the decreased function of DCN1 [4, 176-178]. Previous studies also suggest a highly diverse, cell-specific effect on NEDDylation levels upon *DCN1* ablation [4, 176, 179, 180]. I, therefore, measured the extent of inhibition of CUL1- and CUL3-NEDDylation upon inhibitor application in atherosclerosis-relevant mouse and human cell types *in vitro*.

The NAcM-inhibitors appeared less potent than MLN4924 in all tested cell types **(Figure 6, Figure 13)**. In primary human monocytes, NAcM-COV and NAcM-OPT significantly downregulated the steady-state levels of NEDDylated CUL1 but not CUL3 **(Figure 6)**. In primary human und murine macrophages, the effect of NAcM-COV, but not of NAcM-OPT, on CUL1- and CUL3-NEDDylation was significant **(Figure 13)**, except for steady-state levels of NEDDylated CUL3 in murine macrophages, due to too few repeats to test for significance. Overall, these results align with the results published by Scott et al. **(Figure 4)**.

Compared to the HCC95 cell line employed by Scott et al., the monocytes and macrophages used in this thesis have a lower expression of DCN1. According to the human protein atlas [181], HCC95 yields 45.2nTPM DCUN1D1, whereas human monocytes have an expression of 36.2nTPM and human macrophages of 38.7nTPM DCUN1D1. However, I did not perform comparative Western blot experiments to further confirm this notion and to find out whether this difference also manifests on protein level.

Even though the cell types used in this thesis likely have a lower expression of DCN1, the results suggest that especially NAcM-COV impairs steady-state levels of NEDDylated CUL1 and CUL3 but does not lead to a complete blocking of NEDDylation. However, at the time of writing this thesis, it is not yet thoroughly studied to which extent only partial impairment of NEDDylation compared to full obliteration of CUL1- and CUL3-NEDDylation affects the activity of the CRL [172, 182, 183]. This makes it difficult to distinguish between the effect of the residual NEDDylation in CUL1 and CUL3 and the other cullins' NEDDylation patterns. Still, the extent of the decrease in NEDDylation was overall mirrored in the results of this thesis.

MLN4924 seems to have the most potent effect on human monocyte migration and viability *in vitro*, followed by the covalently binding small molecule inhibitor NAcM-COV. In contrast, the non-covalently binding NAcM-OPT did not show significant results except for a dosage of 30 µM **(Figure 7, Figure 8, Figure 10)**. Also, in the context of atherosclerosis in murine and human macrophages *in vitro*, the novel DCN1 inhibitors did not present the anti-inflammatory potential shown in cells treated with MLN4924 [47, 93, 136]. However, NAcM-COV presented anti-inflammatory tendencies than NAcM-OPT by negatively, but still non-significantly, impacting Il-1β secretion *in vitro* in BMDMs, which might point towards an anti-inflammatory potential of the substance [184] **(Figure 14)**.

These preliminary findings suggest that NAcM-COV rather than NAcM-OPT might be the more promising candidate to further explore the underlying signaling mechanisms and effects of CUL1- and CUL3-NEDDylation in atherosclerosis-relevant cell types. Considering the more potent results of NAcM-COV, the general advantages and disadvantages of irreversibly binding covalent drugs compared to non-covalent inhibitors should be taken into account. In 2017, about 30% of the drugs in the overall market were covalent drugs [185, 186]. These irreversibly binding drugs can be considered advantageous in terms of less frequent dosing and lower risks of drug resistance [187]. Nevertheless, the prolonged impact of these substances as well as the permanent bond between the target-protein and the inhibitor has been associated with adverse events and drug toxicity [186].

6.2 NAcM-COV but not NAcM-OPT impacts monocyte migration and viability *in vitro*

Previous work has revealed that inhibition of CSN5 leads to altered biochemical regulation of actin dynamics due to changed NEDDylation patterns of the actin-binding protein cofilin [138, 147, 164]. Actin remodeling is substantial in immune functions connected to atherosclerosis as monocyte migration, cell differentiation, and intra- and extracellular signaling are only possible because of the rapid assembly and disassembly of filamentous actin [158, 159]. Within this process, cofilin is a crucial protein in regulating actin dynamics [160, 161]. Vogl et al. have suggested that

altered actin remodeling in developing neurons after global inhibition of NEDDylation might be due to lysine 112 of cofilin being a target for NEDDylation [138]. Additionally, actomyosin rearrangement in monocyte-to-macrophage differentiation is controlled by MAP-kinases [164], which are regulated by the CSN [151]. Interestingly, it has previously been suggested that pretreatment with MLN4924 for 30 min before incubation with LPS results in a marginal decrease in neutrophil survival [188]. As MLN4924 has also been suggested to sensitize monocytes for necroptosis [149], I hypothesized that the novel DCN1 inhibitors might impact cellular integrity.

As monocyte mobility depends on cellular remodeling [159], a Transwell-based chemotaxis assay was performed. *In vitro*, in MM6 but not primary human monocytes, NAcM-COV, like MLN4924, significantly reduced monocyte migration **(Figure 7)**. Notably, NAcM-OPT did not negatively impact monocyte migration in either cell type. Still, this assay only measures a cell count and, therefore, fails to evaluate the particular mechanisms resulting in reduced monocyte mobility. Furthermore, the extended migration period of 6-8 h might have been too long as it raises uncertainty regarding cell viabilities. Using a 4 h migration period might have provided more reliable results distinguishing between slow migration and potential cell death [189].

Majolée et al. reported that specific inhibition of CSN5 results in a loss of endothelial integrity. They suggested that this might be attributed to a Rho/ROCK-dependent increased formation of actin-stress fibers [147]. When this group investigated the effects of CSN5 inhibition on endothelial integrity, they sought to determine if the loss of endothelial barrier integrity was due to increased apoptosis. When analyzing caspase-3/7 activity in HUVECs treated with CSN5i-3, they only observed induced caspase-3/7 activity after 24 h of CSN5 inhibition [147]. It was concluded that the initial disruption of endothelial integrity is not caused by apoptosis, but cell death could contribute to reduced cellular integrity at later timepoints [147].

Interestingly, when I did preliminary tests about cleaved caspase 3 levels in MM6 and primary human monocytes after 16 h of *in vitro* inhibitor treatment, the cleaved caspase 3 levels were slightly upregulated in both, cells treated with NAcM-OPT and -COV **(Figure A 1)**, suggesting induced cell death. These results of upregulated cleaved caspase 3 levels at a relatively late time point can be considered in line with previous reports from Majolée et al. [147]. Still, as NAcM-NEG treatment also resulted in an upregulation of cleaved caspase 3 levels, the experimental setup might at least partially explain the increase of apoptosis.

To further evaluate whether the decrease in monocyte viability after inhibitor treatment can be attributed to a loss of endothelial integrity, stainings for actin after inhibitor treatment would be valuable. This setup would be beneficial to assess if actin levels change within cells treated with NEDDylation inhibitors or if the main reason for the impaired cellular remodeling is reduced dynamic actin reorganization itself. To investigate this hypothesis, 3D imaging of the

cells migrating towards a chemoattractant during or after incubation with the inhibitors could be performed to evaluate the underlying mechanisms resulting in reduced monocyte mobility.

To validate my earlier results and observe cell death mechanisms induction by altered NEDDylation patterns, I next performed an Annexin V-FITC/PI cell death assay, which allows a distinction between necrotic and apoptotic cell death.

It has already been shown by El-Mesery et al*.* that *in vitro* treatment of primary human monocytes with MLN4924 affected the cells' anti-necrotic and anti-apoptotic activities. Still, upon treating the primary human monocytes with different doses of MLN4924, a significant decrease in viable monocytes was only detected in the presence of an additional caspase-inhibitor or TNF-α [149]. It was suggested that this reduced cell viability might inhibit the induction of protective proteins controlled by the NF-κB pathway [149, 190]. The data obtained in my thesis suggests that the induction of cell death mechanisms in primary human monocytes *in vitro* depends on the degree of NEDDylation. While NAcM-OPT did not significantly impact cell viability, NAcM-COV, which *in vitro* in primary human monocytes acts as a more potent drug than NAcM-OPT **(Figure 6)**, led to a significant reduction of viable cells **(Figure 9)** from about 70% viable cells in the vehicle control within the population to about 50%. Likewise, MLN4924, which not only abolishes CUL1- and CUL3-NEDDylation but also targets other cullins, led to significantly fewer, namely about 10% viable cells within the population **(Figure 9)**. Notably, the primary type of cell death induced by altering CUL1- and CUL3-NEDDylation was apoptotic cell death. MLN4924's well-studied impact on DNA replication and cell cycle arrest might also explain why this was the driving mechanism of cell death [152]. Still, MLN4924 and NAcM-COV also significantly elevated the proportion of cells in necrosis *in vitro* **(Figure 9).**

These results are partially consistent with El-Mesery et al*.* [149]. Whereas they only observed a significant induction of cell death mechanisms when adding an external stimulus [149], I observed a significant reduction of primary human monocyte viability after 16 h of MLN4924-treatment in doses from 0.1 µM to 5 µM without adding external stimuli **(Figure 9, Figure 11)**. The usage of different cell death assays might explain the different experimental outcomes. El-Mesery et al*.* used a 3-(4,5-dimethylthiazol-2-yl)-2,5-diphenyltetrazolium bromide (MTT) assay, which colorimetrically assesses cell metabolic activity. In contrast, an Annexin V-FITC/PI cell death assay, a flow cytometry-based method, was used in this thesis [191].

Furthermore, the experiments have been executed on primary human monocytes, with only three to four biological repeats. Hence, further investigation is necessary for solid, conclusive results [149]. As primary human monocytes are not monoclonal cell lines but stem from healthy individuals with different ages and genders, higher numbers of repeats might be beneficial to

equal out the interindividual differences. Also, higher numbers of repeats would be beneficial for the dose- and time-dependent assays. As these assays have only been performed with technical replicates rather than biological repeats in this thesis, they only present the effect of the inhibitors on one individual. Consequently, the results in these assays slightly differ from their equivalent in the assay for 16 h of treatments and dosages of 10 µM for the DCN1 inhibitors and 1 µM for MLN4924 that were performed with three biological repeats **(Figure 9-Figure 11)**.

It has previously been shown that NEDDylation also regulates macrophage survival. Li et al. reported in 2013 that ongoing treatment of RAW264.7 macrophages with MLN4924 significantly decreased cell survival and resulted in macrophage apoptosis due to induced G2 cell-cycle arrest [172]. Furthermore, the increase of IκBα and subsequently reduced production of cytokines promoting inflammation like TNF-α and IL-6 in macrophages treated with MLN4924 has been suggested to result in apoptosis in macrophages [142].
Interestingly, in this thesis, primary human monocyte-derived macrophage viability was not reduced after inhibitor treatment *in vitro* **(Figure 12)**, which was contrary to the results in monocytes **(Figure 9)** and not in line with the findings of Li et al. [172]. Still, the analysis of the macrophage viability in this thesis was mainly executed to ensure that the cells were viable before performing further analyses rather than repeating the experimental setup used by Li et al. with the novel DCN1 inhibitors.

Overall, the effect of NEDDylation on dynamic actin remodeling should be investigated further. The impact of MLN4924 and NAcM-COV on the induction of monocyte death might be a therapeutical target for suppressing chronic inflammation. Various studies suggesting that inhibition of NEDDylation has anti-inflammatory potential could be considered supportive for this usage [47, 173, 192]. Still, as it has already been shown in clinical trials with MLN4924, such a broad impact might result in severe side effects. For example, in a 2018 phase 1b study of Pevonedistat in 64 patients with treatment-naive acute myeloid leukemia, 69% experienced severe adverse events [152]. Interestingly, some of the most common adverse events reported in this clinical study were thrombocytopenia (28%) and neutropenia (23%), as well as pneumonia (22%), suggesting an impact of MLN4924 on the immune cell viability [152]. Thus, a more specific inhibitor, such as the DCN1 inhibitors, might be beneficial to decrease the number of adverse events. To make this approach feasible, further research on the compounds, especially *in vivo* analyses, must be done. Still, the DCN1 inhibitors used in this thesis have several limitations, such as lacking three-dimensional character, leading to a less potent impact on cullin NEDDylation, and a moderate murine half-life of 3-4 h that might make it difficult to further work with these compounds in murine *in vivo* models [2, 145]. For this reason, further improved DCN1 inhibitors, like the novel “compound 27” presented by Kim et al. [2], could

be promising candidates to further validate the implications of decreased NEDDylation on dynamic actin remodeling.

6.3 The DCN1 inhibitors do not significantly alter inflammatory gene expression or murine Il-1β protein secretion *in vitro*

Previous studies have demonstrated that MLN4924 negatively affects NF-κB signaling in murine macrophages [47, 136, 172]. When treating BMDMs with MLN4924 *in vitro,* Asare et al. observed reduced mRNA levels of *Tnf-α*, *Il-12,* and *Ccl2.* Furthermore, M2-markers like *Arg1* and *Il-13* were increased after treatment with MLN4924 [47]. It has also been suggested that *in vivo* treatment of MLN4924 in mouse models not only negatively impacts protein serum levels of Il-6 and Tnf-α [47] but also results in decreased Il-1β and Il-6 protein levels in lung tissues in mouse models of adenovirus-induced pulmonary inflammation [192].

In the context of NF-κB signaling, no significantly reduced Il-1β protein levels in BMDMs treated with the NAcM inhibitors and stimulated with Tnf-α were observed **(Figure 14)**. Still, there might be a slight tendency towards reduced Il-1β levels. This result is therefore not completely in line with other works that have described a negative effect of inhibited NEDDylation on murine Il-1β levels *in vitro* in neutrophils [188] and blastocysts [193] as well as *in vivo* in mice treated with MLN4924 [173] and in models of inflamed lung tissues [192].

Interestingly, also no significant alterations were found when analyzing murine and human gene expression after NAcM-OPT and NAcM-COV treatment *in vitro*. On the contrary, in BMDMs, treatment with the novel DCN1 inhibitors resulted in an upregulation of M1 markers like *Il-12* and *Ccl2* **(Figure 14)**. Still, in primary human monocyte-derived macrophages and BMDMs, the novel DCN1 inhibitors caused a non-significant shift towards upregulating some genes connected to the anti-inflammatory M2-skewing **(Figure 14)**. These results do not align with Asare et al.'s observations, who reported significantly reduced mRNA levels of *Tnf-α, Ccl2, Il-6,* and *Il-12* after MLN4924 treatment in the LPS-stimulated BMDMs [47].

The experimental setup might partially explain these non-conclusive effects of the novel DCN1 inhibitors. As I have employed and experimented with the primary immune cells of different individuals, various additional factors outside the inhibitor treatments, such as unnoticed infections or pre-medication of the anonymous donors in the human samples, might have affected the results. Therefore, technical repeats of specific donors might lead to more comparable results.

Furthermore, additional experiments are necessary to analyze the effects of the novel DCN1 inhibitors conclusively:

Firstly, the DCN1 inhibitors' impact on the gene expression in BMDMs should also be checked after an additional pre-incubation with LPS to mirror the entire setup of Asare et al. thoroughly. [47, 136]. Next, for the M1-/M2-profile skewing, treating the macrophages with either IL-4 or LPS and IFN-ɣ before adding the DCN1 inhibitors might be beneficial. In this setup, the macrophages would already be skewed towards M1 or M2 [194]. Therefore, it could be analyzed if a significant shift in phenotype occurs when altering CUL1- and CUL3-NEDDylation. Importantly, it must also be considered that even though the traditional pro-inflammatory M1 and anti-inflammatory M2 classifications were chosen for this thesis, it has since been reported that they cannot fully depict the complexity of macrophage skewing [43]. Furthering the spectrum analyses towards the recently identified three macrophage sub-groups (aortic resident, inflammatory, foamy Trem2^{hi} macrophages) [43] might provide more conclusive findings. Furthermore, technical replicates rather than biological replicates should be employed for further analyses to take the variability and anonymity of the human donors into account.

Importantly, although no apparent impact of the DCN1 inhibitors on gene expression could be observed in this work, NAcM-COV's slight effect on murine Il-1β protein secretion could still point towards anti-inflammatory capacities of this inhibitor. As NEDDylation not only impacts gene expression *in vitro* but also directly affects protein turnover, the decreased level of protein secretion might instead result from altered Il-1β protein degradation rather than altered gene expression. This interplay of a directly affected turnover of critical regulatory proteins and the subsequent changes in signaling pathways is already known to be crucial for the targeted cancer therapy of MLN4924 [195]. IL-1β, which is mainly secreted by monocytes, macrophages, and DCs [184], is a critical pro-inflammatory cytokine in all stages of atherogenesis [196]. For this reason, IL-1β signal transduction has been a target in various animal experiments and clinical trials in the context of inflammation and atherosclerosis [184]. For instance, Anakinra, a recombinant human IL-1α and IL-1β receptor antagonist, has been connected to a significant decrease in the immediate inflammatory reaction in individuals with MI and subsequent cardiovascular events within a median observation period of 365 days [197]. It has also been shown in the CANTOS trial that specific IL-1β-inhibition with the monoclonal antibody Canakinumab significantly decreases cardiovascular events like non-fatal MI and stroke, as well as cardiovascular death [83]. Consequently, the effect of NAcM-COV on murine Il-1β protein levels could point towards an atheroprotective impact of the substance and should therefore be investigated further.

6.4 Foam cell- formation is not impacted by the novel DCN1 inhibitors *in vitro*

Asare et al. have shown that in a murine *in vivo* model, inhibition of NEDDylation by MLN4924 treatment reduces the formation of initial atherosclerotic lesions in the aorta and aortic root [47]. Also, it has been demonstrated by Raghavan et al. that ABCA1 degradation is regulated by

CUL3-NEDDylation [150]. The same group also studied the connection between cullin NEDDylation and foam cell formation by implementing transfection of macrophages with CSN3-siRNA, suggesting an increase in foam cell formation upon CSN3 depletion. They concluded that CSN3 is essential in regulating ABCA1 ubiquitination and might be a therapeutical target against atherosclerosis [198].
I, therefore, hypothesized that the novel DCN1 inhibitors, by impacting CUL3-NEDDylation in macrophages, might affect foam cell formation, as reduced ABCA1 protein degradation might result in higher cholesterol reflux. Thus, an *in vitro* foam cell assay, which consisted of pre-treated murine and human macrophages in a surrounding of oxLDL, was performed.

These experiments found no significant reductions in intracellular lipid levels after the inhibitor treatments in BMDMs **(Figure 16)** or human primary monocyte-derived macrophages **(Figure 15)**.

The DCN1 inhibitors might still impact foam cell formation since an *in vitro* assay cannot replicate the complex microenvironment and interactome within the atherosclerotic lesion. Moreover, foam cells within the atherosclerotic plaque originate not solely from macrophages but also from SMCs, stem/progenitor cells, and endothelium cells [56]. Still, it has to be determined whether further investigating this approach would be beneficial due to the non-significant and non-conclusive results.

It might instead be interesting to replicate this experiment with MLN4924 to further decipher whether complete abolishment of NEDDylation significantly impacts foam cell formation *in vitro.* This would be crucial before further analyzing the effects of partial inhibition of NEDDylation*.* Furthermore, investigation of intracellular ABCA1 protein levels *in vitro* upon inhibitor treatment might give valuable insight. To the best of my knowledge, this approach has yet to be published in any cell type at the time of writing this thesis. Therefore, further analyses on how NEDDylation impacts ABCA1 protein degradation, rather with MLN4924 than the novel DCN1 inhibitors, might further explain why MLN4924 has shown to be atheroprotective.

If that approach yields more promising results than the setup with the novel DCN1 inhibitors, the interconnection of NEDDylation and ABCA1 degradation might be a valuable therapeutical target in treating atherosclerosis.

7 Summary and future perspectives

This thesis aimed to investigate the impact of cullin-NEDDylation on atherosclerosis-relevant mediators of immune response via evaluation of the effects of two novel DCN1 inhibitors, NAcM-OPT and NAcM-COV, on CUL1- and CUL3-NEDDylation in monocyte and macrophage models *in vitro*. The results indicate that NAcM-COV has a more potent impact on CUL1- and CUL3-NEDDylation levels than NAcM-OPT but less pronounced than MLN4924, a well-known NEDDylation inhibitor.

In *in vitro* monocyte models, treatment with NAcM-COV and MLN4924 significantly reduced cell mobility, while treatment with NAcM-OPT did not. Furthermore, treatment with NAcM-COV and MLN4924 resulted in a significant reduction in primary human monocyte viability, suggesting that altering cullin-NEDDylation may impair actin dynamics and reduce cellular integrity. However, treatment with NAcM-OPT and -COV did not significantly impact inflammatory signaling or Il-1β protein levels in murine macrophages in an inflammatory microenvironment. Furthermore, neither NAcM-COV nor NAcM-OPT affected foam cell formation in human and murine *in vitro* models.

In conclusion, further *in vitro* and *in vivo* evaluation is crucial to understand the potential and limitations of the novel DCN1 inhibitors. The development of improved DCN1 inhibitors, such as "compound 27," may be a promising next step to increase their effectiveness *in vivo*. Still, given the central role of myeloid cells in atherosclerosis, targeting cullin-NEDDylation with small molecule inhibitors could be a promising strategy in researching, preventing, and treating this disease.

8 References

1. Libby P, Ridker PM and Hansson GK. Progress and challenges in translating the biology of atherosclerosis. *Nature*. 2011;473:317-325.
2. Kim HS, Hammill JT, Scott DC, Chen Y, Min J, Rector J, Singh B, Schulman BA and Guy RK. Discovery of Novel Pyrazolo-pyridone DCN1 Inhibitors Controlling Cullin Neddylation. *Journal of Medicinal Chemistry*. 2019;62:8429-8442.
3. Deshaies RJ. Structural biology: Corralling a protein-degradation regulator. *Nature*. 2014;512:145-6.
4. Scott DC, Hammill JT, Min J, Rhee DY, Connelly M, Sviderskiy VO, Bhasin D, Chen Y, Ong S-S, Chai SC, Goktug AN, Huang G, Monda JK, Low J, Kim HS, Paulo JA, Cannon JR, Shelat AA, Chen T, Kelsall IR, Alpi AF, Pagala V, Wang X, Peng J, Singh B, Harper JW, Schulman BA and Guy RK. Blocking an N-terminal acetylation–dependent protein interaction inhibits an E3 ligase. *Nature Chemical Biology*. 2017;13:850-857.
5. Joseph P, Leong D, McKee M, Anand SS, Schwalm JD, Teo K, Mente A and Yusuf S. Reducing the Global Burden of Cardiovascular Disease, Part 1: The Epidemiology and Risk Factors. *Circulation Research*. 2017;121:677-694.
6. Milutinović A, Šuput D and Zorc-Pleskovič R. Pathogenesis of atherosclerosis in the tunica intima, media, and adventitia of coronary arteries: An updated review. *Bosnian Journal of Basic Medical Sciences*. 2019.
7. Gisterå A and Hansson GK. The immunology of atherosclerosis. *Nature Reviews Nephrology*. 2017;13:368-380.
8. Weber C and Noels H. Atherosclerosis: current pathogenesis and therapeutic options. *Nature Medicine*. 2011;17:1410-22.
9. Packard RR and Libby P. Inflammation in atherosclerosis: from vascular biology to biomarker discovery and risk prediction. *Clinical Chemistry*. 2008;54:24-38.
10. Zernecke A, Shagdarsuren E and Weber C. Chemokines in atherosclerosis: an update. *Arteriosclerosis, Thrombosis, and Vascular Biology*. 2008;28:1897-908.
11. Wolf D and Ley K. Immunity and Inflammation in Atherosclerosis. *Circulation Research*. 2019;124:315-327.
12. Yoshida H and Kisugi R. Mechanisms of LDL oxidation. *Clinica Chimica Acta*. 2010;411:1875-1882.
13. Ley K, Miller YI and Hedrick CC. Monocyte and Macrophage Dynamics During Atherogenesis. *Arteriosclerosis, Thrombosis, and Vascular Biology*. 2011;31:1506-1516.
14. Tchernof A and Després J-P. Pathophysiology of Human Visceral Obesity: An Update. *Physiological Reviews*. 2013;93:359-404.
15. Tacke F and Randolph GJ. Migratory fate and differentiation of blood monocyte subsets. *Immunobiology*. 2006;211:609-18.
16. Moroni F, Ammirati E, Norata GD, Magnoni M and Camici PG. The Role of Monocytes and Macrophages in Human Atherosclerosis, Plaque Neoangiogenesis, and Atherothrombosis. *Mediators of Inflammation*. 2019;2019:7434376.
17. Vallejo J, Cochain C, Zernecke A and Ley K. Heterogeneity of immune cells in human atherosclerosis revealed by scRNA-Seq. *Cardiovascular Research*. 2021;117:2537-2543.
18. Groh L, Keating ST, Joosten LAB, Netea MG and Riksen NP. Monocyte and macrophage immunometabolism in atherosclerosis. *Seminars in Immunopathology*. 2018;40:203-214.
19. Fernandez DM, Rahman AH, Fernandez NF, Chudnovskiy A, Amir E-aD, Amadori L, Khan NS, Wong CK, Shamailova R, Hill CA, Wang Z, Remark R, Li JR, Pina C, Faries C, Awad AJ, Moss N, Bjorkegren JLM, Kim-Schulze S, Gnjatic S, Ma'ayan A, Mocco J, Faries P, Merad M and Giannarelli C. Single-cell immune landscape of human atherosclerotic plaques. *Nature Medicine*. 2019;25:1576-1588.
20. Galkina E, Kadl A, Sanders J, Varughese D, Sarembock IJ and Ley K. Lymphocyte recruitment into the aortic wall before and during development of atherosclerosis is partially L-selectin dependent. *Journal of Experimental Medicine*. 2006;203:1273-1282.

21. Barrett TJ. Macrophages in Atherosclerosis Regression. *Arteriosclerosis, Thrombosis, and Vascular Biology*. 2020;40:20-33.
22. Smith JD, Trogan E, Ginsberg M, Grigaux C, Tian J and Miyata M. Decreased atherosclerosis in mice deficient in both macrophage colony-stimulating factor (op) and apolipoprotein E. *Proc Natl Acad Sci U S A*. 1995;92:8264-8.
23. Jonasson L, Holm J, Skalli O, Bondjers G and Hansson GK. Regional accumulations of T cells, macrophages, and smooth muscle cells in the human atherosclerotic plaque. *Arteriosclerosis*. 1986;6:131-8.
24. Chistiakov DA, Melnichenko AA, Myasoedova VA, Grechko AV and Orekhov AN. Mechanisms of foam cell formation in atherosclerosis. *Journal of Molecular Medicine*. 2017;95:1153-1165.
25. Maguire EM, Pearce SWA and Xiao Q. Foam cell formation: A new target for fighting atherosclerosis and cardiovascular disease. *Vascular Pharmacology*. 2019;112:54-71.
26. Libby P. Inflammation in Atherosclerosis. *Arteriosclerosis, Thrombosis, and Vascular Biology*. 2012;32:2045-2051.
27. Kapellos TS, Bonaguro L, Gemünd I, Reusch N, Saglam A, Hinkley ER and Schultze JL. Human Monocyte Subsets and Phenotypes in Major Chronic Inflammatory Diseases. *Frontiers in Immunology*. 2019;10:2035.
28. Wong KL, Tai JJ, Wong WC, Han H, Sem X, Yeap WH, Kourilsky P and Wong SC. Gene expression profiling reveals the defining features of the classical, intermediate, and nonclassical human monocyte subsets. *Blood*. 2011;118:e16-31.
29. Menezes S, Melandri D, Anselmi G, Perchet T, Loschko J, Dubrot J, Patel R, Gautier EL, Hugues S, Longhi MP, Henry JY, Quezada SA, Lauvau G, Lennon-Duménil AM, Gutiérrez-Martínez E, Bessis A, Gomez-Perdiguero E, Jacome-Galarza CE, Garner H, Geissmann F, Golub R, Nussenzweig MC and Guermonprez P. The Heterogeneity of Ly6C(hi) Monocytes Controls Their Differentiation into iNOS(+) Macrophages or Monocyte-Derived Dendritic Cells. *Immunity*. 2016;45:1205-1218.
30. Belge KU, Dayyani F, Horelt A, Siedlar M, Frankenberger M, Frankenberger B, Espevik T and Ziegler-Heitbrock L. The proinflammatory CD14+CD16+DR++ monocytes are a major source of TNF. *The Journal of Immunology*. 2002;168:3536-42.
31. Boyette LB, Macedo C, Hadi K, Elinoff BD, Walters JT, Ramaswami B, Chalasani G, Taboas JM, Lakkis FG and Metes DM. Phenotype, function, and differentiation potential of human monocyte subsets. *PLoS One*. 2017;12:e0176460.
32. Schmidl C, Renner K, Peter K, Eder R, Lassmann T, Balwierz PJ, Itoh M, Nagao-Sato S, Kawaji H, Carninci P, Suzuki H, Hayashizaki Y, Andreesen R, Hume DA, Hoffmann P, Forrest AR, Kreutz MP, Edinger M and Rehli M. Transcription and enhancer profiling in human monocyte subsets. *Blood*. 2014;123:e90-9.
33. Xu H, Jiang J, Chen W, Li W and Chen Z. Vascular Macrophages in Atherosclerosis. *Journal of immunology research* 2019;2019:4354786-4354786.
34. Dansky HM, Barlow CB, Lominska C, Sikes JL, Kao C, Weinsaft J, Cybulsky MI and Smith JD. Adhesion of monocytes to arterial endothelium and initiation of atherosclerosis are critically dependent on vascular cell adhesion molecule-1 gene dosage. *Arteriosclerosis, Thrombosis, and Vascular Biology*. 2001;21:1662-7.
35. Čejková S, Králová-Lesná I and Poledne R. Monocyte adhesion to the endothelium is an initial stage of atherosclerosis development. *Cor et Vasa*. 2016;58:e419-e425.
36. Narasimhan PB, Marcovecchio P, Hamers AAJ and Hedrick CC. Nonclassical Monocytes in Health and Disease. *Annual Review of Immunology*. 2019;37:439-456.
37. Allahverdian S, Pannu PS and Francis GA. Contribution of monocyte-derived macrophages and smooth muscle cells to arterial foam cell formation. *Cardiovascular Research*. 2012;95:165-72.
38. Hilgendorf I, Swirski FK and Robbins CS. Monocyte Fate in Atherosclerosis. *Arteriosclerosis, Thrombosis, and Vascular Biology*. 2015;35:272-279.
39. Berg KE, Ljungcrantz I, Andersson L, Bryngelsson C, Hedblad B, Fredrikson GN, Nilsson J and Björkbacka H. Elevated CD14⁺⁺CD16[−]

Monocytes Predict Cardiovascular Events. *Circulation: Cardiovascular Genetics*. 2012;5:122-131.
40. Tapp LD, Wrigley BJ, Pamukcu B and Lip GYH. The CD14++CD16+ monocyte subset and monocyte-platelet interactions in patients with ST-elevation myocardial infarction. *Journal of Thrombosis and Haemostasis*. 2012;10:1231-1241.
41. Benoit M, Desnues B and Mege JL. Macrophage polarization in bacterial infections. *The Journal of Immunology*. 2008;181:3733-9.
42. Kuznetsova T, Prange KHM, Glass CK and de Winther MPJ. Transcriptional and epigenetic regulation of macrophages in atherosclerosis. *Nature Reviews Cardiology*. 2020;17:216-228.
43. Zernecke A, Erhard F, Weinberger T, Schulz C, Ley K, Saliba A-E and Cochain C. Integrated single-cell analysis-based classification of vascular mononuclear phagocytes in mouse and human atherosclerosis. *Cardiovascular Research*. 2022;119:1676-1689.
44. Xue J, Schmidt SV, Sander J, Draffehn A, Krebs W, Quester I, De Nardo D, Gohel TD, Emde M, Schmidleithner L, Ganesan H, Nino-Castro A, Mallmann MR, Labzin L, Theis H, Kraut M, Beyer M, Latz E, Freeman TC, Ulas T and Schultze JL. Transcriptome-based network analysis reveals a spectrum model of human macrophage activation. *Immunity*. 2014;40:274-88.
45. Ginhoux F, Schultze JL, Murray PJ, Ochando J and Biswas SK. New insights into the multidimensional concept of macrophage ontogeny, activation and function. *Nature Immunology*. 2016;17:34-40.
46. Willemsen L and de Winther MP. Macrophage subsets in atherosclerosis as defined by single-cell technologies. *The Journal of Pathology*. 2020;250:705-714.
47. Asare Y, Ommer M, Azombo FA, Alampour-Rajabi S, Sternkopf M, Sanati M, Gijbels MJ, Schmitz C, Sinitski D, Tilstam PV, Lue H, Gessner A, Lange D, Schmid JA, Weber C, Dichgans M, Jankowski J, Pardi R, De Winther MPJ, Noels H and Bernhagen J. Inhibition of atherogenesis by the COP9 signalosome subunit 5 in vivo. *Proc Natl Acad Sci U S A.* 2017;114(13):E2766-E2775.
48. Mills CD, Kincaid K, Alt JM, Heilman MJ and Hill AM. M-1/M-2 macrophages and the Th1/Th2 paradigm. *The Journal of Immunology*. 2000;164:6166-73.
49. Schultze JL, Schmieder A and Goerdt S. Macrophage activation in human diseases. *Seminars in Immunology*. 2015;27:249-56.
50. Martinez FO, Sica A, Mantovani A and Locati M. Macrophage activation and polarization. *Frontiers in Bioscience*. 2008;13:453-61.
51. Martinez FO, Gordon S, Locati M and Mantovani A. Transcriptional profiling of the human monocyte-to-macrophage differentiation and polarization: new molecules and patterns of gene expression. *The Journal of Immunology*. 2006;177:7303-11.
52. Gordon S and Martinez FO. Alternative activation of macrophages: mechanism and functions. *Immunity*. 2010;32:593-604.
53. Tugal D, Liao X and Jain MK. Transcriptional control of macrophage polarization. *Arteriosclerosis, Thrombosis, and Vascular Biology*. 2013;33:1135-44.
54. Rőszer T. Understanding the Mysterious M2 Macrophage through Activation Markers and Effector Mechanisms. *Mediators of Inflammation*. 2015;2015:816460.
55. He Y, Hara H and Núñez G. Mechanism and Regulation of NLRP3 Inflammasome Activation. *Trends in Biochemical Sciences*. 2016;41:1012-1021.
56. Gui Y, Zheng H and Cao RY. Foam Cells in Atherosclerosis: Novel Insights Into Its Origins, Consequences, and Molecular Mechanisms. *Frontiers in Cardiovascular Medicine*. 2022;9:845942.
57. Moore KJ and Freeman MW. Scavenger receptors in atherosclerosis: beyond lipid uptake. *Arteriosclerosis, Thrombosis, and Vascular Biology*. 2006;26:1702-11.
58. Mäkinen PI, Lappalainen JP, Heinonen SE, Leppänen P, Lähteenvuo MT, Aarnio JV, Heikkilä J, Turunen MP and Ylä-Herttuala S. Silencing of either SR-A or CD36 reduces atherosclerosis in hyperlipidaemic mice and reveals reciprocal upregulation of these receptors. *Cardiovascular Research*. 2010;88:530-538.

59. Dai X-Y, Cai Y, Mao D-D, Qi Y-F, Tang C, Xu Q, Zhu Y, Xu M-J and Wang X. Increased stability of phosphatase and tensin homolog by intermedin leading to scavenger receptor A inhibition of macrophages reduces atherosclerosis in apolipoprotein E-deficient mice. *Journal of Molecular and Cellular Cardiology*. 2012;53:509-520.
60. McLaren JE, Michael DR, Ashlin TG and Ramji DP. Cytokines, macrophage lipid metabolism and foam cells: Implications for cardiovascular disease therapy. *Progress in Lipid Research*. 2011;50:331-347.
61. Perrey S, Legendre C, Matsuura A, Guffroy C, Binet J, Ohbayashi S, Tanaka T, Ortuno JC, Matsukura T, Laugel T, Padovani P, Bellamy F and Edgar AD. Preferential pharmacological inhibition of macrophage ACAT increases plaque formation in mouse and rabbit models of atherogenesis. *Atherosclerosis*. 2001;155:359-370.
62. Wintergerst ES, Jelk J, Rahner C and Asmis R. Apoptosis induced by oxidized low density lipoprotein in human monocyte-derived macrophages involves CD36 and activation of caspase-3. *European Journal of Biochememistry*. 2000;267:6050-9.
63. Napoli C, Quehenberger O, De Nigris F, Abete P, Glass CK and Palinski W. Mildly oxidized low density lipoprotein activates multiple apoptotic signaling pathways in human coronary cells. *The FASEB Journal*. 2000;14:1996-2007.
64. Vieira O, Escargueil-Blanc I, Jürgens G, Borner C, Almeida L, Salvayre R and Nègre-Salvayre A. Oxidized LDLs alter the activity of the ubiquitin-proteasome pathway: potential role in oxidized LDL-induced apoptosis. *The FASEB Journal*. 2000;14:532-542.
65. Khan M, Pelengaris S, Cooper M, Smith C, Evan G and Betteridge J. Oxidised lipoproteins may promote inflammation through the selective delay of engulfment but not binding of apoptotic cells by macrophages. *Atherosclerosis*. 2003;171:21-29.
66. Phillips MC. Molecular Mechanisms of Cellular Cholesterol Efflux*. *Journal of Biological Chemistry*. 2014;289:24020-24029.
67. Ertek S. High-density Lipoprotein (HDL) Dysfunction and the Future of HDL. *Current Vascular Pharmacology*. 2018;16:490-498.
68. Baraniecki Ł, Tokarz-Deptuła B, Syrenicz A and Deptuła W. Macrophage efferocytosis in atherosclerosis. *Scandinavian Journal of Immunology*. 2023;97:e13251.
69. D'Arcy MS. Cell death: a review of the major forms of apoptosis, necrosis and autophagy. *Cell Biology International*. 2019;43:582-592.
70. Davidovich P, Kearney CJ and Martin SJ. Inflammatory outcomes of apoptosis, necrosis and necroptosis. *Biological Chemistry*. 2014;395.
71. Zhang Y, Morgan MJ, Chen K, Choksi S and Liu Z-g. Induction of autophagy is essential for monocyte-macrophage differentiation. *Blood*. 2012;119:2895-2905.
72. Tonnus W, Meyer C, Paliege A, Belavgeni A, von Mässenhausen A, Bornstein SR, Hugo C, Becker JU and Linkermann A. The pathological features of regulated necrosis. *The Journal of Pathology*. 2019;247:697-707.
73. Galluzzi L, Vitale I, Aaronson SA, Abrams JM, Adam D, Agostinis P, Alnemri ES, Altucci L, Amelio I, Andrews DW, Annicchiarico-Petruzzelli M, Antonov AV, Arama E, Baehrecke EH, Barlev NA, Bazan NG, Bernassola F, Bertrand MJM, Bianchi K, Blagosklonny MV, Blomgren K, Borner C, Boya P, Brenner C, Campanella M, Candi E, Carmona-Gutierrez D, Cecconi F, Chan FK, Chandel NS, Cheng EH, Chipuk JE, Cidlowski JA, Ciechanover A, Cohen GM, Conrad M, Cubillos-Ruiz JR, Czabotar PE, D'Angiolella V, Dawson TM, Dawson VL, De Laurenzi V, De Maria R, Debatin KM, DeBerardinis RJ, Deshmukh M, Di Daniele N, Di Virgilio F, Dixit VM, Dixon SJ, Duckett CS, Dynlacht BD, El-Deiry WS, Elrod JW, Fimia GM, Fulda S, García-Sáez AJ, Garg AD, Garrido C, Gavathiotis E, Golstein P, Gottlieb E, Green DR, Greene LA, Gronemeyer H, Gross A, Hajnoczky G, Hardwick JM, Harris IS, Hengartner MO, Hetz C, Ichijo H, Jäättelä M, Joseph B, Jost PJ, Juin PP, Kaiser WJ, Karin M, Kaufmann T, Kepp O, Kimchi A, Kitsis RN, Klionsky DJ, Knight RA, Kumar S, Lee SW, Lemasters JJ, Levine B, Linkermann A, Lipton SA, Lockshin RA, López-Otín C, Lowe SW, Luedde T, Lugli E, MacFarlane M, Madeo F, Malewicz M, Malorni W, Manic G, Marine JC, Martin SJ, Martinou JC, Medema JP, Mehlen P, Meier P, Melino S, Miao EA, Molkentin JD, Moll UM, Muñoz-Pinedo C, Nagata S, Nuñez G, Oberst A, Oren M, Overholtzer M, Pagano M, Panaretakis T, Pasparakis M, Penninger JM, Pereira DM, Pervaiz S, Peter ME, Piacentini M, Pinton P, Prehn

JHM, Puthalakath H, Rabinovich GA, Rehm M, Rizzuto R, Rodrigues CMP, Rubinsztein DC, Rudel T, Ryan KM, Sayan E, Scorrano L, Shao F, Shi Y, Silke J, Simon HU, Sistigu A, Stockwell BR, Strasser A, Szabadkai G, Tait SWG, Tang D, Tavernarakis N, Thorburn A, Tsujimoto Y, Turk B, Vanden Berghe T, Vandenabeele P, Vander Heiden MG, Villunger A, Virgin HW, Vousden KH, Vucic D, Wagner EF, Walczak H, Wallach D, Wang Y, Wells JA, Wood W, Yuan J, Zakeri Z, Zhivotovsky B, Zitvogel L, Melino G and Kroemer G. Molecular mechanisms of cell death: recommendations of the Nomenclature Committee on Cell Death 2018. *Cell Death & Differentiation*. 2018;25:486-541.

74. Shi J, Gao W and Shao F. Pyroptosis: Gasdermin-Mediated Programmed Necrotic Cell Death. *Trends in Biochemical Sciences*. 2017;42:245-254.

75. Jia C, Chen H, Zhang J, Zhou K, Zhuge Y, Niu C, Qiu J, Rong X, Shi Z, Xiao J, Shi Y and Chu M. Role of pyroptosis in cardiovascular diseases. *International Immunopharmacology*. 2019;67:311-318.

76. Ofengeim D and Yuan J. Regulation of RIP1 kinase signalling at the crossroads of inflammation and cell death. *Nature Reviews Molecular Cell Biology*. 2013;14:727-36.

77. Boada-Romero E, Martinez J, Heckmann BL and Green DR. The clearance of dead cells by efferocytosis. *Nature Reviews Molecular Cell Biology*. 2020;21:398-414.

78. Adhyaru BB and Jacobson TA. Safety and efficacy of statin therapy. *Nature Reviews Cardiology*. 2018;15:757-769.

79. Zhan S, Tang M, Liu F, Xia P, Shu M and Wu X. Ezetimibe for the prevention of cardiovascular disease and all-cause mortality events. *Cochrane Database of Systematic Reviews*. 2018.

80. Mach F, Baigent C, Catapano AL, Koskinas KC, Casula M, Badimon L, Chapman MJ, De Backer GG, Delgado V, Ference BA, Graham IM, Halliday A, Landmesser U, Mihaylova B, Pedersen TR, Riccardi G, Richter DJ, Sabatine MS, Taskinen M-R, Tokgozoglu L, Wiklund O and Group ESD. 2019 ESC/EAS Guidelines for the management of dyslipidaemias: lipid modification to reduce cardiovascular risk: The Task Force for the management of dyslipidaemias of the European Society of Cardiology (ESC) and European Atherosclerosis Society (EAS). *European Heart Journal*. 2019;41:111-188.

81. Wang Y and Liu ZP. PCSK9 Inhibitors: Novel Therapeutic Strategies for Lowering LDLCholesterol. *Mini-Reviews in Medicinal Chemistry*. 2019;19:165-176.

82. Ridker PM. Anti-inflammatory therapy for atherosclerosis: interpreting divergent results from the CANTOS and CIRT clinical trials. *Journal of Internal Medicine*. 2019;285:503-509.

83. Hansson GK. Inflammation and Atherosclerosis. *Circulation*. 2017;136:1875-1877.

84. Gamad N, Shafiq N and Malhotra S. Effect size in CANTOS trial. *BMJ Evidence-Based Medicine*. 2018;23:44-44.

85. Hedin U and Matic LP. Recent advances in therapeutic targeting of inflammation in atherosclerosis. *Journal of Vascular Surgery*. 2019;69:944-951.

86. Ibañez B and Fuster V. CANTOS. *Circulation Research*. 2017;121:1320-1322.

87. Capodanno D and Angiolillo DJ. Canakinumab for secondary prevention of atherosclerotic disease. *Expert Opinion on Biological Therapy*. 2018;18:215-220.

88. Chan ES and Cronstein BN. Methotrexate--how does it really work? *Nature Reviews Rheumatology*. 2010;6:175-8.

89. Ridker PM, Everett BM, Pradhan A, Macfadyen JG, Solomon DH, Zaharris E, Mam V, Hasan A, Rosenberg Y, Iturriaga E, Gupta M, Tsigoulis M, Verma S, Clearfield M, Libby P, Goldhaber SZ, Seagle R, Ofori C, Saklayen M, Butman S, Singh N, Le May M, Bertrand O, Johnston J, Paynter NP and Glynn RJ. Low-Dose Methotrexate for the Prevention of Atherosclerotic Events. *New England Journal of Medicine*. 2019;380:752-762.

90. Tardif J-C, Kouz S, Waters DD, Bertrand OF, Diaz R, Maggioni AP, Pinto FJ, Ibrahim R, Gamra H, Kiwan GS, Berry C, López-Sendón J, Ostadal P, Koenig W, Angoulvant D, Grégoire JC, Lavoie M-A, Dubé M-P, Rhainds D, Provencher M, Blondeau L, Orfanos A, L'Allier PL, Guertin M-C and Roubille F. Efficacy and Safety of Low-Dose Colchicine after Myocardial Infarction. *New England Journal of Medicine*. 2019;381:2497-2505.

91. Vaidya K, Arnott C, Martínez GJ, Ng B, McCormack S, Sullivan DR, Celermajer DS and Patel S. Colchicine Therapy and Plaque Stabilization in Patients With Acute Coronary Syndrome: A CT Coronary Angiography Study. *JACC Cardiovasc Imaging*. 2018;11:305-316.
92. Pan Z, Cheng J, Yang W, Chen L and Wang J. Effect of colchicine on inflammatory markers in patients with coronary artery disease: A meta-analysis of clinical trials. *European Journal of Pharmacology*. 2022;927:175068.
93. Milic, Tian and Bernhagen. Role of the COP9 Signalosome (CSN) in Cardiovascular Diseases. *Biomolecules*. 2019;9:217.
94. Chamovitz DA, Wei N, Osterlund MT, von Arnim AG, Staub JM, Matsui M and Deng XW. The COP9 complex, a novel multisubunit nuclear regulator involved in light control of a plant developmental switch. *Cell*. 1996;86:115-21.
95. Seeger M, Kraft R, Ferrell K, Bech-Otschir D, Dumdey R, Schade R, Gordon C, Naumann M and Dubiel W. A novel protein complex involved in signal transduction possessing similarities to 26S proteasome subunits. *The FASEB Journal*. 1998;12:469-478.
96. Zhang X-C, Chen J, Su C-H, Yang H-Y and Lee M-H. Roles for CSN5 in control of p53/MDM2 activities. 2008;103:1219-1230.
97. Eckey M, Hong W, Papaioannou M and Baniahmad A. The Nucleosome Assembly Activity of NAP1 Is Enhanced by Alien. 2007;27:3557-3568.
98. Lykke-Andersen K, Schaefer L, Menon S, Deng X-W, Miller JB and Wei N. Disruption of the COP9 Signalosome Csn2 Subunit in Mice Causes Deficient Cell Proliferation, Accumulation of p53 and Cyclin E, and Early Embryonic Death. *Molecular and Cellular Biology*. 2003;23:6790-6797.
99. Claret F-X, Hibi M, Dhut S, Toda T and Karin M. A new group of conserved coactivators that increase the specificity of AP-1 transcription factors. *Nature*. 1996;383:453-457.
100. Wee S, Geyer RK, Toda T and Wolf DA. CSN facilitates Cullin–RING ubiquitin ligase function by counteracting autocatalytic adapter instability. *Nature Cell Biology*. 2005;7:387-391.
101. Lyapina S. Promotion of NEDD8-CUL1 Conjugate Cleavage by COP9 Signalosome. *Science*. 2001;292:1382-1385.
102. Cope GA, Suh GSB, Aravind L, Schwarz SE, Zipursky SL, Koonin EV and Deshaies RJ. Role of Predicted Metalloprotease Motif of Jab1/Csn5 in Cleavage of Nedd8 from Cul1. *Science*. 2002;298:608-611.
103. Wu J-T, Lin H-C, Hu Y-C and Chien C-T. Neddylation and deneddylation regulate Cul1 and Cul3 protein accumulation. *Nature Cell Biology*. 2005;7:1014-1020.
104. Enchev RI, Schulman BA and Peter M. Protein neddylation: beyond cullin–RING ligases. *Nature Reviews Molecular Cell Biology*. 2015;16:30-44.
105. Lingaraju GM, Bunker RD, Cavadini S, Hess D, Hassiepen U, Renatus M, Fischer ES and Thomä NH. Crystal structure of the human COP9 signalosome. *Nature*. 2014;512:161-165.
106. Schwechheimer C, Serino G and Deng X-W. Multiple Ubiquitin Ligase–Mediated Processes Require COP9 Signalosome and AXR1 Function. *The Plant Cell*. 2002;14:2553-2563.
107. Chamovitz DA and Glickman M. The COP9 signalosome. *Current Biology*. 2002;12:R232.
108. Cope GA and Deshaies RJ. COP9 Signalosome. *Cell*. 2003;114:663-671.
109. Wei N and Deng XW. The COP9 Signalosome. *Annual Review of Cell and Developmental Biology*. 2003;19:261-286.
110. Qu J, Zou T and Lin Z. The Roles of the Ubiquitin–Proteasome System in the Endoplasmic Reticulum Stress Pathway. *International Journal of Molecular Sciences*. 2021;22:1526.
111. Skaar JR, Pagan JK and Pagano M. Mechanisms and function of substrate recruitment by F-box proteins. *Nature Reviews Molecular Cell Biology*. 2013;14:369-381.
112. Park J, Cho J and Song EJ. Ubiquitin–proteasome system (UPS) as a target for anticancer treatment. *Archives of Pharmacal Research*. 2020;43:1144-1161.

113. Goldberg AL, Cascio P, Saric T and Rock KL. The importance of the proteasome and subsequent proteolytic steps in the generation of antigenic peptides. *Molecular Immunology*. 2002;39:147-64.
114. Hershko A. Roles of ubiquitin-mediated proteolysis in cell cycle control. *Current Opinion in Cell Biology*. 1997;9:788-99.
115. Jesenberger V and Jentsch S. Deadly encounter: ubiquitin meets apoptosis. *Nature Reviews Molecular Cell Biology*. 2002;3:112-21.
116. Desterro J, Rodriguez MS and Hay R. Regulation of transcription factors by protein degradation. *Cellular and molecular life sciences : CMLS*. 2000;57:1207-19.
117. Ciechanover A, Orian A and Schwartz AL. Ubiquitin-mediated proteolysis: biological regulation via destruction. *Bioessays*. 2000;22:442-51.
118. Tisdale MJ. Pathogenesis of cancer cachexia. *The Journal of Supportive Oncology*. 2003;1:159-68.
119. van Wijk SJL and Timmers HTM. The family of ubiquitin-conjugating enzymes (E2s): deciding between life and death of proteins. *The FASEB Journal*. 2010;24:981-993.
120. Nguyen HC, Wang W and Xiong Y. Cullin-RING E3 Ubiquitin Ligases: Bridges to Destruction: Springer International Publishing; 2017: 323-347.
121. Berndsen CE and Wolberger C. New insights into ubiquitin E3 ligase mechanism. *Nature Structural & Molecular Biology*. 2014;21:301-307.
122. Sarikas A, Hartmann T and Pan Z-Q. The cullin protein family. *Genome Biology*. 2011;12:220.
123. Duda DM, Scott DC, Calabrese MF, Zimmerman ES, Zheng N and Schulman BA. Structural regulation of cullin-RING ubiquitin ligase complexes. *Current Opinion in Structural Biology*. 2011;21:257-64.
124. Deshaies RJ, Emberley ED and Saha A. Control of cullin-ring ubiquitin ligase activity by nedd8. *Sub-Cellular Biochemistry*. 2010;54:41-56.
125. Whitby FG, Xia G, Pickart CM and Hill CP. Crystal structure of the human ubiquitin-like protein NEDD8 and interactions with ubiquitin pathway enzymes. *Journal of Biological Chemistry*. 1998;273:34983-91.
126. Huang DT, Paydar A, Zhuang M, Waddell MB, Holton JM and Schulman BA. Structural Basis for Recruitment of Ubc12 by an E2 Binding Domain in NEDD8's E1. *Molecular Cell*. 2005;17:341-350.
127. Deshaies RJ and Joazeiro CA. RING domain E3 ubiquitin ligases. *Annual Review of Biochemistry*. 2009;78:399-434.
128. Hotton SK and Callis J. Regulation of cullin RING ligases. *Annual Review of Plant Biology*. 2008;59:467-89.
129. Mosadeghi R, Reichermeier KM, Winkler M, Schreiber A, Reitsma JM, Zhang Y, Stengel F, Cao J, Kim M, Sweredoski MJ, Hess S, Leitner A, Aebersold R, Peter M, Deshaies RJ and Enchev RI. Structural and kinetic analysis of the COP9-Signalosome activation and the cullin-RING ubiquitin ligase deneddylation cycle. *eLife*. 2016;5.
130. Du W, Zhang R, Muhammad B and Pei D. Targeting the COP9 signalosome for cancer therapy. *Cancer Biology & Medicine*. 2022;19:573-90.
131. Wang L, Du WQ, Xie M, Liu MR, Huo FC, Yang J and Pei DS. Jab1 promotes gastric cancer tumorigenesis via non-ubiquitin proteasomal degradation of p14ARF. *Gastric Cancer*. 2020;23:1003-1017.
132. Li J, Li Y, Wang B, Ma Y and Chen P. CSN5/Jab1 facilitates non-small cell lung cancer cell growth through stabilizing survivin. *Biochem Biophys Res Commun*. 2018;500:132-138.
133. Zhu Y, Qiu Z, Zhang X, Qian F, Wang B, Wang L, Shi H and Yu R. Jab1 promotes glioma cell proliferation by regulating Siah1/β-catenin pathway. *Journal of Neuro-Oncology*. 2017;131:31-39.
134. Schweitzer K, Bozko PM, Dubiel W and Naumann M. CSN controls NF-κB by deubiquitinylation of IκBα. *The EMBO Journal*. 2007;26:1532-1541.
135. Schweitzer K and Naumann M. Control of NF-kappaB activation by the COP9 signalosome. *Biochemical Society Transactions*. 2010;38:156-61.

136. Asare Y, Shagdarsuren E, Schmid JA, Tilstam PV, Grommes J, El Bounkari O, Schütz AK, Weber C, de Winther MP, Noels H and Bernhagen J. Endothelial CSN5 impairs NF-κB activation and monocyte adhesion to endothelial cells and is highly expressed in human atherosclerotic lesions. *Thrombosis and Haemostasis*. 2013;110:141-52.
137. Bech-Otschir D, Kraft R, Huang X, Henklein P, Kapelari B, Pollmann C and Dubiel W. COP9 signalosome-specific phosphorylation targets p53 to degradation by the ubiquitin system. *The EMBO Journal*. 2001;20:1630-9.
138. Vogl AM, Phu L, Becerra R, Giusti SA, Verschueren E, Hinkle TB, Bordenave MD, Adrian M, Heidersbach A, Yankilevich P, Stefani FD, Wurst W, Hoogenraad CC, Kirkpatrick DS, Refojo D and Sheng M. Global site-specific neddylation profiling reveals that NEDDylated cofilin regulates actin dynamics. *Nature Structural & Molecular Biology*. 2020;27:210-220.
139. Khera N and Rajput S. Therapeutic Potential of Small Molecule Inhibitors. *Journal of Cellular Biochemistry*. 2017;118:959-961.
140. Brownell JE, Sintchak MD, Gavin JM, Liao H, Bruzzese FJ, Bump NJ, Soucy TA, Milhollen MA, Yang X, Burkhardt AL, Ma J, Loke HK, Lingaraj T, Wu D, Hamman KB, Spelman JJ, Cullis CA, Langston SP, Vyskocil S, Sells TB, Mallender WD, Visiers I, Li P, Claiborne CF, Rolfe M, Bolen JB and Dick LR. Substrate-assisted inhibition of ubiquitin-like protein-activating enzymes: the NEDD8 E1 inhibitor MLN4924 forms a NEDD8-AMP mimetic in situ. *Molecular Cell*. 2010;37:102-11.
141. Milhollen MA, Traore T, Adams-Duffy J, Thomas MP, Berger AJ, Dang L, Dick LR, Garnsey JJ, Koenig E, Langston SP, Manfredi M, Narayanan U, Rolfe M, Staudt LM, Soucy TA, Yu J, Zhang J, Bolen JB and Smith PG. MLN4924, a NEDD8-activating enzyme inhibitor, is active in diffuse large B-cell lymphoma models: rationale for treatment of NF-{kappa}B-dependent lymphoma. *Blood*. 2010;116:1515-23.
142. Zhou L, Jiang Y, Luo Q, Li L and Jia L. Neddylation: a novel modulator of the tumor microenvironment. *Molecular Cancer*. 2019;18.
143. Soucy TA, Smith PG, Milhollen MA, Berger AJ, Gavin JM, Adhikari S, Brownell JE, Burke KE, Cardin DP, Critchley S, Cullis CA, Doucette A, Garnsey JJ, Gaulin JL, Gershman RE, Lublinsky AR, McDonald A, Mizutani H, Narayanan U, Olhava EJ, Peluso S, Rezaei M, Sintchak MD, Talreja T, Thomas MP, Traore T, Vyskocil S, Weatherhead GS, Yu J, Zhang J, Dick LR, Claiborne CF, Rolfe M, Bolen JB and Langston SP. An inhibitor of NEDD8-activating enzyme as a new approach to treat cancer. *Nature*. 2009;458:732-736.
144. Swords RT, Erba HP, DeAngelo DJ, Bixby DL, Altman JK, Maris M, Hua Z, Blakemore SJ, Faessel H, Sedarati F, Dezube BJ, Giles FJ and Medeiros BC. Pevonedistat (MLN4924), a First-in-Class NEDD8-activating enzyme inhibitor, in patients with acute myeloid leukaemia and myelodysplastic syndromes: a phase 1 study. *British Journal of Haematology*. 2015;169:534-543.
145. Hammill JT, Bhasin D, Scott DC, Min J, Chen Y, Lu Y, Yang L, Kim HS, Connelly MC, Hammill C, Holbrook G, Jeffries C, Singh B, Schulman BA and Guy RK. Discovery of an Orally Bioavailable Inhibitor of Defective in Cullin Neddylation 1 (DCN1)-Mediated Cullin Neddylation. *Journal of Medicinal Chemistry*. 2018;61:2694-2706.
146. Zheng Y-C, Guo Y-J, Wang B, Wang C, Mamun MAA, Gao Y and Liu H-M. Targeting neddylation E2s: a novel therapeutic strategy in cancer. *Journal of Hematology & Oncology*. 2021;14.
147. Majolée J, Pronk MCA, Jim KK, Van Bezu JSM, Van Der Sar AM, Hordijk PL and Kovačević I. CSN5 inhibition triggers inflammatory signaling and Rho/ROCK-dependent loss of endothelial integrity. *Scientific Reports*. 2019;9.
148. Schlierf A, Altmann E, Quancard J, Jefferson AB, Assenberg R, Renatus M, Jones M, Hassiepen U, Schaefer M, Kiffe M, Weiss A, Wiesmann C, Sedrani R, Eder J and Martoglio B. Targeted inhibition of the COP9 signalosome for treatment of cancer. *Nature Communications*. 2016;7:13166.
149. El-Mesery M, Seher A, Stühmer T, Siegmund D and Wajant H. MLN4924 sensitizes monocytes and maturing dendritic cells for TNF-dependent and -independent necroptosis. *British Journal of Pharmacology*. 2015;172:1222-1236.

150. Raghavan S, Singh NK, Mani AM and Rao GN. Protease-activated receptor 1 inhibits cholesterol efflux and promotes atherogenesis via cullin 3-mediated degradation of the ABCA1 transporter. *Journal of Biological Chemistry*. 2018;293:10574-10589.
151. Schwarz A, Bonaterra GA, Schwarzbach H and Kinscherf R. Oxidized LDL-induced JAB1 influences NF-κB independent inflammatory signaling in human macrophages during foam cell formation. *Journal of Biomedical Science*. 2017;24.
152. Swords RT, Coutre S, Maris MB, Zeidner JF, Foran JM, Cruz J, Erba HP, Berdeja JG, Tam W, Vardhanabhuti S, Pawlikowska-Dobler I, Faessel HM, Dash AB, Sedarati F, Dezube BJ, Faller DV and Savona MR. Pevonedistat, a first-in-class NEDD8-activating enzyme inhibitor, combined with azacitidine in patients with AML. *Blood*. 2018;131:1415-1424.
153. Schindelin J, Arganda-Carreras I, Frise E, Kaynig V, Longair M, Pietzsch T, Preibisch S, Rueden C, Saalfeld S, Schmid B, Tinevez J-Y, White DJ, Hartenstein V, Eliceiri K, Tomancak P and Cardona A. Fiji: an open-source platform for biological-image analysis. *Nature Methods*. 2012;9:676-682.
154. Rueden CT, Schindelin J, Hiner MC, DeZonia BE, Walter AE, Arena ET and Eliceiri KW. ImageJ2: ImageJ for the next generation of scientific image data. *BMC Bioinformatics*. 2017;18:529.
155. Ziegler-Heitbrock HW, Thiel E, Fütterer A, Herzog V, Wirtz A and Riethmüller G. Establishment of a human cell line (Mono Mac 6) with characteristics of mature monocytes. *International Journal of Cancer*. 1988;41:456-61.
156. Heap RE, Marín-Rubio JL, Peltier J, Heunis T, Dannoura A, Moore A and Trost M. Proteomics characterisation of the L929 cell supernatant and its role in BMDM differentiation. *Life Science Alliance*. 2021;4:e202000957.
157. Taylor SC and Posch A. The Design of a Quantitative Western Blot Experiment. *BioMed Research International*. 2014;2014:1-8.
158. Kopitar AN, Markelj G, Oražem M, Blazina Š, Avčin T, Ihan A and Debeljak M. Flow Cytometric Determination of Actin Polymerization in Peripheral Blood Leukocytes Effectively Discriminate Patients With Homozygous Mutation in ARPC1B From Asymptomatic Carriers and Normal Controls. *Frontiers in Immunology*. 2019;10:1632-1632.
159. Moulding DA, Record J, Malinova D and Thrasher AJ. Actin cytoskeletal defects in immunodeficiency. *Immunological Reviews*. 2013;256:282-99.
160. Bamburg JR and Bernstein BW. Actin dynamics and cofilin-actin rods in alzheimer disease. *Cytoskeleton (Hoboken)*. 2016;73:477-97.
161. Ostrowska Z and Moraczewska J. Cofilin - a protein controlling dynamics of actin filaments. *Postepy Hig Med Dosw (Online)*. 2017;71:339-351.
162. Dupire J, Puech PH, Helfer E and Viallat A. Mechanical adaptation of monocytes in model lung capillary networks. *Proc Natl Acad Sci U S A*. 2020;117:14798-14804.
163. Lämmermann T and Sixt M. Mechanical modes of 'amoeboid' cell migration. *Current Opinion in Cell Biology*. 2009;21:636-44.
164. Bhattacharya A, Ghosh P, Prasad R, Ghosh A, Das K, Roy A, Mallik S, Sinha DK and Sen P. MAP Kinase driven actomyosin rearrangement is a crucial regulator of monocyte to macrophage differentiation. *Cell Signalling*. 2020;73:109691.
165. Liu H, Bei Q and Luo X. MLN4924 inhibits cell proliferation by targeting the activated neddylation pathway in endometrial carcinoma. *Journal of International Medical Research*. 2021;49:3000605211018592.
166. Torka P, Mavis C, Kothari S, Belliotti S, Gu J, Sundaram S, Barth M and Hernandez-Ilizaliturri FJ. Pevonedistat, a NEDD8-Activating Enzyme Inhibitor, Induces Apoptosis and Augments Efficacy of Chemotherapy and Small Molecule Inhibitors in Pre-clinical Models of Diffuse Large B-cell Lymphoma. *EJHaem*. 2020;1:122-132.
167. El-Mesery M, Anany MA, Hazem SH and Shaker ME. The NEDD8-activating enzyme inhibition with MLN4924 sensitizes human cancer cells of different origins to apoptosis and necroptosis. *Archives of Biochemistry and Biophysics*. 2020;691:108513.
168. Lewno MT, Cui T and Wang X. Cullin Deneddylation Suppresses the Necroptotic Pathway in Cardiomyocytes. *Frontiers in Physiology*. 2021;12:690423.

169. Xu J, Huang Y, Zhao J, Wu L, Qi Q, Liu Y, Li G, Li J, Liu H and Wu H. Cofilin: A Promising Protein Implicated in Cancer Metastasis and Apoptosis. *Frontiers in Cell and Developmental Biology*. 2021;9:599065.
170. Crowley LC and Waterhouse NJ. Detecting Cleaved Caspase-3 in Apoptotic Cells by Flow Cytometry. *Cold Spring Harbor Protocols*. 2016;2016.
171. Reuter S and Lang D. Life span of monocytes and platelets: importance of interactions. *FBL*. 2009;14:2432-2447.
172. Li L, Liu B, Dong T, Lee HW, Yu J, Zheng Y, Gao H, Zhang Y, Chu Y, Liu G, Niu W, Zheng S, Jeong LS and Jia L. Neddylation pathway regulates the proliferation and survival of macrophages. *Biochemical and Biophysical Research Communications*. 2013;432:494-8.
173. Segovia JA, Tsai SY, Chang TH, Shil NK, Weintraub ST, Short JD and Bose S. Nedd8 regulates inflammasome-dependent caspase-1 activation. *Molecular and Cellular Biology*. 2015;35:582-97.
174. Dergunov AD and Baserova VB. Different Pathways of Cellular Cholesterol Efflux. *Cell Biochemistry and Biophysics*. 2022;80:471-481.
175. Azuma Y, Takada M, Maeda M, Kioka N and Ueda K. The COP9 signalosome controls ubiquitinylation of ABCA1. *Biochemical and Biophysical Research Communications*. 2009;382:145-148.
176. Keuss MJ, Thomas Y, McArthur R, Wood NT, Knebel A and Kurz T. Characterization of the mammalian family of DCN-type NEDD8 E3 ligases. *Journal of Cell Science*. 2016;129:1441-54.
177. Lydeard JR, Schulman BA and Harper JW. Building and remodelling Cullin-RING E3 ubiquitin ligases. *EMBO Reports*. 2013;14:1050-1061.
178. Monda JK, Scott DC, Miller DJ, Lydeard J, King D, Harper JW, Bennett EJ and Schulman BA. Structural conservation of distinctive N-terminal acetylation-dependent interactions across a family of mammalian NEDD8 ligation enzymes. *Structure*. 2013;21:42-53.
179. Meyer-Schaller N, Chou YC, Sumara I, Martin DD, Kurz T, Katheder N, Hofmann K, Berthiaume LG, Sicheri F and Peter M. The human Dcn1-like protein DCNL3 promotes Cul3 neddylation at membranes. *Proc Natl Acad Sci U S A*. 2009;106:12365-70.
180. Kim AY, Bommeljé CC, Lee BE, Yonekawa Y, Choi L, Morris LG, Huang G, Kaufman A, Ryan RJ, Hao B, Ramanathan Y and Singh B. SCCRO (DCUN1D1) is an essential component of the E3 complex for neddylation. *Journal of Biological Chemistry*. 2008;283:33211-20.
181. Uhlén M, Fagerberg L, Hallström BM, Lindskog C, Oksvold P, Mardinoglu A, Sivertsson Å, Kampf C, Sjöstedt E, Asplund A, Olsson I, Edlund K, Lundberg E, Navani S, Szigyarto CA, Odeberg J, Djureinovic D, Takanen JO, Hober S, Alm T, Edqvist PH, Berling H, Tegel H, Mulder J, Rockberg J, Nilsson P, Schwenk JM, Hamsten M, von Feilitzen K, Forsberg M, Persson L, Johansson F, Zwahlen M, von Heijne G, Nielsen J and Pontén F. Proteomics. Tissue-based map of the human proteome. *Science*. 2015;347:1260419.
182. Kim YM, Kim HJ, Kim DK, Jung DH, Cho HJ, Kim S, Nah J and Jang SM. Differential dynamics of cullin deneddylation via COP9 signalosome subunit 5 interaction. *Biochemical and Biophysiological Research Communications*. 2022;637:341-347.
183. Zhang S and Sun Y. Cullin RING Ligase 5 (CRL-5): Neddylation Activation and Biological Functions. *Advances in Experimental Medicine and Biology*. 2020;1217:261-283.
184. Weber A, Wasiliew P and Kracht M. Interleukin-1β (IL-1β) processing pathway. *Science signaling*. 2010;3:cm2-cm2.
185. De Cesco S, Kurian J, Dufresne C, Mittermaier AK and Moitessier N. Covalent inhibitors design and discovery. *European Journal of Medicinal Chemistry*. 2017;138:96-114.
186. Aljoundi A, Bjij I, El Rashedy A and Soliman MES. Covalent Versus Non-covalent Enzyme Inhibition: Which Route Should We Take? A Justification of the Good and Bad from Molecular Modelling Perspective. *The Protein Journal*. 2020;39:97-105.
187. Bjij I, Olotu FA, Agoni C, Adeniji E, Khan S, El Rashedy A, Cherqaoui D and Soliman MES. Covalent Inhibition in Drug Discovery: Filling the Void in Literature. *Current Topics in Medicinal Chemistry*. 2018;18:1135-1145.

188. Jin J, Jing Z, Ye Z, Guo L, Hua L, Wang Q, Wang J, Cheng Q, Zhang J, Xu Y and Wei L. MLN4924 suppresses lipopolysaccharide-induced proinflammatory cytokine production in neutrophils in a dose-dependent manner. *Oncology Letters*. 2018;15:8039-8045.
189. Prangley E, Kumar T and Ponda MP. Quantifying Human Monocyte Chemotaxis In Vitro and Murine Lymphocyte Trafficking In Vivo. *Journal of Visualized Experiments*. 2017.
190. Read MA, Brownell JE, Gladysheva TB, Hottelet M, Parent LA, Coggins MB, Pierce JW, Podust VN, Luo RS, Chau V and Palombella VJ. Nedd8 modification of cul-1 activates SCF(beta(TrCP))-dependent ubiquitination of IkappaBalpha. *Molecular and Cellular Biology*. 2000;20:2326-33.
191. Rieger AM, Nelson KL, Konowalchuk JD and Barreda DR. Modified annexin V/propidium iodide apoptosis assay for accurate assessment of cell death. *Journal of Visualized Experiments*. 2011.
192. Hao R, Song Y, Li R, Wu Y, Yang X, Li X, Qian F, Ye RD and Sun L. MLN4924 protects against interleukin-17A-induced pulmonary inflammation by disrupting ACT1-mediated signaling. *American Journal of Physiology-Lung Cellular and Molecular Physiology*. 2019;316:L1070-L1080.
193. Yang G, Chen J, He Y, Luo H, Yuan H, Chen L, Huang L, Mao F, Hu S, Qian Y, Miao C and Feng R. Neddylation Inhibition Causes Impaired Mouse Embryo Quality and Blastocyst Hatching Failure Through Elevated Oxidative Stress and Reduced IL-1β. *Frontiers in Immunology*. 2022;13:925702.
194. Edin S, Wikberg ML, Rutegård J, Oldenborg P-A and Palmqvist R. Phenotypic Skewing of Macrophages In Vitro by Secreted Factors from Colorectal Cancer Cells. *PLOS ONE*. 2013;8:e74982.
195. Zhou L, Zhang W, Sun Y and Jia L. Protein neddylation and its alterations in human cancers for targeted therapy. *Cell Signalling*. 2018;44:92-102.
196. Mai W and Liao Y. Targeting IL-1β in the Treatment of Atherosclerosis. *Frontiers in Immunology*. 2020;11:589654.
197. Abbate A, Trankle CR, Buckley LF, Lipinski MJ, Appleton D, Kadariya D, Canada JM, Carbone S, Roberts CS, Abouzaki N, Melchior R, Christopher S, Turlington J, Mueller G, Garnett J, Thomas C, Markley R, Wohlford GF, Puckett L, Medina de Chazal H, Chiabrando JG, Bressi E, Del Buono MG, Schatz A, Vo C, Dixon DL, Biondi-Zoccai GG, Kontos MC and Van Tassell BW. Interleukin-1 Blockade Inhibits the Acute Inflammatory Response in Patients With ST-Segment-Elevation Myocardial Infarction. *Journal of the American Heart Association*. 2020;9:e014941.
198. Boro M, Govatati S, Kumar R, Singh NK, Pichavaram P, Traylor JG, Jr., Orr AW and Rao GN. Thrombin-Par1 signaling axis disrupts COP9 signalosome subunit 3-mediated ABCA1 stabilization in inducing foam cell formation and atherogenesis. *Cell Death & Differentiation*. 2021;28:780-798.

Appendix

Supplemental figures

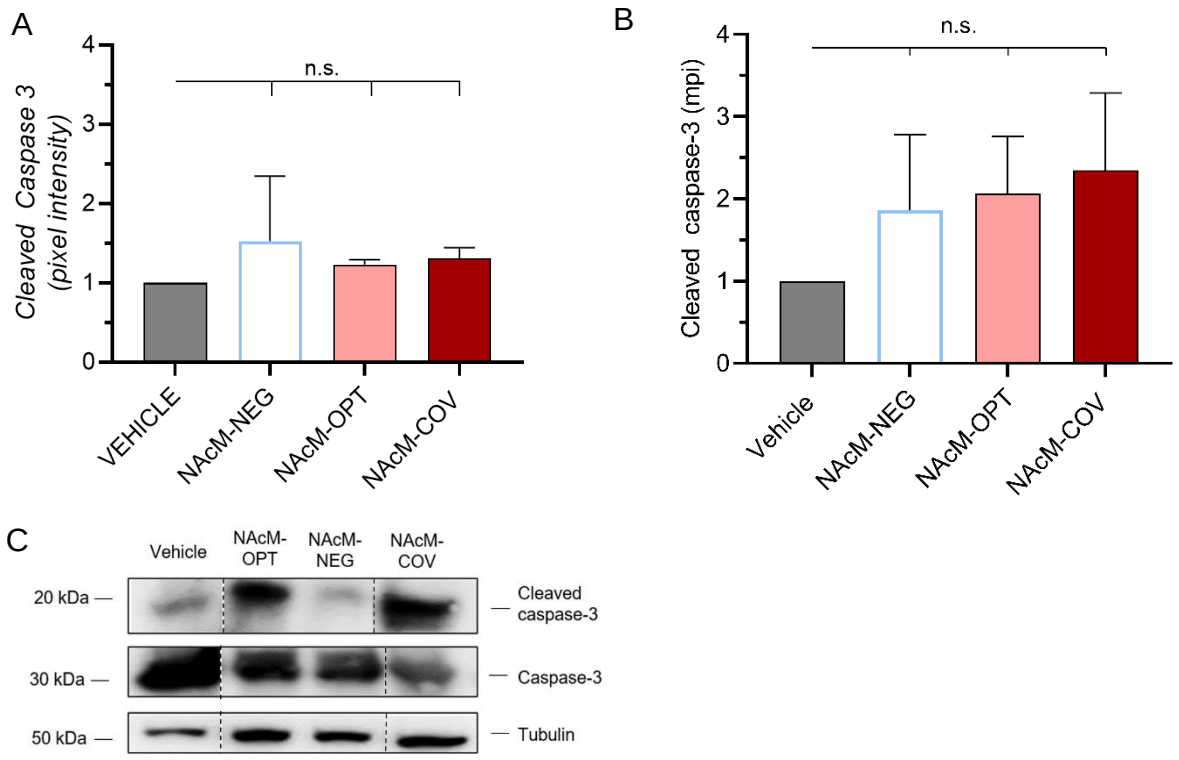

Figure A 1 Cleaved caspase 3 levels in MM6 are upregulated after NAcM-OPT and -COV treatment. Immunoblot quantification of cleaved caspase-3 mean pixel intensities (mpi) of primary human monocytes and MM6 after 16 h of NAcM-NEG, -OPT, -COV (10 µM) treatment. **A:** Quantification of cleaved caspase-3 mpi in MM6 (n=3 independent experiments) **B:** Quantification of cleaved caspase-3 mpi in primary human monocytes (n=3 independent biological replicates) **C:** Representative immunoblots of caspase-3 and cleaved caspase-3 in primary human monocytes. All values were normalized to and calculated as ratios to tubulin mpis. Statistics: one-way ANOVA with Dunnett multiple comparisons test.

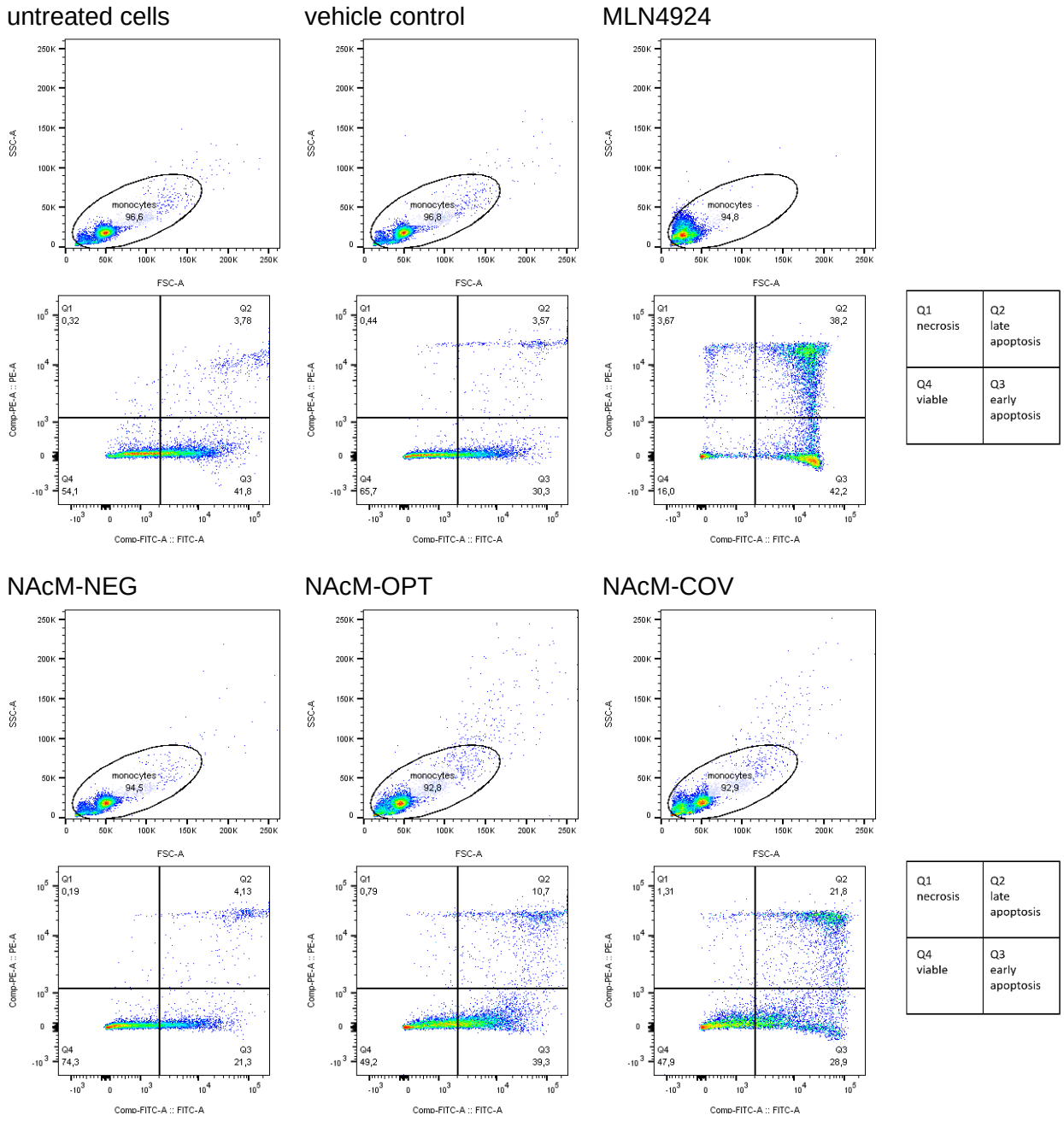

Figure A 2 Exemplary gatings of Annexin V-FITC/PI-double staining of primary human monocytes after 16 h inhibitor treatments. (NAcM-NEG/-OPT/-COV: 10 µM, MLN4924: 1 µM) Gating was performed toward vehicle controls. Q1 represents the percentage of the cell population in necrosis, Q2 the percentage of the cell population in late apoptosis, Q3 the percentage of cells in early apoptosis and Q4 represents the viable percentage of the cell population. Representative of n=165 experiments.

Acknowledgments

First and foremost, I would like to express my gratitude to Univ.-Prof. Dr. rer. nat. Jürgen Bernhagen, whose expertise, guidance, and support have been invaluable throughout my time lab. The culture of learning you created in the lab has made my time there both, challenging and rewarding.

I am profoundly grateful to my direct supervisor in the lab, Dr. Jelena Milic, PhD. Your endless patience, constant encouragement, and constructive criticism have been instrumental for me while working on this thesis. Observing your growth and transformation into the scientist you are today has been a guiding example for me.

Furthermore, I want to thank the whole Bernhagen group, with special recognition to Dr. Omar El Bounkari, Dr. Markus Brandhofer, and Dr. Dzmitry Sinitski. Your collective knowledge and enthusiasm for science have been an essential resource and inspiration for me.

My gratitude in the lab especially extends to Yuan, Mathias, and Verena. My friendships with you made my time working in the lab even more memorable and enjoyable. A special thanks also to Sabi for our much-needed coffee dates.

I would also like to acknowledge my research committee members, Prof. Söhnlein and Prof. Behrends, for their constructive feedback, which has enriched my thesis.

Thank you to my family and friends: your love and support have been the foundation of my medical studies and my research. Lastly, to Max: Thank you for being a constant pillar of support throughout this journey.

To everyone mentioned and the many more who have supported me indirectly:
Thank you!

Affidavit

LMU LUDWIG-MAXIMILIANS-UNIVERSITÄT MÜNCHEN

Promotionsbüro Medizinische Fakultät

MMRS

Affidavit

Preuner, Eva-Maria

Surname, first name

Street

Zip code, town, country

I hereby declare, that the submitted thesis entitled:

Characterization of novel NEDDylation inhibitors in in vitro models of atherogenesis

is my own work. I have only used the sources indicated and have not made unauthorised use of services of a third party. Where the work of others has been quoted or reproduced, the source is always given.

I further declare that the submitted thesis or parts thereof have not been presented as part of an examination degree to any other university.

München, 29.03.2025 — Eva-Maria Preuner

place, date — Signature Eva-Maria Preuner